THE UNIVERSITY OF CALGARY

Fuel Systems for Liquid-fuelled Aerovalved Pulse Combustors

by

Ajay Kumar

A THESIS

SUBMITTED TO THE FACULTY OF GRADUATE STUDIES

IN PARTIAL FULFILMENT OF THE REQUIREMENTS

FOR THE DEGREE OF MASTER OF SCIENCE

IN MECHANICAL ENGINEERING

DEPARTMENT OF MECHANICAL ENGINEERING

CALGARY, ALBERTA

AUGUST, 1993

THE UNIVERSITY OF CALGARY

FACULTY OF GRADUATE STUDIES

The undersigned certify that they have read, and recommend to the faculty of graduate studies for acceptance, a thesis entitled, "Fuel Systems for Liquid-fuelled Aerovalved Pulse Combustors" submitted by Ajay Kumar in partial fulfilment of the requirements for the degree of Master of Science in Mechanical Engineering.

J.A.C. Kentfield.

Dr J.A.C. Kentfield, Supervisor
Department of Mechanical Engineering

Dr. G.A. Karim
Department of Mechanical Engineering

Dr. I. Wierzba
Department of Mechanical Engineering

Dr. R.G. Moore
Department of Chemical Engineering

Date: August 17, 1993

ABSTRACT

The ability of pulse combustors to generate a combustion driven pressure rise has led to their potential application in gas turbines. This results in an increase in the power output of the turbine. Previous work carried out in this field at the University of Calgary employed a gas-fuelled aerovalved pulse combustor. As a majority of gas turbines run on liquid fuel there is a need to develop a liquid-fuelled pulse combustor for a similar application.

In the current work four types of fuel systems were investigated: carburettor, high pressure steady flow fuel injection, low pressure steady flow fuel injection and high pressure fuel interrupter. Gas analysis of the exhaust gases for the four fuel systems was conducted to determine the levels of CO emissions. The results from the present study indicate that the pulse combustor has the ability to handle fuel injection at high pressure. Also it is possible to supply the fuel to the pulse combustor intermittently. Although the pulse combustor ran on all four fuel systems further work is required to optimize a fuel system for liquid-fuelled pulse combustor for gas turbine application.

ACKNOWLEDGEMENTS

To Dr. J.A.C. Kentfield for his support and guidance during the course of this work. His suggestions during the writing of the manuscript were invaluable.

The exhaust gas analysis carried out would not have been possible without the dedicated help of Reginald Gustafson. His suggestions and innovative ideas during the experiments were of immense value.

Thanks are also extended to Gregory East, Rob Scorey, Charles Imer, Paul Lavoie, Roy Bechtold, Jack VanBenthem, Brandon Ferguson and Art Moehrle for the construction of the experimental set up. Thanks are due to Bert Unterberger for the photographs of the experimental equipment.

I would like to acknowledge the help extended by Rovin Karunanayake throughout the work. The effort of Lynn Banach for typing the manuscript and tolerating me in her office is greatly appreciated.

Last of all, my thanks to Nayani for being a constant support during the course of this work.

Dedicated to my parents and wife for their love and sacrifice

TABLE OF CONTENTS

LIST OF TABLES

LIST OF FIGURES

NOMENCLATURE

A	area (m^2)
a	acceleration (m/s^2)
a_1	velocity of sound in the gas in connector pipe (m/s)
a_2	velocity of sound in kerosene (m/s)
F	force (N)
K	spring constant (N/m)
m	mass (kg)
P	fuel pressure (kPa)
Δp	pressure difference (kPa)
R	gas constant (J/(kg.K))
S	spool displacement (mm)
s	non-return valve lift (mm)
T	thrust produced by pulse combustor (N)
T_1	temperature of gas in combustion chamber (K)
T_2	ambient temperature (K)
T_{av}	average temperature of gas in connector pipe (K)
t	time (ms)
t_1	time required for the pressure wave to travel from pulse combustor to interrupter (ms)
t_2	time required to displace spool (ms)
t_3	time required for the pressure wave to travel from interrupter to nozzle tip (ms)

t_4	time required to open the delivery valve (ms)
u	velocity (m/s)
W	weight of thrust plate (N)
x	length (m), valve thickness (mm)
y	length of chains suspending thrust plates (mm)

GREEK

ρ	density (kg/m^3)
γ	specific heat ratio

ABBREVIATIONS

S.F.C.	specific fuel consumption (kg/(h.N))

CHAPTER 1 INTRODUCTION

1.1 BACKGROUND

Combustion driven oscillations appear to have been first observed by Higgins in 1777 (1). He found that by changing the axial position of a small diffusion flame in a tube an audible sound, or note, was produced for particular locations of the flame. This phenomenon was explained by Rayleigh in 1878 (2). It was used in a variety of applications (e.g. propulsion, heating etc.) around the turn of the century.

Rayleigh stated that the requirement necessary for sustained combustion driven oscillations is that the point of energy release must be in phase with and at the point of maximum pressure to reinforce the resonant pressure wave. If energy is given to a gas at the moment of highest pressure, or taken from it at the moment of lowest pressure, the oscillations are encouraged. On the other hand, if energy is supplied at the instant of lowest pressure, or taken away at the moment of highest pressure, the oscillations are discouraged. In both cases the frequency is unaltered. If the gas is at its normal density at the instant when the transfer of heat takes place, the oscillations are neither encouraged nor discouraged, but the frequency is altered depending on the phase of heat transfer.

Figure 1.1 (3) shows Rayleigh's criterion for combustion driven oscillations graphically. Q is the instantaneous source of energy release which causes an instantaneous pressure rise. The undisturbed combustion chamber pressure is represented by the solid curve and the dashed curve represents the combustion chamber pressure after modification by the instantaneous release of energy. Case 1 shows that if the energy release is at the point of maximum pressure, 3Π/2, 7Π/2, etc, the amplitude of pressure oscillation increases but the frequency remains unchanged. The amplitude of the pressure oscillation decreases, with no effect on the frequency when heat is added at the moment of minimum pressure, Π/2, 5Π/2, etc, as depicted in case 2. Case 3 shows that if the energy release occurs at Π, 3Π, etc, the frequency increases with no effect on the pressure amplitude. If the energy release occurs at 2Π, 4Π, etc, the frequency decreases with no effect on the pressure amplitude as shown in case 4. If the energy release is at some location other than the cases presented above, then both the amplitude and frequency of the pressure wave will be affected.

Keller and Westbrook (4) studied the response of a valved, Helmholtz pulse combustor to changes in the chemical kinetic ignition delay time and found that by decreasing the chemical kinetic ignition delay, the Helmholtz-type pulse combustor became de-tuned and operated less stably. This was attributed to the mismatch in the phase relationship between the instantaneous energy release rate and the resonant pressure wave.

Strictly speaking there is no difference between combustion driven oscillations and pulse combustion as the underlying principle, the Rayleigh criterion, is same for both.

The major distinction is that in the case of combustion driven oscillations in nominally steady flow systems the aim is usually to suppress the pressure oscillations, whereas in the case of pulse combustion the aim is to sustain the pressure oscillations and put these to a worthwhile use. Table 1.1 (5) summarizes the principle differences between pulse combustion and combustion driven oscillations such as can occur in nominally steady flow systems.

In a valved pulse combustor (described in section 1.2) the oscillations are of the standing wave mode (6). Valveless or aerovalved pulse combustors exhibit a combined standing and travelling wave type of oscillations. A standing wave is characterised by a 1/4 cycle phase difference and a travelling wave by a 1/2 cycle phase difference between pressure and velocity.

According to Putnam et al (5) the first mechanical valved pulse combustor and aerovalved pulse combustor were reported in 1906 and 1909 respectively. In pulse combustors the interaction between chemical kinetics and fluid dynamics is very complex and the situation is aggravated by the unsteady, cyclic nature of the pressure, temperature and velocity variations. There is also a difficulty in scaling up existing laboratory designs to large scale units. Hence, the design of pulse combustors relies heavily on trial and error. Putnam (7) divides the analytical approaches used for predicting the performance of a pulse combustor into three categories.

(a) Considering the phenomenon as a perturbation phenomenon.

(b) Treating the phenomenon by the method of characteristics.

(c) Dividing the process into components as is sometimes done for the various phases of operation of an internal combustion engine.

In the most recent symposium on pulsating combustion a number of analytical and numerical methods for pulse combustion system modelling were presented (8). Most of the models dealt with the pulse combustor in one space dimension only.

Pulse combustors have the ability to handle gaseous, liquid or solid fuel. Gaseous fuels (e.g. propane, methane) can be premixed with fresh air before entering the combustor (3, 9), fed continuously to the combustion chamber (10,11) or supplied from a separate aerodynamic or mechanical valve (3). Keller et al (3) compared the operations of a valved pulse combustor for both premixed and conventional injection system (fuel and air supplied separately to the combustion chamber) and found that the combustor operated favourably in the premixed mode. Liquid fuel (e.g. gasoline, kerosene) can be injected into the combustor with air as a fuel rich mixture using a carburettor (12,13,14), injected into the combustion chamber continuously through the cycle (15) or vaporized before being injected into the combustion chamber (16). Solid fuel (eg. coal) can be burnt in Rikje type combustors of the "singing tube" type, in unpulverized (17,18) or pulverized form in other types of pulse combustors (19).

1.2 TYPES OF PULSE COMBUSTORS

On the basis of the air inlet valve design the pulse combustors can be divided into three categories - flapper and reed valve, rotary valve and the aerodynamic valve.

Figure 1.2 (20,21) shows an example of a reed and flapper valved pulse combustors. The reed valve shown is similar to the type in the Argus-Schmidt tube used for propelling the V-1 "buzz bomb", or cruise missile, of World War II. An advantage of the flapper valve shown is that a considerable range of flow can be achieved by changing the spacer, which governs the area of the annular orifice between the two plates. In a reed or flapper valved pulse combustor there is no back flow from the inlet because when the pressure inside the combustor rises above inlet pressure the inlet valves close to inhibit any back flow. As the combustor pressure drops below inlet pressure the reed or flapper inlet valves open automatically to let in fresh air or a mixture of fresh air and fuel. The main disadvantage of valved pulse combustors with these valve types is the failure of the valve from fatigue and, or, thermal damage from coming in contact with hot combustion gases or, indeed, in some applications heated inlet air. The working cycle of a valved pulse combustor has been described by Kentfield (20), Arpaci et al (22) and many other authors.

Compared to flapper and reed valves, rotary valves are less complicated. They are also less susceptible to fatigue and thermal failure. Figure 1.3(a) shows a perforated rotor disk, driven by a d.c. motor, used for the inlet valve by Kunsagi (23). In a rotary valved pulse combustor the system frequency is fixed by the rotation of the valve. Thus for the optimum performance some feedback mechanism would be required in which the valve would rotate at a rate permitting the combustor to operate at its natural frequency.

Aerovalved or valveless pulse combustors are characterized by no moving parts. Thus the risk of inlet valve failure is eliminated. This is an important consideration for heavy duty combustors (such as those that might be used for gas turbine applications) in which the inlet valves are subject to an adverse operating environment. The back flow from the inlet can be used for pumping, pressure boosting or thrust generation. The SNECMA design (24) shown in Figure 1.3(b) has a forward facing inlet arranged coaxially with the tail pipe on opposite sides of the combustion chamber. Figure 1.3(c) shows a design by Persechino (25) in which the inlet and tail pipe are on the same side of the combustor, parallel to each other.

Aerovalved pulse combustors can have more than one inlet. Spiers (10) showed that by using four inlets the overall length of the pulse combustor could be reduced by 40%. This was attributed to the fact that the mixing time for the fuel and air decreases with multiple inlets which allows the length of the pulse combustor to be decreased without altering the performance of the machine. This is of great significance if the pulse combustor was to be installed on an aviation gas turbine, where engine weight and volume become critical factors. The working cycle of an aerovalved pulse combustor is described in the next section.

A distinction should be made between pulse and pulsed combustors as these two terms are sometimes used synonymously. A pulsed combustor is a device that runs at a frequency other than its natural frequency. The frequency of a pulsed combustor is determined by ignition timing, fuel injection or valve sequence as distinct from a pulse combustor which fires at its natural frequency controlled by the wave events. A device which falls between a pulse combustor and a pulsed combustor is called the Rikje tube referred to previously. It consists of a vertical tube open at both ends with a heat source situated at one quarter of the tube length above the lower end. As it is not self aspirating and its frequency is wave controlled it is neither a pulse combustor nor a pulsed combustor.

1.3 WORKING CYCLE OF PULSE COMBUSTOR

Figure 1.4 (5) shows various processes taking place in a single cycle of an aerovalved pulse combustor. The operating cycle of a valved pulse combustor (20, 22) is slightly different form an aerovalved pulse combustor in that there is no back flow from the inlet of the valved unit. There are typically four phases in a cycle. Phase 1 is characterized by ignition of the mixture of fresh air, fuel and combustion gases from the previous cycle. This is depicted by point A on the pressure vs specific volume diagram. It has been confirmed that the ignition of the combustion mixture takes place due to the presence of residual products of combustion from previous cycle (20). Keller and Saito (26) used OH chemiluminescence to confirm that the residual combustion process serves as the ignition source for the next combustion cycle. According to their finding the combustion process never ceases between cycles and is responsible for the ignition of the following cycle.

After ignition the burning region expands towards the inlet and exit of the combustion chamber till point B, the peak pressure point of the PV diagram is attained. In phase 2, the gases expand and move outward until the pressure inside the combustion chamber falls below atmospheric pressure (point C) because of momentum effect. In phase 3 the gas flow reverses (first in the inlet and then in the long tail pipe). In phase 4, fresh charge is drawn in from the inlet and some exhaust gases from the tail pipe. The momentum effect of the gases coming in causes the pressure inside the combustion chamber to rise above atmospheric pressure. Fuel is supplied during this phase and it mixes with the fresh air and the exhaust gases to form a heated combustible mixture for the next cycle.

1.4 OBJECTIVES OF CURRENT WORK

The main objectives of the current work were:

(1) To develop a pulse combustor to run on liquid fuel. One of the main applications of such a liquid fuelled pulse combustor would be on a gas turbine. Tests carried out earlier (11, 27, 28) on a gas turbine showed that the power output of the engine increased as a direct result of the stagnation pressure rise achieved due to the substitution of the conventional combustion chamber of the gas turbine with a gas fired pulse combustor. As a majority of gas turbines run on liquid fuel there is a need to conduct similar tests with a liquid fuelled pulse combustor. A number of liquid fuel systems were to be evaluated and tested:

   (a) Carburettor fuel system.

   (b) High pressure steady flow fuel injection system.

   (c) Low pressure steady flow fuel injection system.

   (d) High pressure fuel interrupter system.

(2) To evaluate and try to reduce the exhaust emissions from the various liquid fuel systems listed above.

1.5 ORGANIZATION OF TEXT

The advantages, disadvantages and the applications of pulse combustor are discussed in Chapter 2. Special emphasis is given to the potential application of pulse combustors in gas turbines. In Chapter 3 the experimental set up is discussed including the four types of fuel systems tested - carburettor, high and low pressure steady flow fuel injection systems and high pressure fuel interrupter. The dynamic analysis of the non-return valve of the carburettor and the Mark 1 fuel interrupter is carried out in Chapter 4.

Chapter 5 is devoted to a description of the operating procedure of the carburettor fuel system, observations made, the results obtained and finally a discussion of the results. Similar analysis is made for both the high and low pressure steady flow fuel systems as reported in Chapter 6. Likewise Chapter 7 deals with the high pressure fuel interrupter system. Finally Chapter 8 summarizes the conclusions of the present work. It also includes some recommendations for future work.

DISTINGUISHING PARAMETERS	PULSE COMBUSTION	COMBUSTION DRIVEN OSCILLATIONS
Aim	Utilize	Eliminate
Operating range	Increase	Decrease
Damping	Minimize while meeting environmental noise requirements	Maximise sufficiently to eliminate
Pumping	Positive pumping of air required	May occur in either direction or not at all
Initiation	Small fan usually needed for starting	Usually self starting
Air supply	Usually self pumping	Blower, fuel momentum or buoyancy

Table 1.1: Principal differences between pulse combustion and combustion driven oscillations as can occur in nominally steady systems (5).

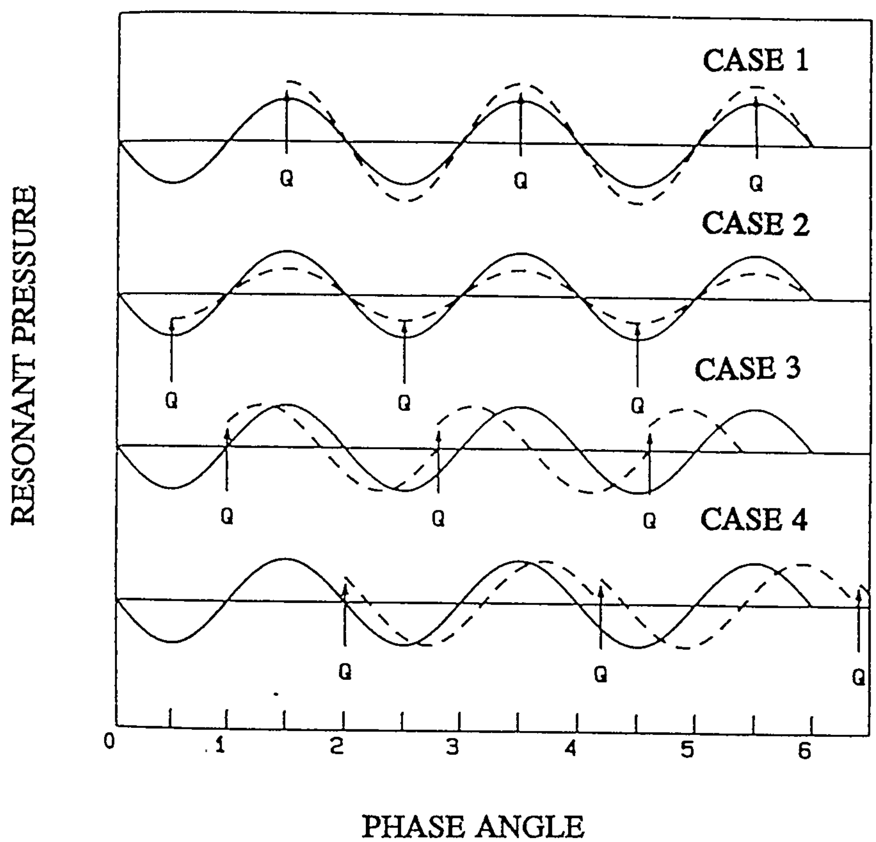

Figure 1.1: Schematic representation of Rayleigh's criterion (3)

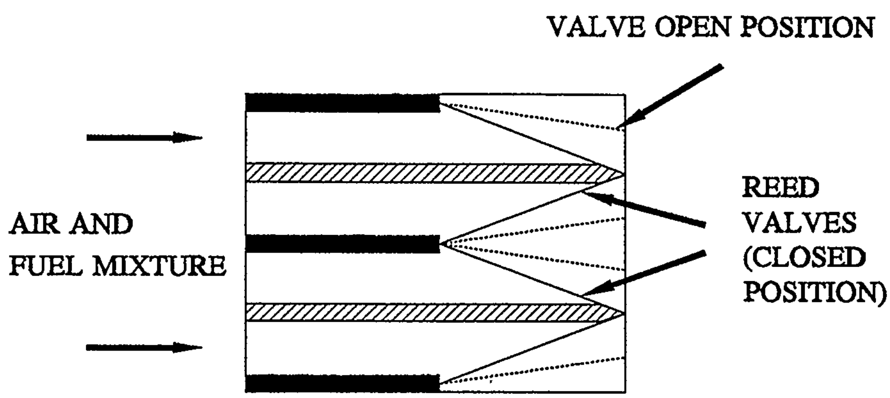

(a) Reed Valve (20)

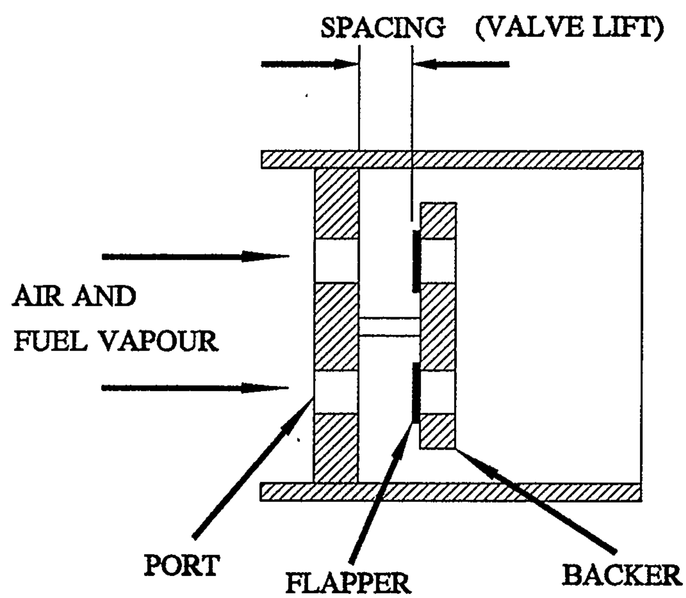

(b) Flapper Valve (21)

Figure 1.2: Pulse combustor equipped with (a) Reed valve (b) Flapper valve

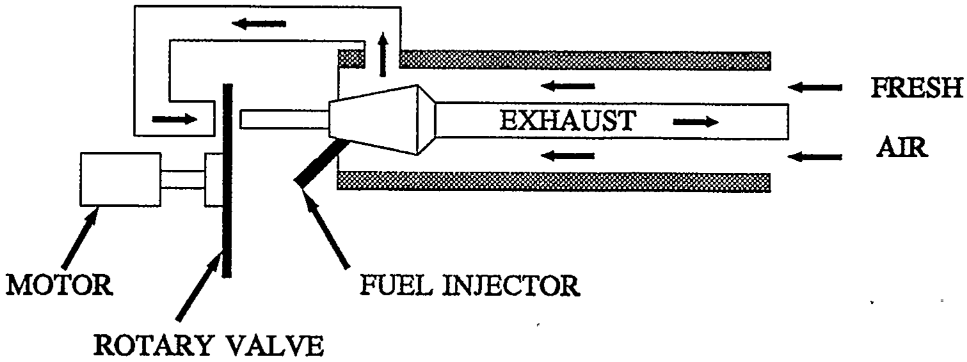

(a) Rotary valve (23)

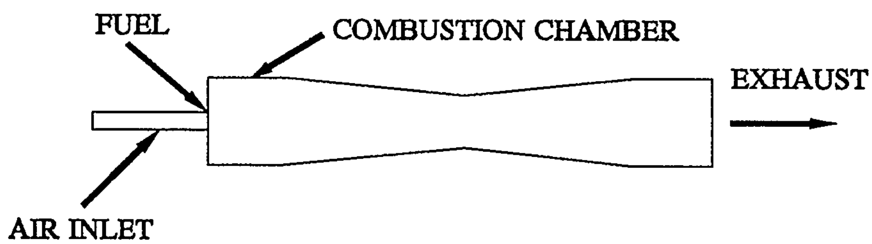

(b) Aerovalved (SNECMA (24))

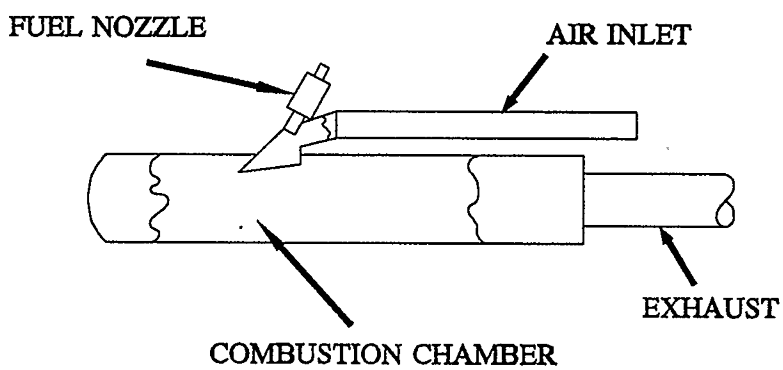

(c) Aerovalved (Persechino (25))

Figure 1.3: (a) Pulse combustor with rotary valve (b) Aerovalved pulse combustor with forward facing inlet (c) Aerovalved pulse combustor with rearward facing inlet

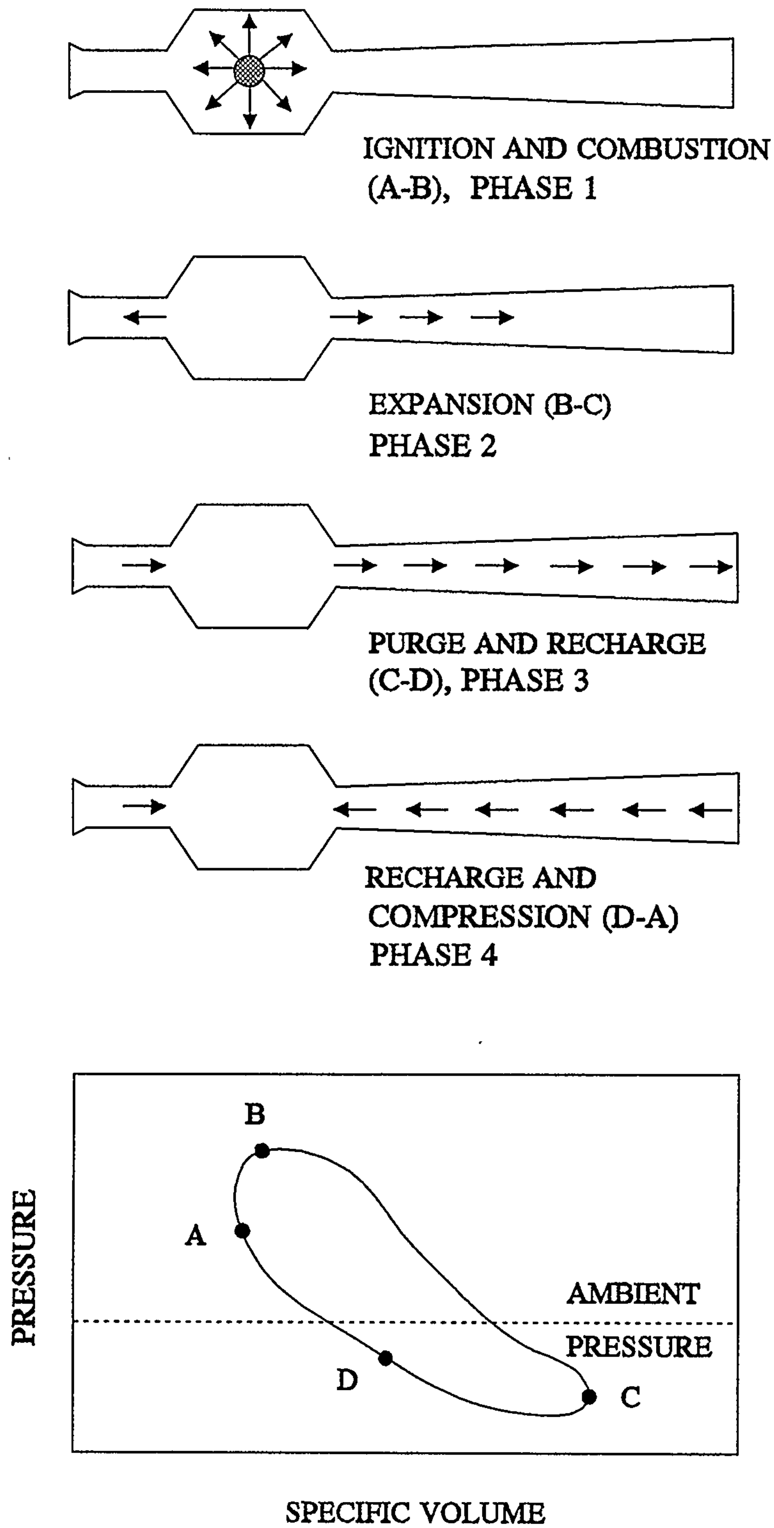

Figure 1.4: Operating phases of an idealized pulse combustor (7)

CHAPTER 2 PULSE COMBUSTOR: ADVANTAGES, DISADVANTAGES AND APPLICATIONS

2.1 ADVANTAGES AND DISADVANTAGES

2.1.1 Advantages

The main advantages of pulse combustors over steady flow combustors are as follows.

(a) Low NO_x Emissions: Pulse combustors inherently have been found to produce low NO_x emissions compared to steady flow combustors of comparable size. Corliss et al (29) found that the NO_x emissions from pulse combustors were 34-46 ppm compared to 58-138 ppm for conventional boilers. According to some authors (5) the low NO_x concentrations from pulse combustors are the outcome of very rapid combustion resulting from the high mixing rate, followed by a rapid quenching of the products. Keller and Hongo (30) investigated the mechanism of NO_x production in pulsating flow and concluded that the low NO_x emissions in pulse combustors were a result of the rapid mixing of residual products with the hot products producing a short residence time at high temperature. Typically the residence time of the charge in pulse combustors is half that in internal combustion engines and steady flow burners.

NO_x emissions from pulse combustors has been found to be reduced by flue gas, or exhaust, recirculation, fuel staging, air staging or a combination of both fuel and air staging. In flue gas recirculation cooled products of combustion are mixed with fresh air and introduced into the combustion chamber. This leads to lower peak temperatures and hence lower NO_x concentrations. Michel (31) achieved a 50% reduction in NO_x emissions with exhaust gas recirculation for a hot water boiler. In fuel and air staging, combustion is divided into two sequential flame zones and fuel or air is admitted in stages. This results in low peak temperatures and production of thermal NO_x is limited. Kelly (32) reduced the NO_x concentration for a propane fuelled aerovalved pulse combustor by 17% for fuel staging and 28% for air staging. A combination of both, fuel and air staging, led to a 54% reduction in NO_x concentration.

(b) High Rate of Heat Transfer: Another major advantage of pulse combustors is that convective heat transfer rates in the tail pipe are enhanced by as much as 2.5 times over those in steady turbulent flows at the same mean Reynold's number (33, 34). Hanby (33) obtained heat transfer coefficients with pulsating flow that were over 100% that obtained with steady flow. Dec and Keller (34) tested the affect of pulsating frequency, pulsation amplitude and mean flow rate on heat transfer rate. The Nusselt number was found to increase with both pulsation amplitude and frequency with a maximum enhancement of 2.5 times than for steady flow at the same mean Reynold's number.

With an increase in the mass flow rate the Nusselt number enhancement decreased for a given combustor pulsation frequency and amplitude. Perry and Culick (35) found that the wall heat transfer in the presence of large amplitude combustion driven oscillations varied approximately as the square root of the oscillations amplitude and as the fourth root of the frequency.

(c) High Energy Transfer Efficiency and Combustion Intensity: Energy transfer efficiencies in pulse combustor heaters have been found to be much higher than in conventional steady flow combustion heaters. Lockwood (36) calculated the energy transfer efficiency of a pulse combustor water heater to be around 95%. This is a marked improvement over the corresponding efficiencies of conventional water heaters which are around 45 to 60% (36). Adams (37) conducted tests on Lennox pulse combustor furnaces and found that their efficiencies were in the range of 91 to 94 %. Similar values were also quoted by Woodworth (38). Also combustion intensities for pulse combustors have been reported to be ten times those for conventional burners (39).

(d) Multi-Fuel Capability: Pulse combustors are known to have the ability to run on liquid, gas and solid fuels. Some of the fuels that have been tested on pulse combustors are propane (10, 28), methane (40), gasoline (12, 13, 14), kerosene (16), residual fuel (41), wood (42) and coal (16, 17, 18). The ability of pulse combustors to handle multiple fuels is an asset considering the depleting resources of some fuels. Generally some adjustments are required to switch over from one fuel to another.

(e) Combustion Driven Pressure Gain: Pulse combustors produce a combustion driven pressure gain instead of a combustion driven pressure loss associated with a conventional steady flow combustion chamber. This has led to the potential application of pulse combustors in gas turbines. In the conventional combustion chamber of a gas turbine there is a pressure loss due to friction losses. Further there is a fundamental heat addition loss associated with the reduction of fluid density due to heat addition to a moving fluid. This can result in a 2 to 8% pressure loss in the combustion chamber of a gas turbine. This leads to a reduction in the power output and an increase in fuel consumption. By using a pulse combustor on a gas turbine Kentfield and Fernandes (43) achieved an increase of 4% of the compressor delivery pressure. According to Kentfield (20) this would translate to about 1 to 2% increase in net power output, with a corresponding reduction in specific fuel consumption, for each 1% reduction in combustion pressure loss or increase in pressure gain.

(f) Simplicity in Construction: Aerovalved pulse combustors, with no moving parts, are one of the simplest thrust generators known. The simplicity in design makes the aerovalved pulse combustors very economical to fabricate. In addition pulse combustors do not require a fan or a blower for operating, making them even more economically feasible.

2.1.2. Disadvantages

The main disadvantages of pulse combustors over steady flow combustors are as follows:

(a) High Noise and Vibration Level: An inherent problem of pulse combustor is noise generation. This has proved to be the main deterrent in using pulse combustors for residential applications. Sran and Kentfield (44) obtained a 20 db reduction in the noise level of a twin valveless pulse combustor by operating the twin combustors in anti-phase.

(b) Lack of Fundamental Understanding: Because of the complexity of the working cycle of a pulse combustor there is a lack of information on fundamental fluid dynamics, combustion and heat transfer processes occurring in pulse combustors. As a result the design and development of pulse combustors have proceeded largely by trial and error. This has been found to be time consuming and costly and does not necessarily guarantee an optimum design.

2.2 PULSE COMBUSTOR ON A GAS TURBINE

The ability of a pulse combustor to generate a combustion driven pressure gain led to their potential application in gas turbines. The pioneering proposal in this field was due to Reynst (45). The advantage of using a pulse combustor on a gas turbine is illustrated in Figure 2.1 (20). It is clear from the figure that the additional temperature drop available in the turbine results in an increase in the power output of the engine with a resultant reduction in specific fuel consumption. Thus the use of pulse combustor in a gas turbine leads to either a reduction in the number of stages of the compressor, without modifying the turbine, or an increase in the power of the turbine, without altering the compressor. Porter (46) developed a valveless combustor for a gas turbine that operated on pressures ranging from 1 to 3 atmospheres and found that the discharge pressure was higher than the inlet pressure. He studied the effect of pressure pulsations on turbine efficiency and concluded that the loss of turbine efficiency due to pulsations originating from the combustor was likely to be small. Yemeni (27) carried out tests on a small gas turbine installed with a gas fired pulse combustor. The system produced about a 0.5 % stagnation pressure gain. The advantage of using a pulse combustor was not fully realized because of the crude design of the system. Work carried out by O'Blenes (28) on the same system increased the stagnation pressure gain to approximately 1.5 %. Fernandes (11) further improved the performance of the gas turbine by achieving a 4 % increase in stagnation pressure and a 27 % increase in thermal efficiency using a pulse combustor configuration shown in Figure 2.2. The principal disadvantage of using a pulse combustor on a gas turbine is the increase in the weight and volume of the total system. Spiers (10) designed a four inlet pulse combustor for a gas turbine. By using multiple inlets he was able to achieve a 40 % reduction in length as compared to a single inlet pulse combustor without altering the performance of the unit.

2.3 OTHER APPLICATIONS OF PULSE COMBUSTORS

Over the years pulse combustors have been used in a number of applications. The high energy transfer efficiency obtained from pulse combustors plus their ability to pump products of combustion past heat transfer surfaces has led to their use in steam raising and water heating. Similar machines have also been used as air heaters for warming cabins, vehicle interiors, house heating etc. Pulse combustors have also been applied for drying (eg. food for livestock), fogging, gasification, propulsion, hot gas recirculation, power generation, heating railway track switches, etc. A detailed description of their applications can be found elsewhere (5, 7, 12, 20).

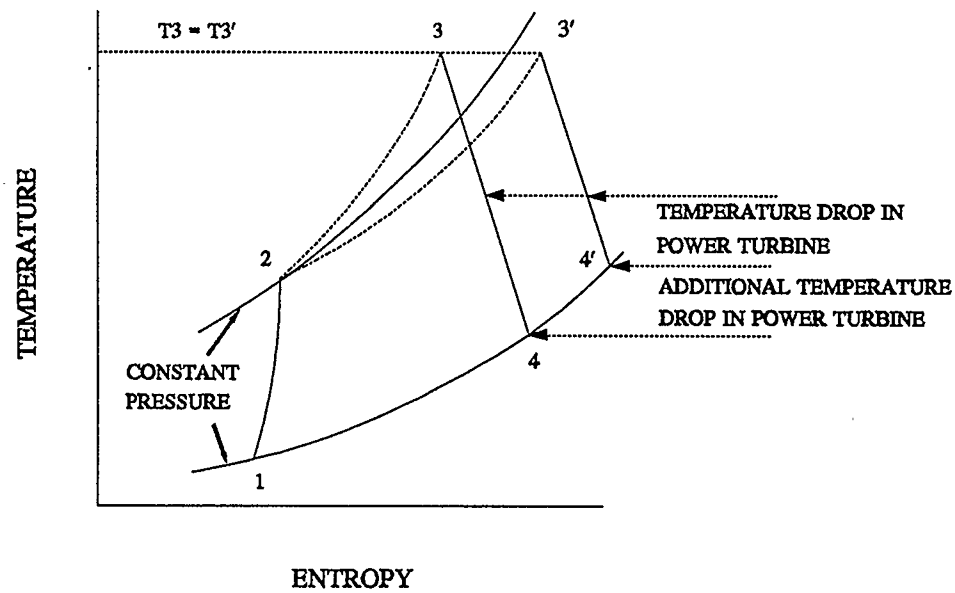

Figure 2.1: Simple shaft-power gas turbine cycles on the temperature vs entropy diagram
Cycle 123′4′ with combustor pressure loss
Cycle 1234 with combustor pressure gain (20)

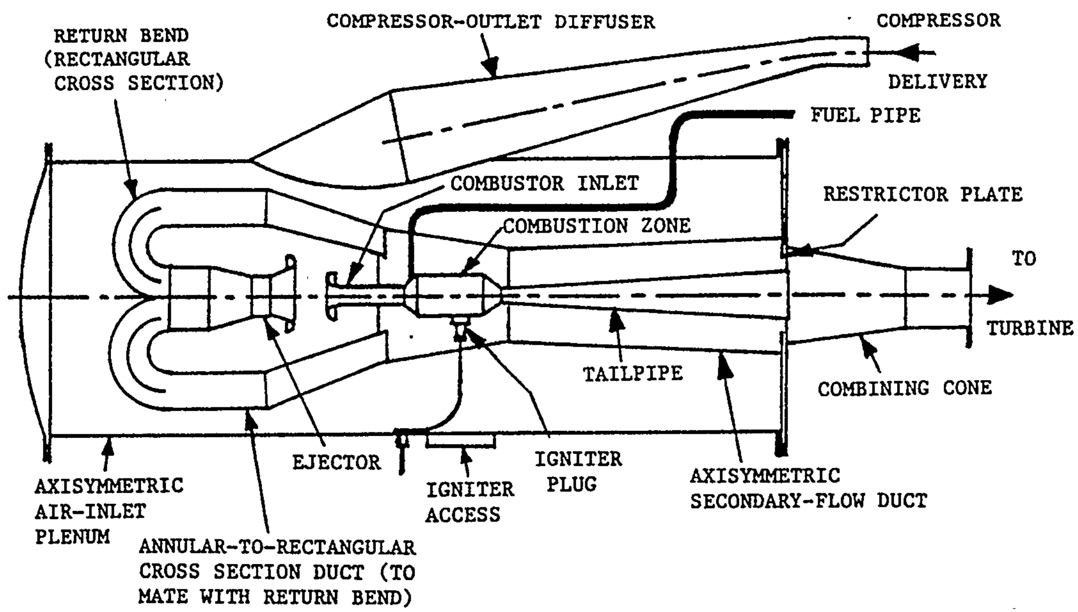

Figure 2.2: Configuration of prototype pulse combustor used on a gas turbine (11)

CHAPTER 3 EXPERIMENTAL SET UP AND EQUIPMENT

3.1 INTRODUCTION

As outlined in sections 1.4 of Chapter 1 the objective of the study was to convert a gas fuelled pulse combustor to run on liquid fuel. Although most of the designing of the fuel system was done with the idea of using the liquid fuelled pulse combustor on a gas turbine, it could also be used for other applications such as warm air blowing, etc.

Four types of liquid fuel systems were investigated. The carburettor used was modified from that used on a gasoline fired hand held warm air blower (47). In the high and low pressure steady flow fuel injection systems the fuel was injected directly into the combustion chamber, nominally continuously, at a pressure ranging from 345 kPa gauge to 1034 kPa gauge and from 69 kPa gauge to 345 kPa gauge respectively. In the high pressure fuel interrupter system the fuel was supplied intermittently to the pulse combustor at a pressure ranging from 345 kPa gauge to 1034 kPa gauge.

The following sections provide a description of the pulse combustor, fuel systems, experimental set up and the instrumentation used.

3.2 PULSE COMBUSTOR

The pulse combustor used for the experiments was similar to the 76.2 mm (internal diameter of the combustion chamber) pulse combustor used by Rehman (13). This unit was based upon the design of a carburetted gasoline fuelled combustor developed by Kentfield (48) which, in turn, was based on the valveless Hiller HH-M1 unit (15). Figure 3.1 shows the combustor details. All dimensions shown are internal (mm).

The pulse combustor comprised of three main parts - an inlet pipe, a cylindrical combustion chamber and a tail pipe. The combustion chamber was 76.2 mm in diameter and 134.9 mm in length. Two stainless steel bosses were welded onto the combustion chamber. The first boss was used for the pressure transducer to pick up the pressure variation in the combustion chamber. When the pressure transducer was not used the hole was plugged with a spark plug. The second boss was for a spark plug to initiate combustion. The frustum of a right cone welded at the rear end of the combustion chamber reduced the diameter from 76.2 mm to 26.7 mm in a length of 25.4 mm. A 914.4 mm long diverging tail pipe was welded to the end of this cone. The diameter of the tail pipe increased from 26.7 mm to 62.5 mm. Another frustum of a right cone welded at the front end of the combustion chamber reduced the diameter from 76.2 mm to 38.1 mm in a length of 19.1 mm. The inlet which consisted of two parts was welded to the frustum. The first part closest to the combustion chamber was 38.1 mm in length and had a uniform diameter of 38.1 mm. The second part was a uniform pipe of 38.1 mm diameter for 25.4 mm and then decreased in diameter from 38.1 mm to 33 mm in a length of 69.9 mm. The two sections were joined by a flange. A Bell mouth was welded to the open end of the inlet. The pulse combustor was supported on the frame at three places. The middle support was bolted to the frame, whereas the other two supports were free to slide longitudinally to accommodate the expansion and contraction of the pulse combustor. The combustor was fabricated out of 0.76 mm thick stainless steel sheets rolled into various cylindrical and conical sections previously referred to.

3.3 FUEL SYSTEMS

The four fuel systems tested are described in the following section.

3.3.1 Carburettor System

3.3.1.1 *Set Up*

Figure 3.2 shows the schematic of the carburettor fuel system. The fuel used for the carburettor was gasoline. An electric pump was used to pump gasoline into an elevated tank mounted four metres above the ground. Fuel from the tank was fed to a float chamber mounted on the wall just below the fuel tank. The purpose of this float chamber was to maintain a constant head in the combustor fuel system regardless of the level of fuel in the fuel tank.

For measuring the fuel flow rate the gasoline was passed through a rotameter before being fed to a second float chamber in the body of the carburettor. A non-return valve helped prevent the back flow of gases from the carburettor. The working principle of the non-return valve is described in the next section. The amount of fuel going into the pulse combustor was controlled with the help of a needle valve in the carburettor. The needle valve was operated remotely via a cable.

3.3.1.2 *Carburettor and Non-Return Valve Assembly*

The carburettor and non-return valve assembly used for the present work were taken from a gasoline fired warm air blower developed by Kentfield (47). The design of the carburettor and valve assembly was slightly different from the one used by Ibrahim (12) and Rehman (13), although the working principle behind both designs was the same. Figure 3.3 shows the non-return valve assembly. The carburettor body (not shown), which contained the fuel float chamber, the fuel jet and the needle valve, was connected to the non-return valve assembly and it supplied a fuel rich mixture to the pulse combustor. The non-return valve was an annular ring cut out of mylar or ,alternately, shim steel. The dynamic analysis of the mylar and shim steel non-return valve is presented in section 4.1 of Chapter 4.

The non-return valve oscillated on the valve guide between the valve seat and the backstop at a frequency equal to the operating frequency of the pulse combustor. During the suction period of the cycle, i.e. when the pressure inside the combustion chamber dropped below atmospheric pressure, the non-return valve moved to the left and allowed the fuel rich mixture to enter the combustor through the eight spokes in the valve guide. During the exhaust period of the cycle, i.e. when the pressure inside the combustion chamber rose above atmospheric pressure and the supply of fuel was not required in the pulse combustor, the non-return valve moved to the right and closed the fuel holes in the valve seat. This prevented the back flow of gases through the carburettor.

3.3.1.3 *Fuel Nozzle*

The fuel and air mixture from the carburettor and the non-return valve assembly was fed to the emulsion nozzle and sprayer as shown in Figure 3.4. A cone was silver soldered around the emulsion nozzle to encourage the spreading of the fuel rich gasoline-air mixture coming out of the sprayer. A six spoked sprayer and a 19.1 mm (maximum) diameter cone were used, as this combination was found by Ibrahim (12) to give the best performance.

To prevent the fuel from adhering to the inner walls of the nozzle a spring having a wire diameter of 0.25 mm was inserted inside the nozzle. Ibrahim (12) attributed the better performance of the pulse combustor with the spring to the breaking up of any fluid film forming on the inner surface of the nozzle.

3.3.2 High Pressure Steady Flow Fuel Injection System

The carburettor system described in the preceding sections operated on atmospheric air. The disadvantage of such a system was that if the pulse combustor was to be installed on the gas turbine the carburettor would have to run on the compressed air (between 4 to 20 times atmospheric pressure) supplied by the turbine compressor. This would warrant the redesigning of the carburettor (float chamber, etc.), to handle the compressed air. To obviate this problem attention was focused on the high pressure steady flow fuel injection system. Although this system also operated with atmospheric air, the design changes required for it to run on compressed air in a gas turbine would be minimal.

3.3.2.1 *Set Up*

A gear pump is the most common fuel pump used in gas turbines (49). Appendix A describes briefly some of the different fuel pumps used in gas turbines for injecting fuel into the combustor of the gas turbine. Therefore, a gear pump was chosen for the present work. The advantage of this was that if this pulse combustor was to be installed on a gas turbine, the original pump in the turbine could, it would seem, be used to inject fuel into the pulse combustor.

A gear pump is a positive displacement device in which the mechanical displacement of the liquid in produced by rotation of toothed gear wheels as shown in Figure 3.5. The liquid enters from the suction side. As the gears pass the inlet port liquid is entrained between adjacent teeth and is then carried around the casing to the discharge opening and then forced out through the exit port. The arrows in the figure indicate the direction of rotation of the gear wheels. As the discharge pressure at the exit of the pump is increased the leakage through the clearance between the casing and the gears also increases.

Several makes and types of gear pumps were considered for the present application. Odgers (50) suggested using a combination of the gear pump and nozzle used for residential burners that run on kerosene. Based on his recommendation an Inglis Sundstrand Model "H" two stage gear pump was selected. This unit is used in residential and industrial burners running on kerosene or diesel fuel. The detailed design features of the pump are described in Appendix B.

A two stage pump had an advantage over the single stage pump in that the air trapped inside the pump could be purged out. As shown in Figure 3.6 (51) the first stage drew oil from the tank into the strainer chamber reservoir. When the strainer chamber was full, excess oil and all the trapped air rose to the top of the chamber. This was drawn into the first stage gear and pumped back to the tank. The second pumping stage drew only air free oil from the bottom of the strainer chamber and delivered it under pressure to the nozzle. Thus, there was no air trapped in the fuel going to the combustor through the fuel nozzle. Cavitation and squawking sounds were eliminated since there was no air in the second stage. Fuel by-passed by the valve returned to the bottom of the strainer chamber reservoir. This fuel, plus that being drawn from the fuel tank by the extra capacity first stage, kept the strainer chamber full at all times. A pressure gauge was attached to the gauge port to read the pressure at which the fuel was pumped. The fuel pressure could be changed with the help of the pressure adjusting screw (operated with a screw driver). This gave a fuel pressure variation of 345 kPa gauge to 1034 kPa gauge. The pump was driven by a 150 W Emerson electric motor rotating at 1725 rev/min. Figure 3.7 shows the set up of the fuel system for the high pressure steady flow fuel injection system. Fuel flow rate was determined with the help of a rotameter. The actual set up of the gear pump and the electric motor is shown in Figure 3.8.

3.3.2.2 *Fuel Nozzles*

The fuel nozzles used in conjunction with the gear pump were Delavan oil burner nozzles used for residential applications. Figure 3.9 shows the internal features of the fuel nozzle. Three different types of (on the basis of spray pattern) nozzles were tested.

A schematic representation of the spray patterns of the three nozzles is shown in Figure 3.10 (52).

Type A: This type of nozzle produced a hollow cone with fine droplets on the outside periphery of the main spray cone and is recommended for stable flame at low flows (52). Hollow cone nozzles generally have more stable spray angles and patterns under adverse conditions than solid cone nozzles of the same flow rate.

Type W: This type of nozzle produced neither a hollow nor a solid spray but had an average spray pattern to fit the average burner.

Type B: This type produced a solid cone that distributed fuel droplets fairly uniformly throughout the complete spray. This nozzle is recommended for large burners to provide smooth ignition.

In addition the type A, W and B nozzles were also identified by their fuel flow rates and spray cone angle. For example, a 4.00, 90^{o}A nozzle identification meant that the nozzle was of type A with a spray cone angle of 90^{o} and delivered 4.00 gallons of fuel in one hour at a fuel pressure of 689 kPa gauge (100 psig). All the fuel nozzles used were rated at this pressure. Table 3.1 shows the flow rates of some of the nozzles used at different fuel pressures. The spray cone angles varied from 45^{o} to 90^{o}. With the high pressure steady flow fuel injection system, 4.00 rated nozzles were mostly used.

The positioning of the fuel nozzle in the combustion chamber of the pulse combustor was carried out by trial and error. Figure 3.11 shows the first configuration of the nozzle in the combustion chamber to be tested. A threaded boss was welded to the frustum cone that joined the combustion chamber to the inlet. The fuel nozzle was screwed into this boss. All three types (A, W and B) of nozzles were used in this set up. It was found that the pulse combustor failed to go into resonance. Instead of a clear bluish flame, normally associated with a resonating pulse combustor, large sporadic pockets of reddish flame were observed in the inlet of the pulse combustor. When the compressed air supply was switched off the combustion process ceased. This was attributed to the fact that the distribution of the fuel in the combustion chamber was not uniform because of the asymmetric location of the fuel nozzle in the combustion chamber. Hence, proper mixing of the fuel, air and combustion products, essential for the proper working of the pulse combustor, was not achieved.

The next recourse was to position the fuel nozzle in the inlet (similar to the location of the carburettor fuel nozzle) to give a more uniform and symmetrical distribution of fuel in the combustion chamber. This configuration is shown in Figure 3.12. To minimize the blockage of the pulse combustor inlet the hexagon nut and the threads on the nozzle (Figure 3.9) were machined off. The strainer at the end of the nozzle was removed and a 9.5 mm (outer diameter) stainless steel pipe was silver soldered in its place. This pipe served as a fuel pipe for conveying fuel to the nozzle. Dispensing with the nozzle strainer did not cause any filtration problems as the fuel passed through two strainers and one filter before reaching the nozzle. A 25 mm long bolt was welded to the fuel pipe, 85 mm back from the nozzle tip. The nozzle assembly was firmly held in the inlet pipe by this bolt and two retaining nuts. A hole had to be drilled in the inlet to accommodate the bolt.

It was found that in this set up the pulse combustor went into resonance but with the type A nozzle only. With type W and B fuel nozzles the compressed air supply could not be switched off. What is believed to be the reason for this is explained in section 6.3.1 of Chapter 6

3.3.3 Low Pressure Steady Flow Fuel Injection System

The only difference between this fuel system and the high pressure steady flow fuel injection system was that the original spring in the pressure regulating valve of the gear pump of the high pressure system was replaced with a weaker spring. The new spring gave a fuel pressure variation from 69 kPa gauge to 345 kPa gauge. The rest of the set up was the same as shown in Figure 3.7. A 8.00 gallons per hour rated nozzle had to be used with this system to get fuel flow rates comparable to those for the high pressure steady flow fuel injection system.

3.3.4 High Pressure Fuel Interrupter System

As described in section 1.3 of Chapter 1 the burning of fuel in the pulse combustor takes place intermittently. The supply of fuel is only required during phases 3 and 4 of the working cycle. During this period the pressure in the combustion chamber is below atmospheric pressure and fuel, fresh air and combustion products (the latter from the previous cycle) mix with one another to form a combustible mixture. Subsequently, ignition and expansion take place and the combustion chamber pressure rises to exceed the atmospheric pressure. During this portion of the cycle the supply of fuel into the combustion chamber is not required because back flow from the inlet of the pulse combustor takes place and this results in a potential for exhausting unburnt fuel from the inlet. This is not much of a problem with a gaseous fuel which is supplied to the combustion chamber at a pressure comparable to the peak firing pressure in the combustion chamber. In such a case the fuel supply is self modulated by the combustion chamber pressure i.e. the fuel is supplied to the combustor when the pressure in the combustion chamber is below atmospheric pressure and the fuel is shut off when the combustion chamber pressure rises above atmospheric pressure.

In the case of liquid fuel being injected into the combustor at high pressure (1000 kPa gauge) the fuel supply modulation by the combustion chamber pressure is minimal. This results in fuel being injected into the combustion chamber throughout the cycle. Therefore, various high pressure fuel interrupter systems, capable of cutting off fuel during phases 1 and 2 (Figure 1.4) of the working cycle were designed and tested.

3.3.4.1 *Mark 1 Interrupter: Details and Set Up*

Figure 3.13 shows the cross section of the Mark 1 interrupter. It consisted of a stainless steel spool which was driven back and forth by the pressure fluctuations in the combustion chamber. The spool was 62.7 mm long and 6.6 mm in diameter. A 11.1 mm long and 1.6 mm deep groove was machined approximately mid way through the spool to facilitate the opening and closing of the fuel ports. The pressure fluctuations in the combustion chamber were sensed by a 1.59 mm thick neoprene diaphragm. The diameter of the diaphragm exposed on both sides was 76.2 mm. The left side of the diaphragm was joined to the combustion chamber by a 7.6 mm (inner diameter) copper connector pipe and the other side was vented to atmosphere through a 6.3 mm hole. The spool was rigidly connected to the diaphragm by a stainless steel hexagon nut. An aluminium washer was provided at the back of the diaphragm to prevent it from deflecting without moving the spool. At the other end of the spool a return spring was provided to help the spool to return to its original position. The tension of the return spring could be adjusted with the help of the return spring tension adjuster. The movement of the spool was restricted with the help of a adjustable backstop. The interrupter body was machined out of brass.

The working principle of the interrupter system is shown in Figure 3.14. When the pressure in the combustion chamber rose above atmospheric pressure it was sensed by the diaphragm and accordingly both the diaphragm and spool moved to the right (Figure 3.14 (b)). This shut off the fuel nozzle port and connected the pump port to the fuel return port and the fuel was diverted back to the float chamber. Thus the fuel supply to the nozzle was cut off when the pressure in the pulse combustor rose above atmospheric pressure. The fuel return was provided so that regardless of the position of the spool the gear pump would provide a continuous fuel supply. This eliminated any pressure waves being sent through the fuel system back towards the pump.

When the pressure in the combustion chamber dropped below atmospheric pressure the spool returned to its original position because of vacuum in the pulse combustor and the force of the return spring. This connected the fuel port to the nozzle port as shown in Figure 3.14 (a). Thus the fuel was supplied to the pulse combustor when the pressure in the combustor fell below atmospheric pressure.

The set up of the fuel system using the Mark 1 interrupter is shown in Figure 3.15. The fuel from the pump [1] was either supplied to the pulse combustor [4] or diverted back to the float chamber [5] depending upon the pressure signal [2] sensed by the diaphragm in the interrupter. The fuel leakage from both sides of the spool [3 and 6] was returned to the float chamber. With this arrangement the rotameter measured only the fuel delivered to the pulse combustor.

The only problem with such a system was the correct phasing of the fuel supply with the combustion chamber pressure in the pulse combustor. The timing of fuel delivery into the combustor could be varied by changing the length of the connector pipe between the combustor and the interrupter. The length of the connector pipe was chosen such that the combined time required for [1] the pressure wave to travel from the combustion chamber to the interrupter, [2] the spool to move the full distance and [3] the pressure wave to travel from the interrupter to the fuel nozzle was equal to the time for one cycle of the pulse combustor. Thus the interrupter worked on the pressure sensed from the cycle previous to the current operating cycle of the pulse combustor i.e. it was one cycle out of phase with the pulse combustor. An approximate evaluation of the connector pipe length is reported in section 4.2 of Chapter 4.

3.3.4.2 ***Mark 2 Interrupter: Details and Set Up***

When the spool in the Mark 1 interrupter was manually moved to the right, it was found that the fuel spray took 3 to 5 seconds (depending on the fuel pressure) to die down in-spite of the fact that the nozzle port was cut off from the fuel port. This was not acceptable because the working cycle of the pulse combustor was approximately 5 ms in duration. Thus for the interrupter to work properly the fuel shut off from the nozzle had to be instantaneous. Initially it was thought that this was due to the rubber fuel hose, used to connect the interrupter to the fuel nozzle, which expanded with the fuel pressure. When the fuel supply was cut off the fuel hose contracted and led to the problem of nozzle dribbling. However, when the rubber hose was replaced with a copper pipe the dribble of the nozzle still persisted.

To circumvent this problem the Mark 2 interrupter was developed. Figure 3.16 shows the cross sections of the Mark 2 interrupter. The operating principle of this interrupter was the same as that of Mark 1 interrupter. The only addition in the new device was a nozzle drain port, provided to eliminate nozzle dribbling. Figure 3.17 (a) shows the spool position when there was vacuum in the combustion chamber. In this configuration the fuel port was connected to the nozzle port. When the pressure rose in the combustion chamber the spool was pushed to the right as shown in Figure 3.17(b). In this position fuel from the pump was diverted back to the float chamber and the nozzle port got connected to the nozzle drain port. This relieved the pressure in the nozzle fuel line, by spilling some fuel back to the float chamber via the nozzle drain, thus eliminating the nozzle dribbling. To confirm this the spool was moved manually to the right (Figure 3.17(b) position) and it was found that the fuel spray from the nozzle was cut off instantly. The fuel system set up using this interrupter is shown in Figure 3.18. The set up was similar to the one for the Mark 1 interrupter with the exception that the fuel from the nozzle drain [7] was returned to the float chamber. The spool displacement required to uncover and cover the various fuel ports in this interrupter was 5 mm.

When the pulse combustor was run with the Mark 2 interrupter it was found that the running was very rough and the combustor ceased to resonate a few seconds after the compressed air supply was switched off. It appeared that the reason for this was that when the nozzle port was opened to the nozzle drain (Figure 3.17(b)) the fuel line was drained excessively. As a result air was entrapped in the nozzle fuel line. This affected the fuel flow through the nozzle for the next cycle. This was confirmed by manually moving the spool from right to left. As the nozzle port was connected to the pump port a squirting noise was heard and the fuel spray was formed after some delay. The squirting sound and the delay in the spray formation were, presumably, because of the air trapped in the fuel line. This led to the rough running and ultimately the blowout of the pulse combustor.

To cope with the excessive draining of the nozzle fuel line a delivery, or drawback, valve was designed as shown in Figure 3.19. This valve was similar to the delivery, or drawback, valve located between the fuel injection pump and the fuel injector in a diesel engine and served the same purpose i.e. to prevent dribbling from the fuel nozzle. As shown in Figure 3.20 this delivery valve was located between the interrupter and the fuel nozzle. The spring loaded valve acted as a non-return valve. When the nozzle port was connected to the fuel port the valve lifted off its seat (Figure 3.21(a)) to uncover the fuel holes. This allowed the fuel to flow to the nozzle. The valve stayed in the open position until the nozzle port was connected to the nozzle drain port. At this point, the reduction in pressure in the fuel line between the interrupter and the delivery valve and the force of the delivery valve spring combined to return the valve to its seat (Figure 3.21(c)). Figure 3.21(b) shows the intermediate position of the delivery valve, on its way back to the closed position, just as the fuel holes in it were covered. Any further displacement of the delivery valve from this position to its closed position caused a sudden drop in pressure in the fuel line between the delivery valve and the nozzle. This helped prevent the dribbling of the nozzle without getting any air trapped in the nozzle fuel line. The actual mounting of the Mark 2 interrupter on the pulse combustor is shown in Figure 3.22. Figure 3.23 shows the close up of the Mark 2 interrupter equipped with the delivery valve.

3.3.4.3 *Mark 3 Interrupter: Details and Set up*

The cross section of the Mark 3 interrupter is shown in Figure 3.24. This interrupter differed from the Mark 2 interrupter in that it had no fuel return port. The advantage of this was that the total spool displacement required to uncover and cover the different fuel ports was reduced from 5 mm for the previous interrupter to 2 mm for this interrupter. Figure 3.25(a) shows the fuel flow path when there was vacuum in the combustion chamber of the pulse combustor. Figure 3.25(b) depicts the fuel flow path when the pressure in the combustion chamber rose above atmospheric pressure. In this configuration the fuel from the nozzle was diverted to the nozzle drain.

3.4 STARTING AIR SYSTEM

To initiate combustion in the pulse combustor compressed air had to be used. Figure 3.4 shows the schematic of the compressed air supply for the carburettor fuel system. The air supply was taken from the laboratory compressed air line. The compressed air served two functions. The air supply going to the emulsion nozzle helped to induce the flow of the fuel rich mixture from the carburettor and spray it into the combustion chamber. The two additional air jets supplied compressed air to dilute the fuel rich mixture from the carburettor and initiate its combustion. For the high and low pressure steady flow fuel injection and the fuel interrupter systems only the two additional air jets shown in Figure 3.4 were used.

3.5 IGNITION SYSTEM

The energy required to initiate combustion was supplied with the help of an automotive spark plug. A step up transformer that generated 10 kV in the secondary coil was used. The main supply of 110 volts A.C. and 60 Hz was connected to the primary side of the transformer. A high tension cable, capable of withstanding temperatures up to 200°C, was used to connect the secondary coil of the transformer to the spark plug thereby supplying a spark at the mains frequency of 60 Hz. The whole circuit was grounded by connecting a wire from the pulse combustor frame to the metal casing of the transformer.

3.6 THRUST MEASUREMENT

The thrust produced by the combustor on both the inlet and tail pipe sides was measured by thrust meters. The thrust meters worked on the principle of conservation of momentum. Morzouk (53) has provided a theoretical justification for using thrust meters for the static thrust measurement. Figure 3.26 shows the thrust measuring equipment for the tail pipe. A similar arrangement was used for the inlet pipe of the combustor. The combustor was not provided with any flow rectification device to turn the inlet backflow downstream.

The following equation was used to measure the thrust produced by the pulse combustor.

$$\frac{T}{x} = \frac{W}{y}$$

where,

T = thrust produced, N

W = weight of the thrust plate, N

y = length of the chains suspending the thrust plate from the frame, mm

x = displacement of the thrust plate, mm

At the start of the experiments the displacement of the thrust plate was measured by a pointer that moved over a scale. The disadvantage of this arrangement was that as there was no damping in the system the pointer oscillated about its mean position. Additionally, it was cumbersome for a single operator to control the fuel flow rate and read the displacement from the scale at the same time.

To counteract these problems a position transducer was used to measure the displacement of the thrust meter (Figure 3.26). The position transducer was capable of measuring displacement up to 254 mm with an accuracy standard of ± 0.15% full scale and a resolution of 0.008% full scale. In addition it was capable of withstanding vibrations from 10 to 2000 Hz without a change in calibration and damage. The transducer cable was attached to the pointer and provided an initial tension of 7.5 newton. This initial tension acted as an effective damper and damped the oscillations of the thrust plate during thrust measurement. An input excitation voltage of 10 volts d.c. was fed into the transducer. The unit provided a voltage output of 3.713 mV/(V.mm) by means of a precision potentiometer. The output voltage could be either read on a 88000A digital multimeter or fed into a Fluke 2200B datalogger to obtain a print-out.

3.7 EXHAUST GAS ANALYSIS

The concentrations of CO, CO_2 and O_2 in the inlet and tail pipe of the pulse combustor were measured by the Beckman Model 804 infrared and paramagnetic analyzers shown in Figure 3.27. Figure 3.28 shows the schematic of the equipment used to measure the exhaust gas composition. The concentration of the NO_x and unburned hydrocarbons in the exhaust gases could not be measured because of the non-availability of equipment required to measure the same.

The sampling probe was made out of 3.17 mm diameter stainless steel tube. In the end of the sampling tube 28 small holes were drilled. Exhaust gases entered the sampling probe through these holes and were water cooled in a heat exchanger before being fed to the analyzer. N_2 was used for drying the exhaust gases before sampling. The instrument was calibrated using standard samples of CO, CO_2 and O_2.

3.8 PRESSURE MEASUREMENT

The dynamic pressure in the combustion chamber of the pulse combustor was measured with the help of a water cooled Kistler model 601B1 piezoelectric transducer. The pressure transducer was inserted into the first boss welded on the combustion chamber (Figure 3.1). When the pressure measurement was not required this boss was plugged with a spark plug. The charge from the transducer was fed via a low noise cable to a Kistler model 504A charge amplifier and subsequently to a Tektronix 5223 digital oscilloscope. The data from the oscilloscope was recorded by a Hewlett Packard 7004B X-Y plotter. The pressure transducer was water cooled to protect it from the temperature within the combustion chamber. A safety device was incorporated in the water circuit that ensured the cut-off of the fuel supply to the combustor in the event of a cooling water circuit failure. This device consisted of a reed switch strapped on the outside of a copper pipe. Water that cooled the transducer was drained via this copper pipe. The flow of water caused a magnetic ball in the pipe to float and close the reed switch thereby opening the solenoid valve that supplied fuel to the nozzle. In the event of a breakdown in the water circuit the magnetic ball stopped floating in the copper pipe leading to the opening of the reed switch and the shutting off of the solenoid valve. This provided an effective safety circuit to safeguard against the heating up of the pressure transducer in case the water cooling circuit broke down.

NOZZLE RATING AT 689 kPa(g)	276 kPa(g)	414 kPa(g)	552 kPa(g)	827 kPa(g)	965 kPa(g)	1103 kPa(g)
3.0	1.90	2.33	2.69	3.29	3.55	3.80
4.0	2.51	3.07	3.55	4.37	4.70	5.05
5.0	3.15	3.85	4.45	5.46	5.90	6.30
6.0	3.78	4.63	5.35	6.56	7.10	7.60
7.0	4.40	5.39	6.22	7.65	8.25	8.85
8.0	5.02	6.19	7.10	8.75	9.43	10.1

Table 3.1: Effect of pressure on nozzle flow rate (nozzle flow rate in gallons per hour)

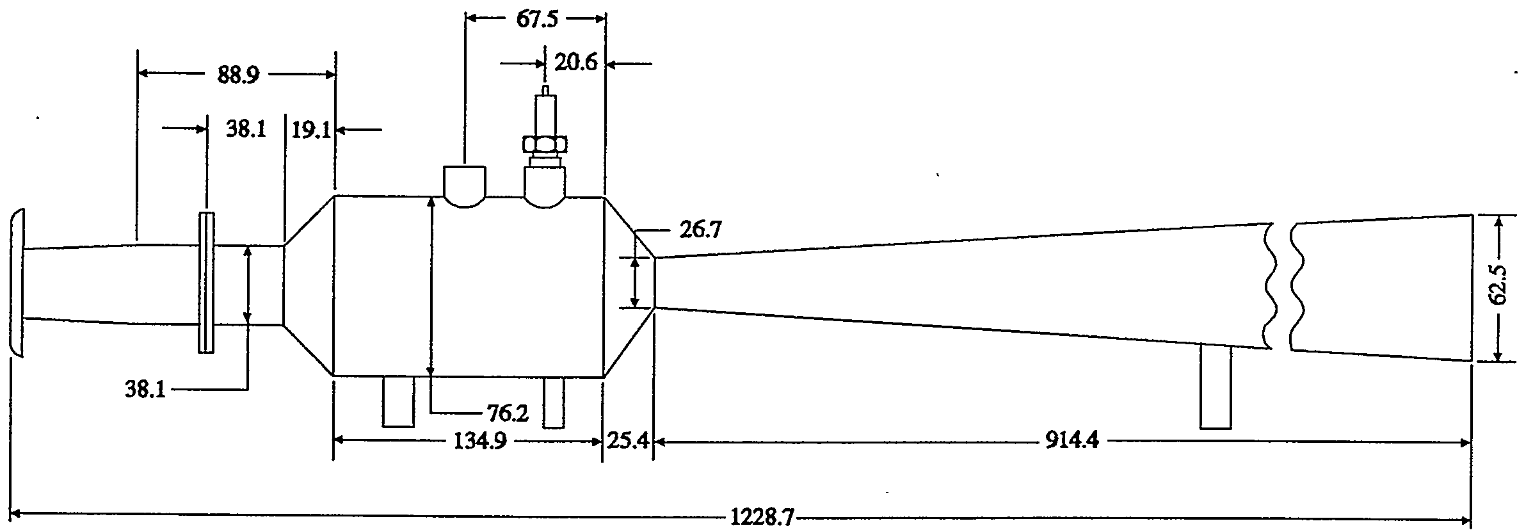

Figure 3.1: The pulse combustor (all dimensions in mm)

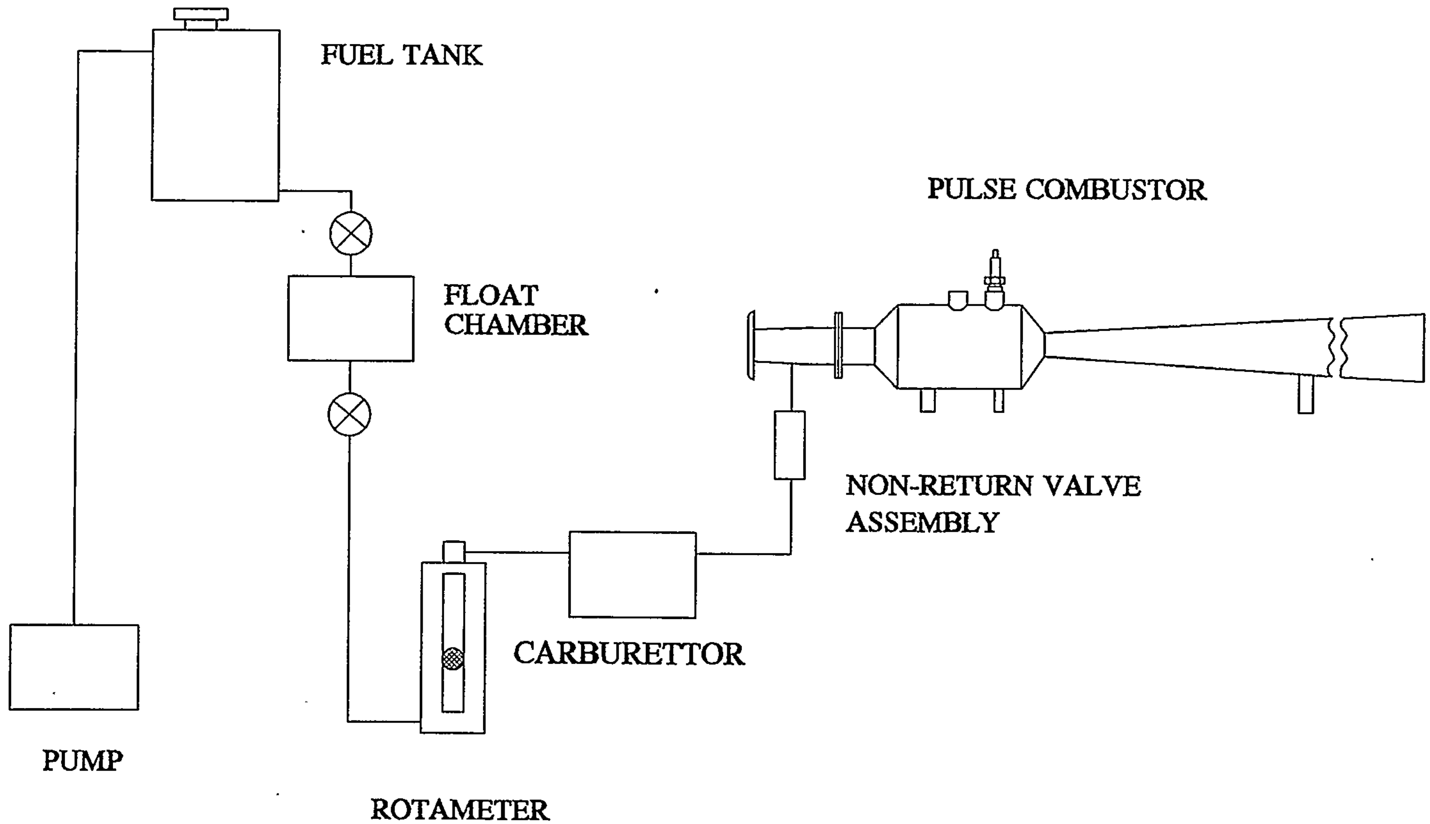

Figure 3.2: Schematic of the fuel system for the carburettor

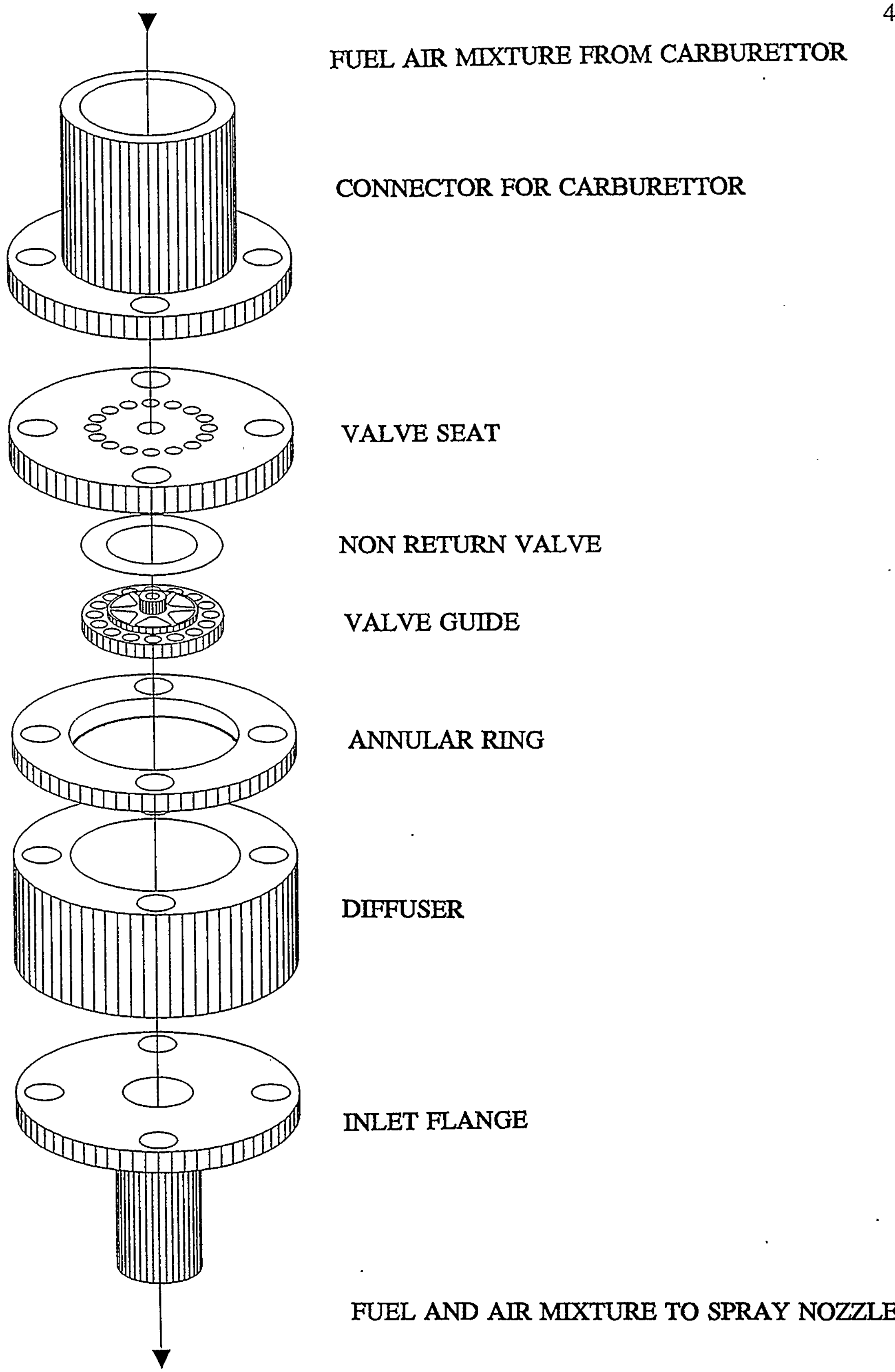

Figure 3.3: Non return valve assembly

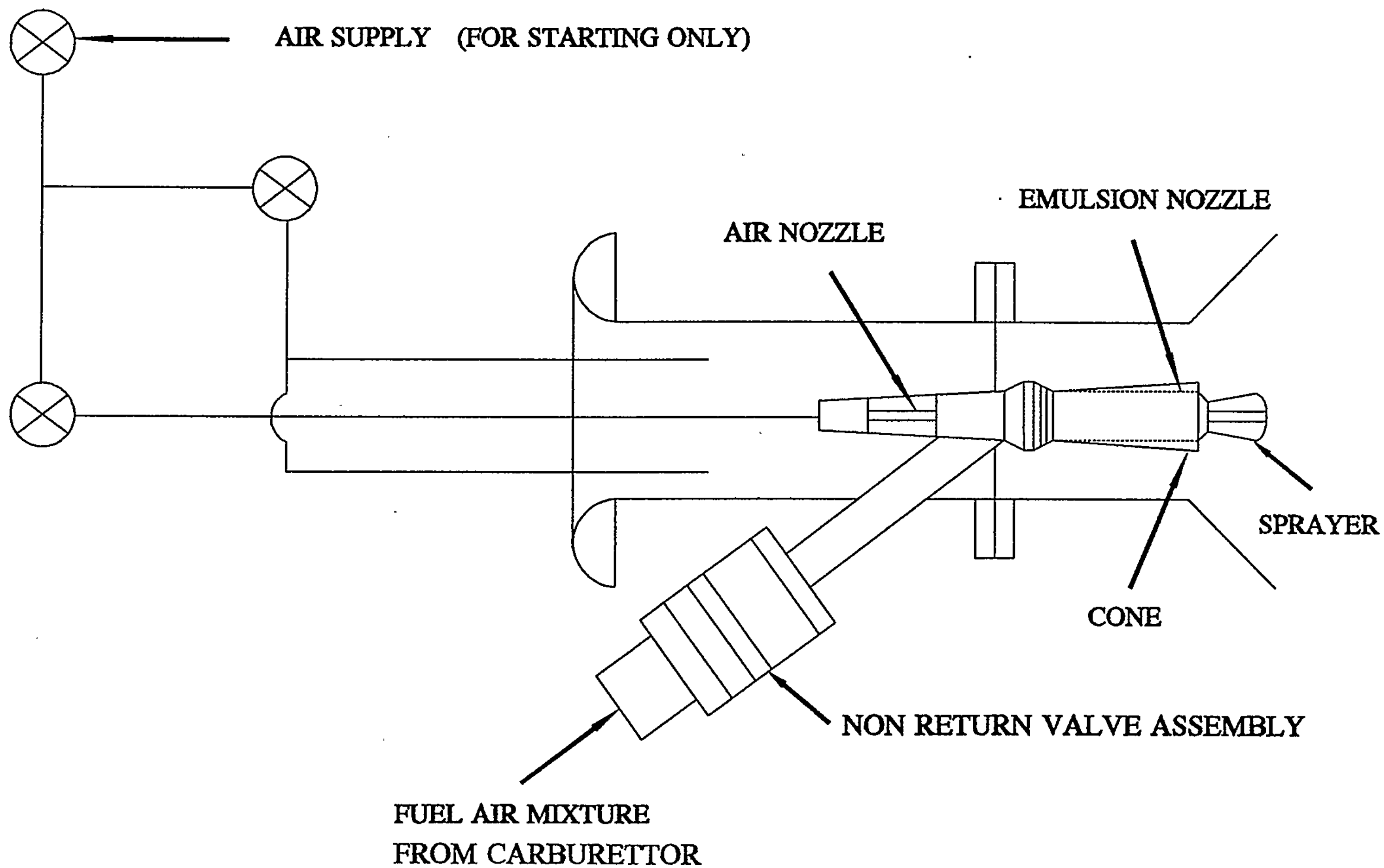

Figure 3.4: Fuel spraying and starting air system

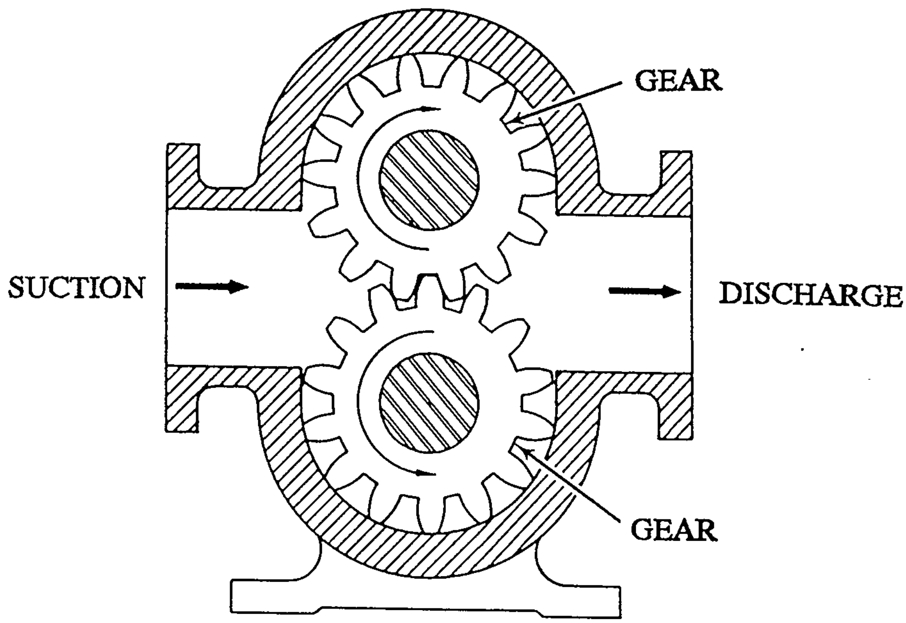

Figure 3.5: Cross section of a basic gear pump

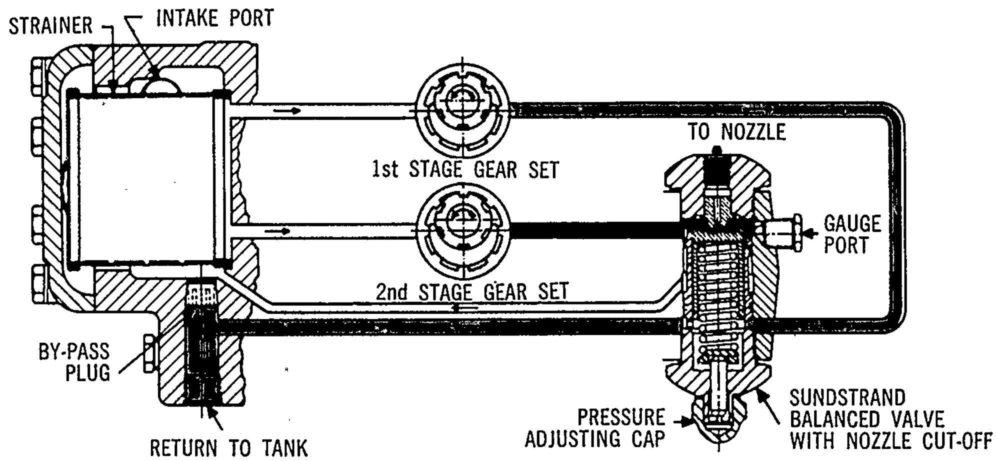

Figure 3.6: Circuit diagram for the two stage gear pump

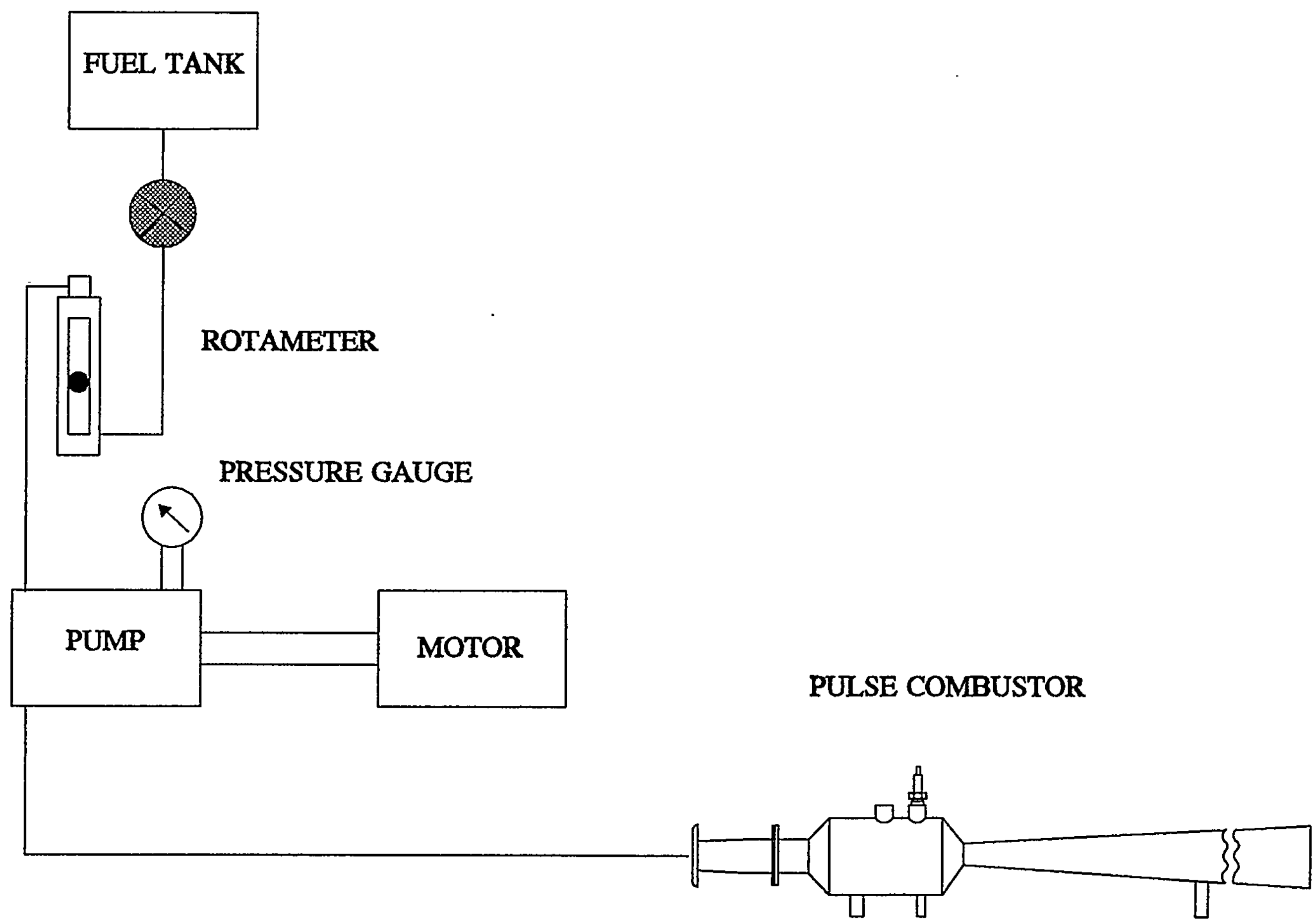

Figure 3.7: Schematic of the fuel setup for the high pressure steady flow fuel injection system

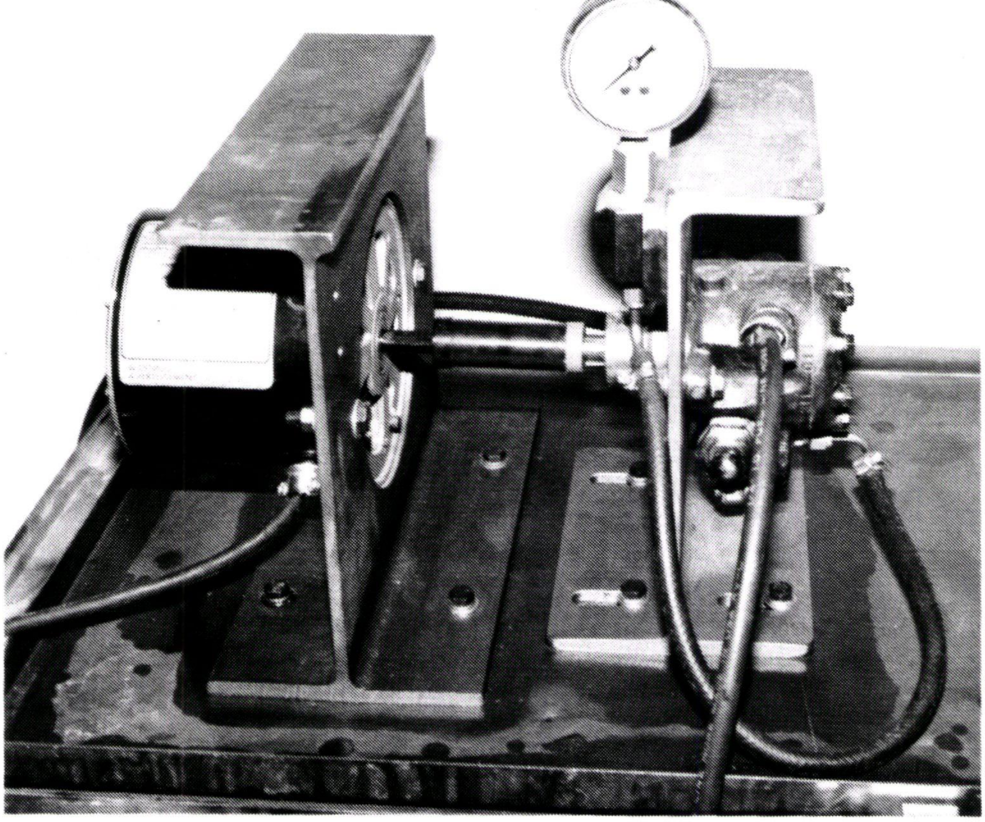

Figure 3.8: Set up of the gear pump and electric motor

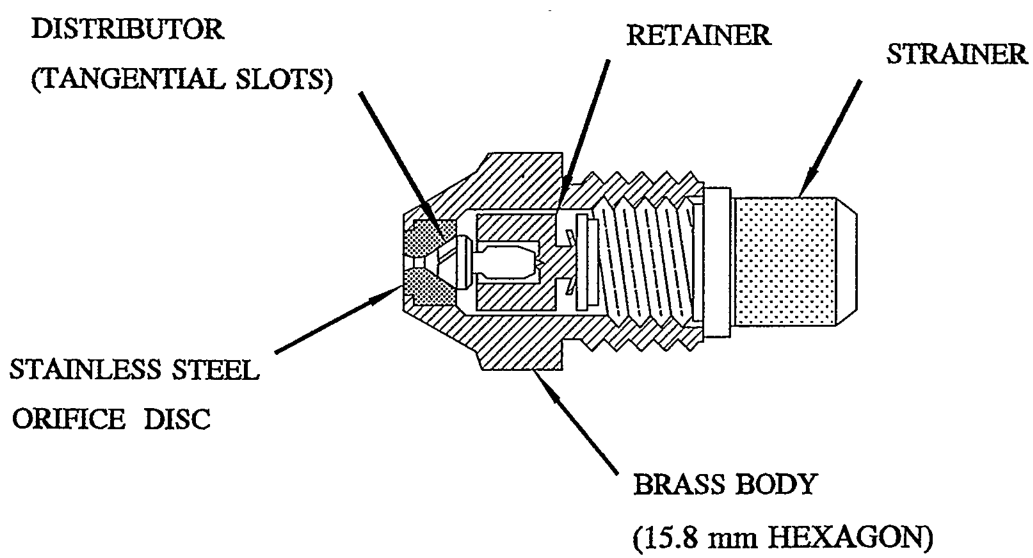

Figure 3.9: Cross section of the fuel nozzle

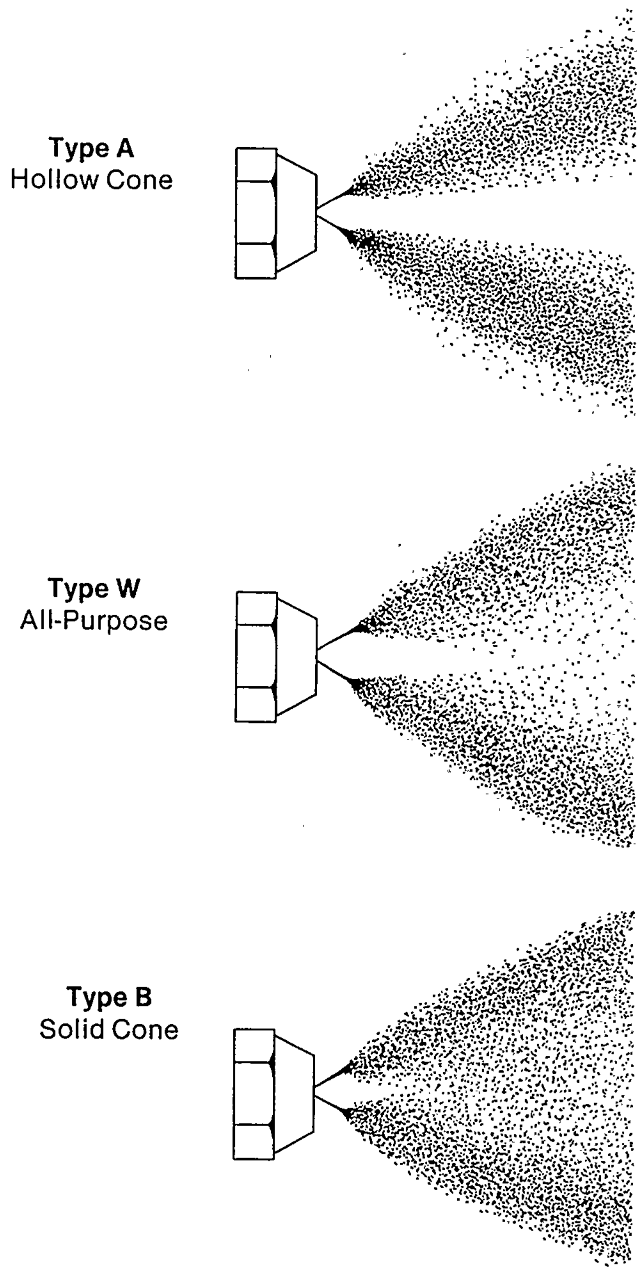

Figure 3.10: Spray pattern produced by fuel nozzle types A, W & B

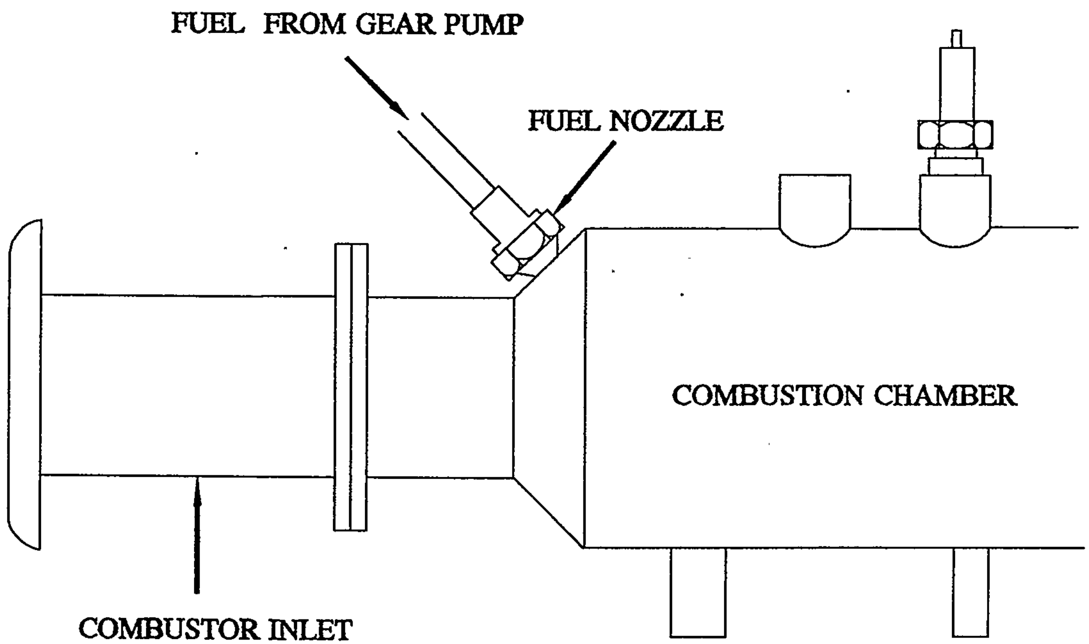

Figure 3.11: Unsuccessful location of the fuel nozzle in the combustion chamber

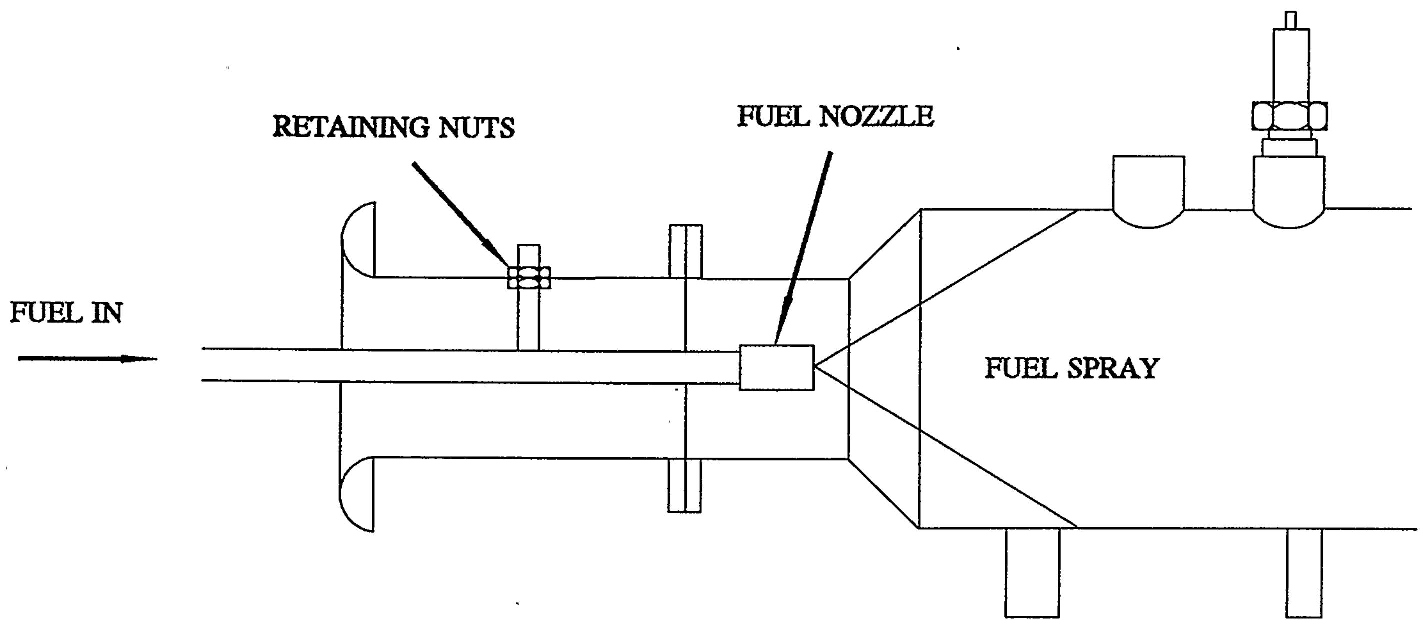

Figure 3.12: Successful location of the fuel nozzle in the combustion chamber

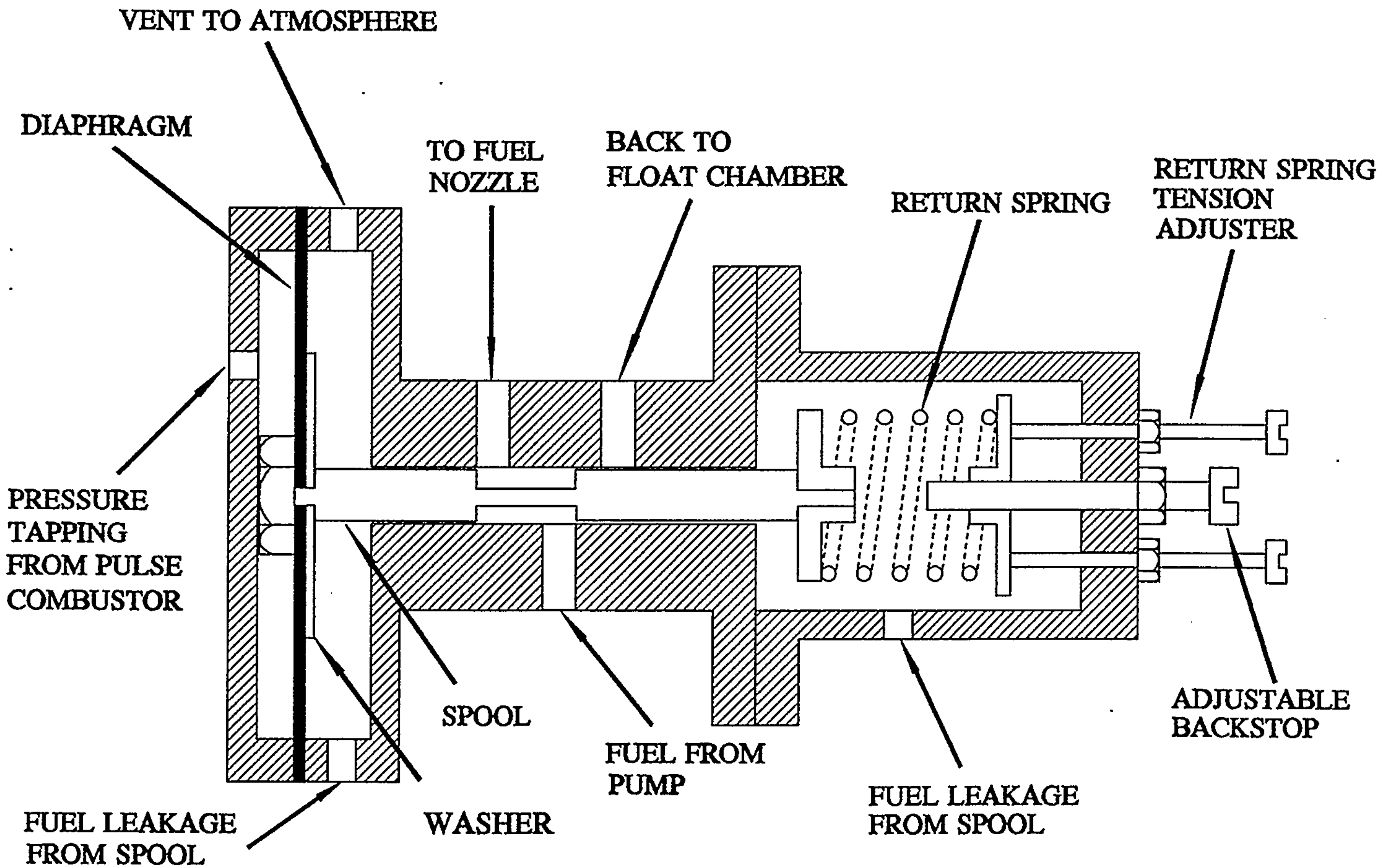

Figure 3.13: Cross section of Mark 1 interrupter

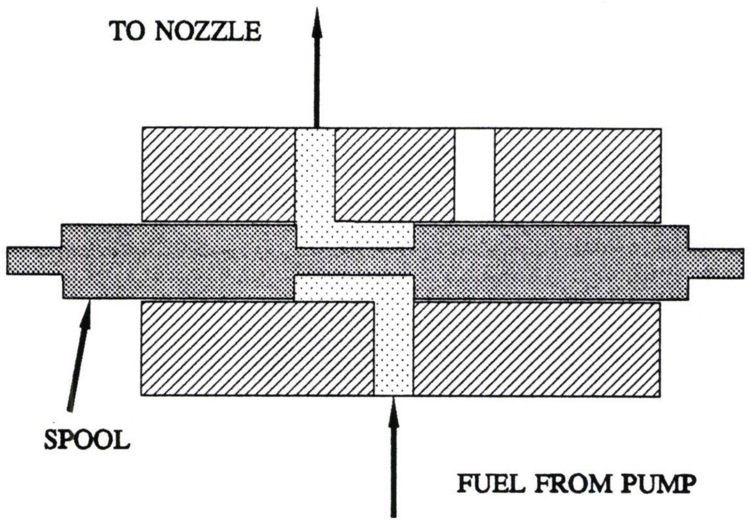

(a) Fuel from pump to the fuel nozzle

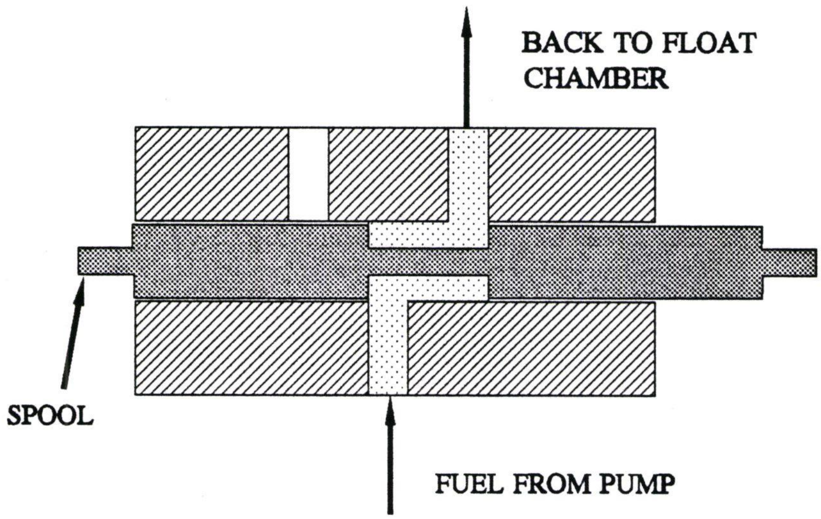

(b) Fuel from pump diverted back to float chamber

Figure 3.14: Working principle of the Mark 1 interrupter

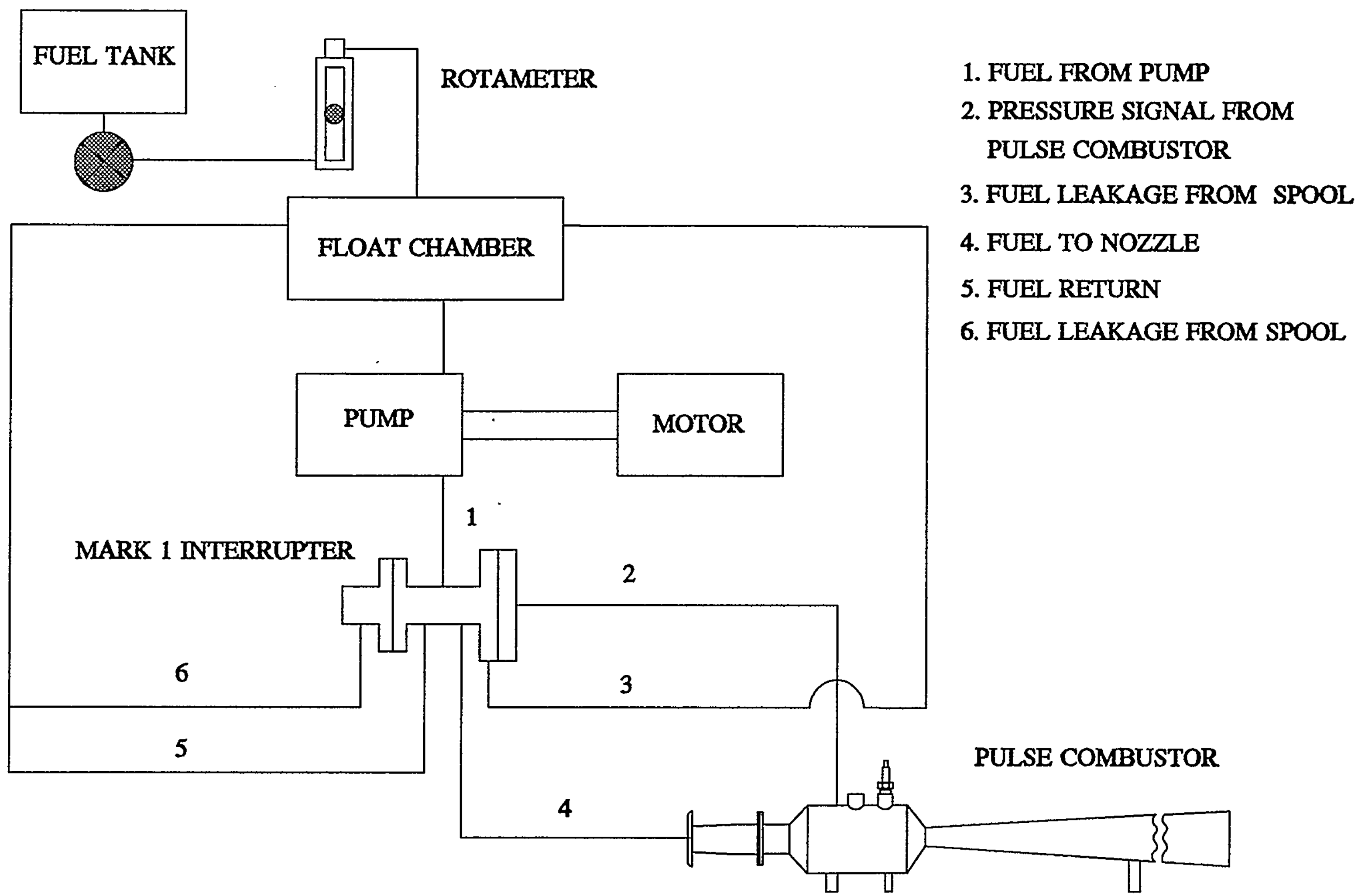

Figure 3.15: Schematic of fuel system for Mark 1 interrupter

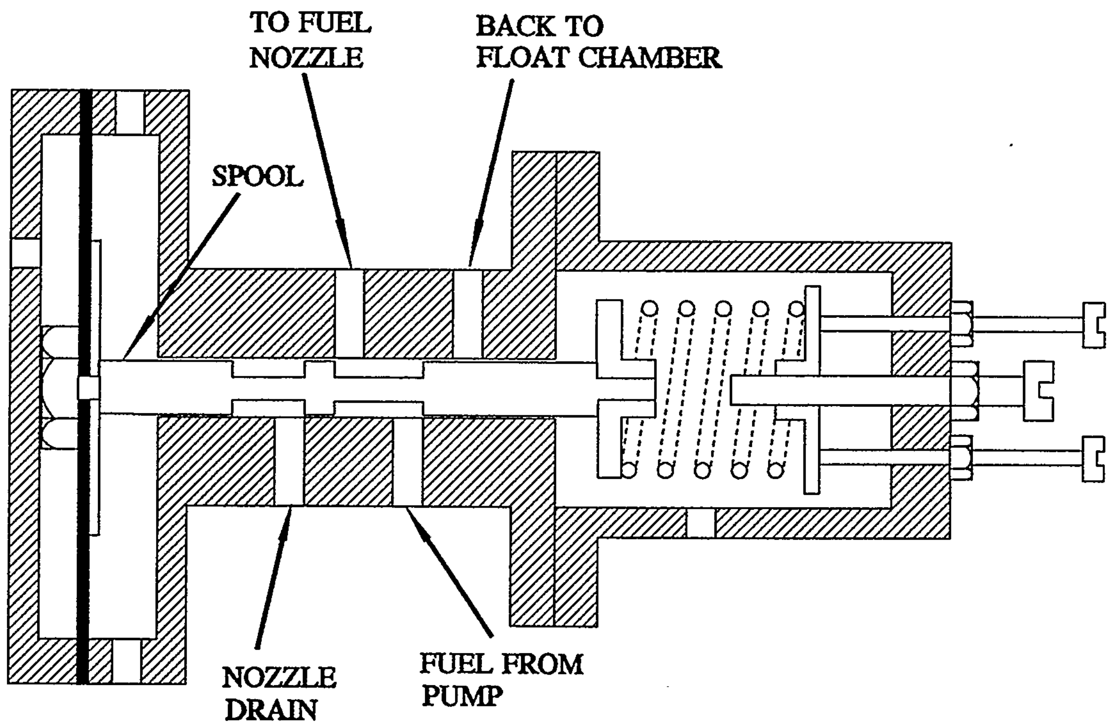

Figure 3.16: Cross section of the Mark 2 interrupter

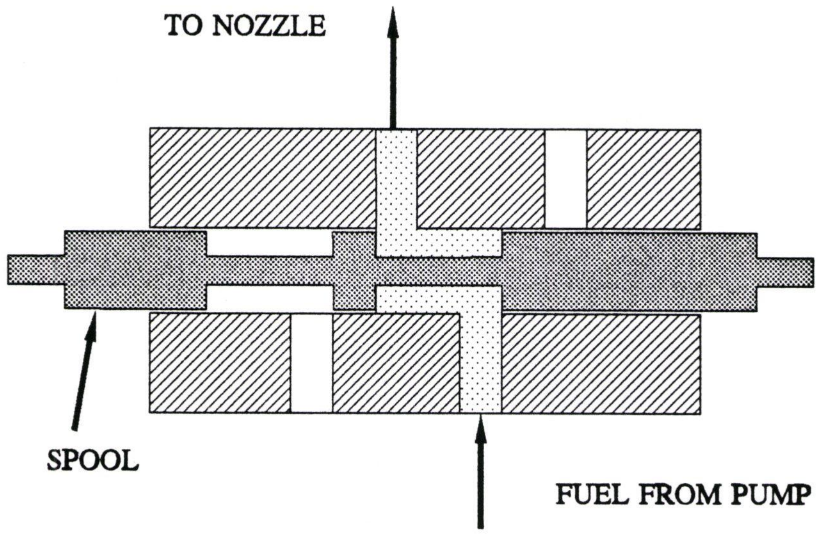

(a) Fuel from pump to fuel nozzle

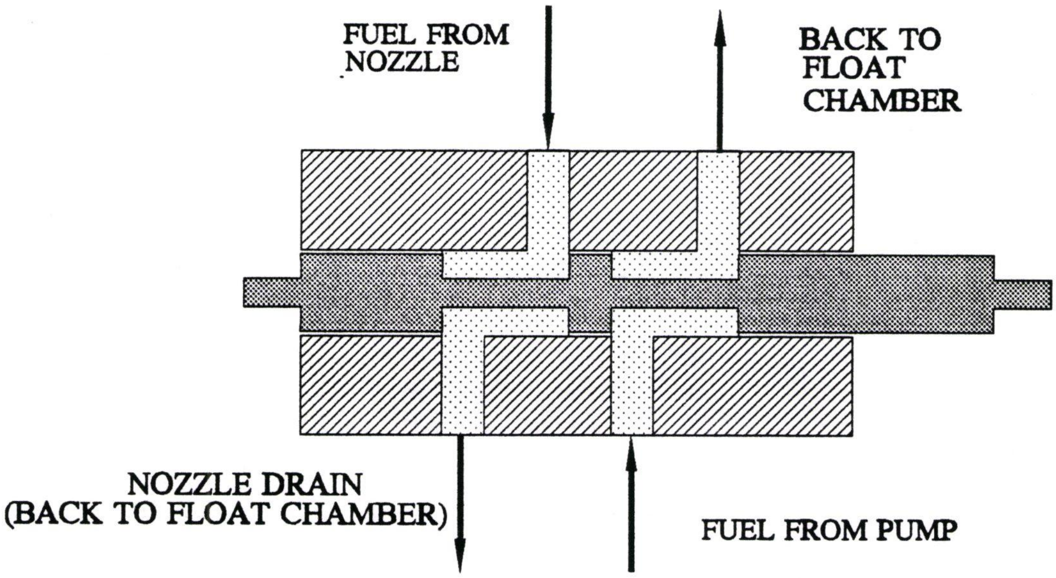

(b) Fuel from pump and nozzle fuel line back to float chamber

Figure 3.17: Working principle of Mark 2 interrupter

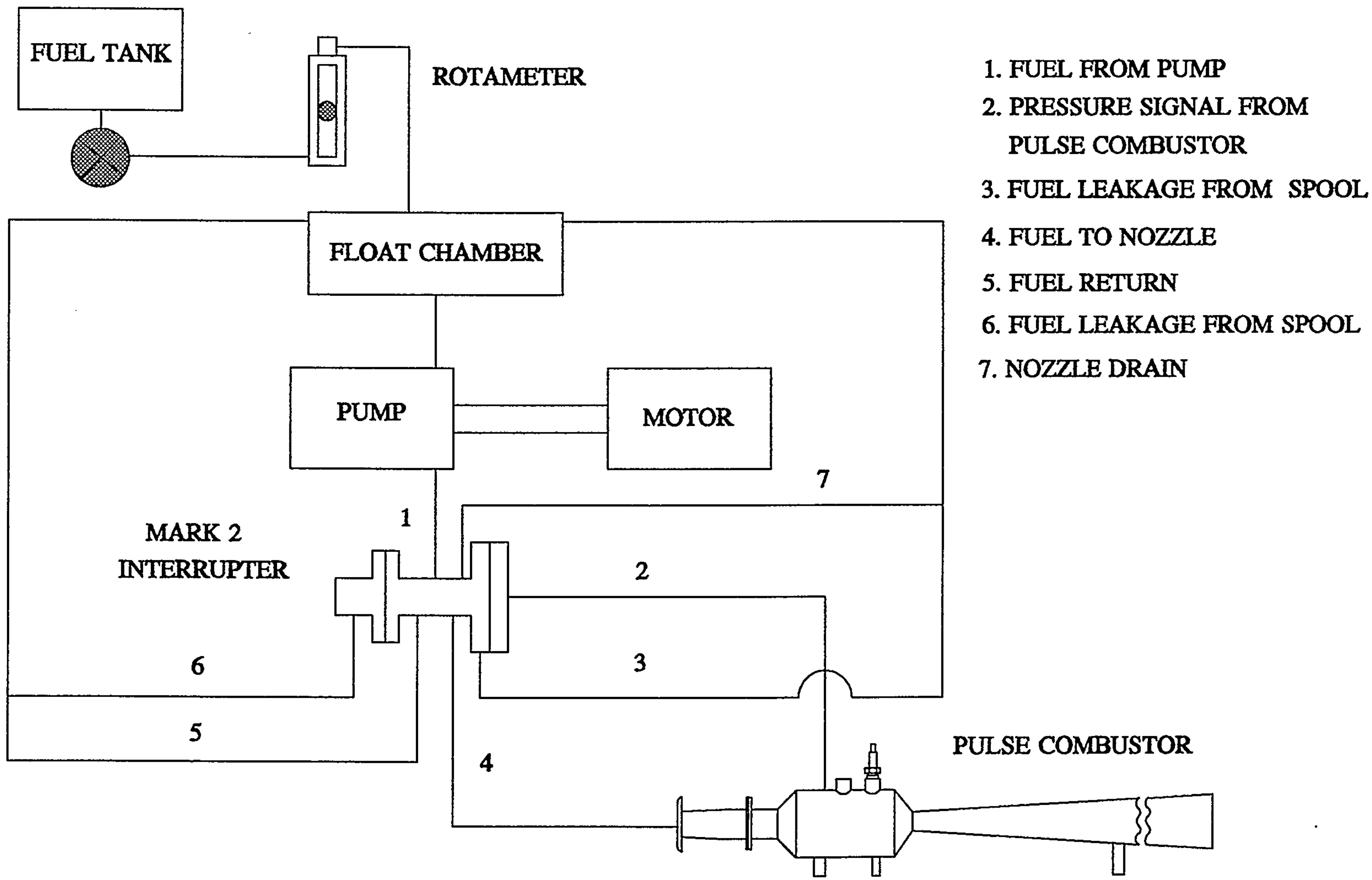

Figure 3.18: Schematic of fuel system for Mark 2 interrupter

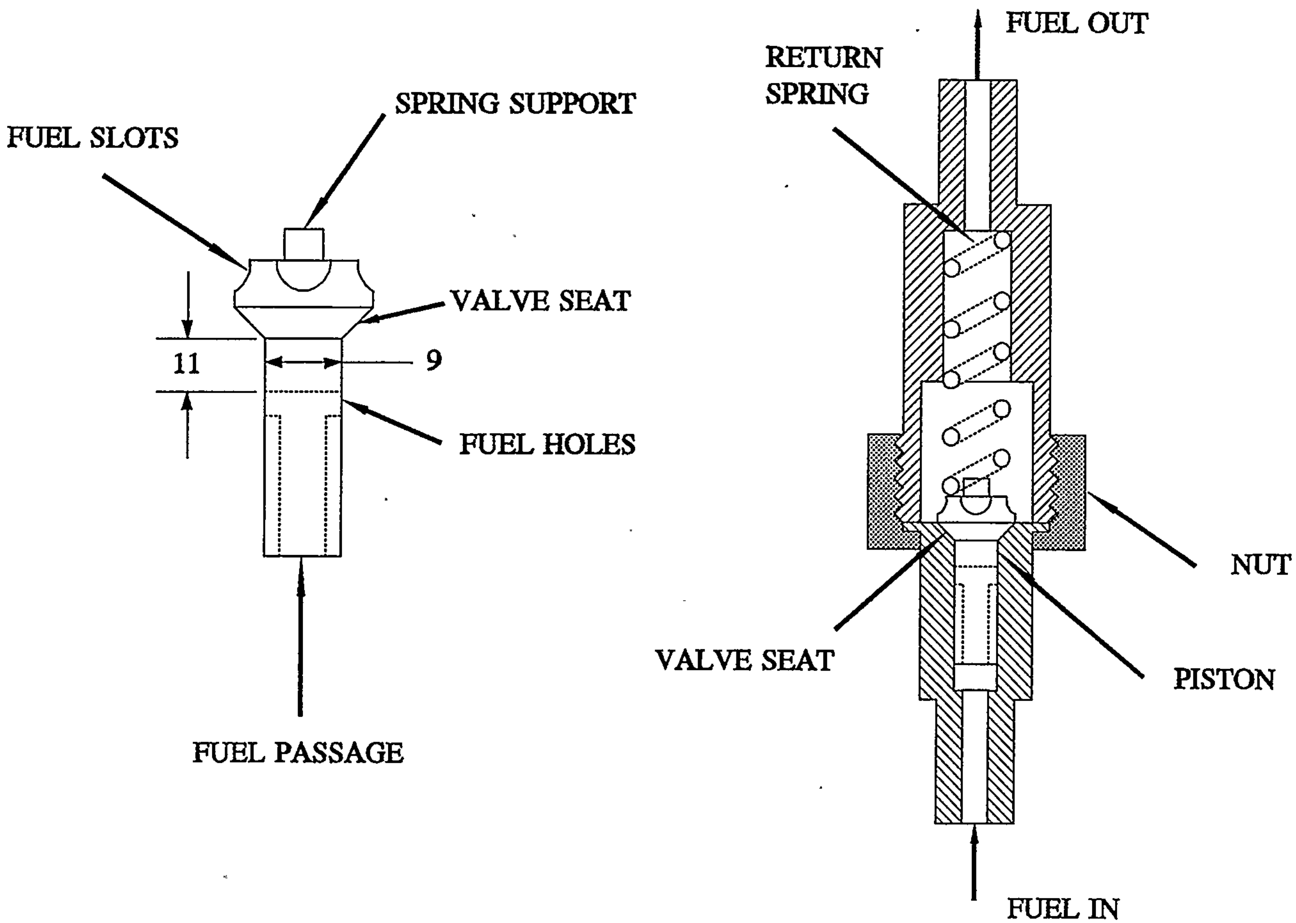

Figure 3.19: Fuel delivery valve used with the Mark 2 interrupter (all dimensions in mm)

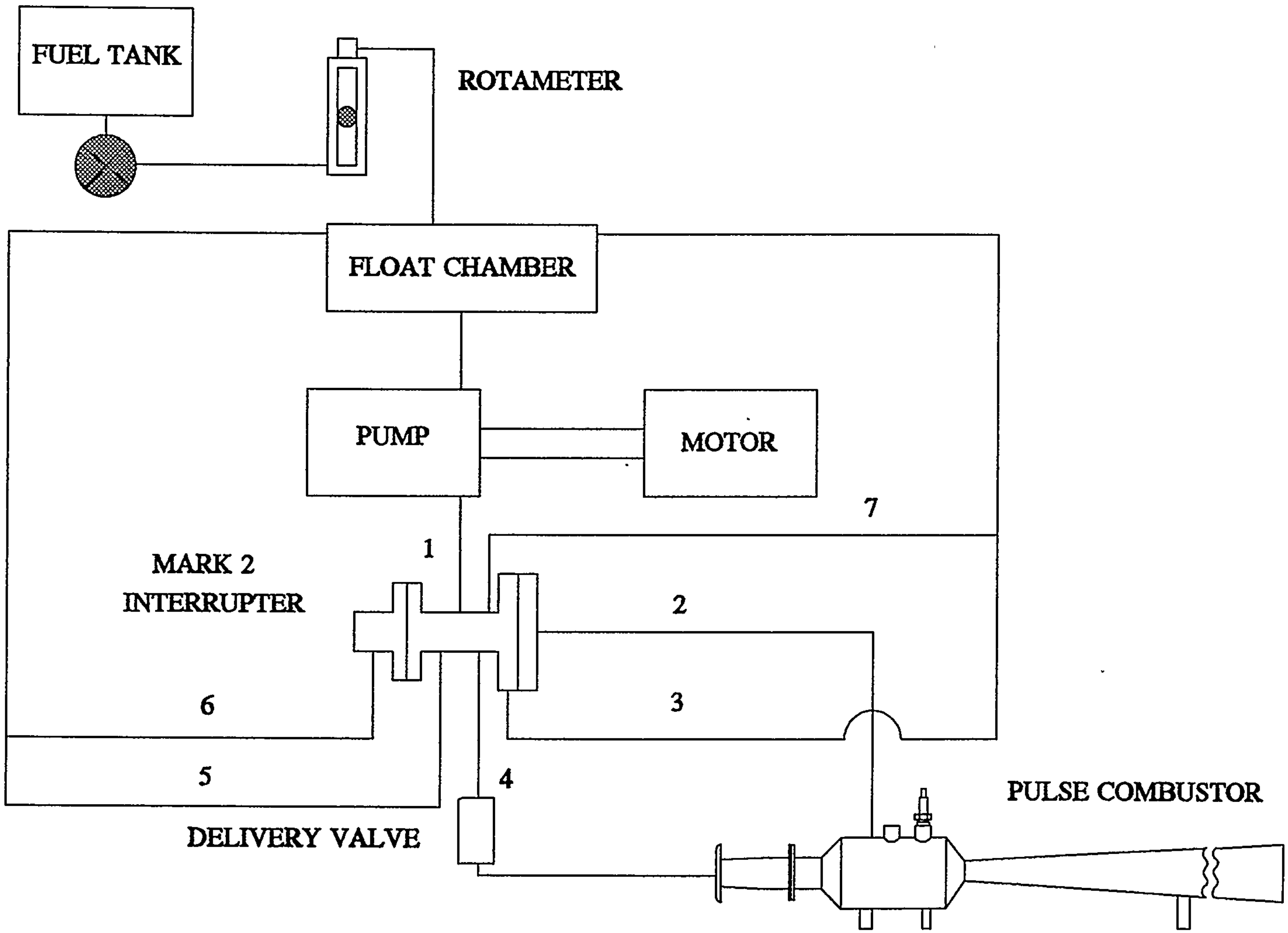

Figure 3.20: Schematic of fuel system for Mark 2 interrupter and delivery valve

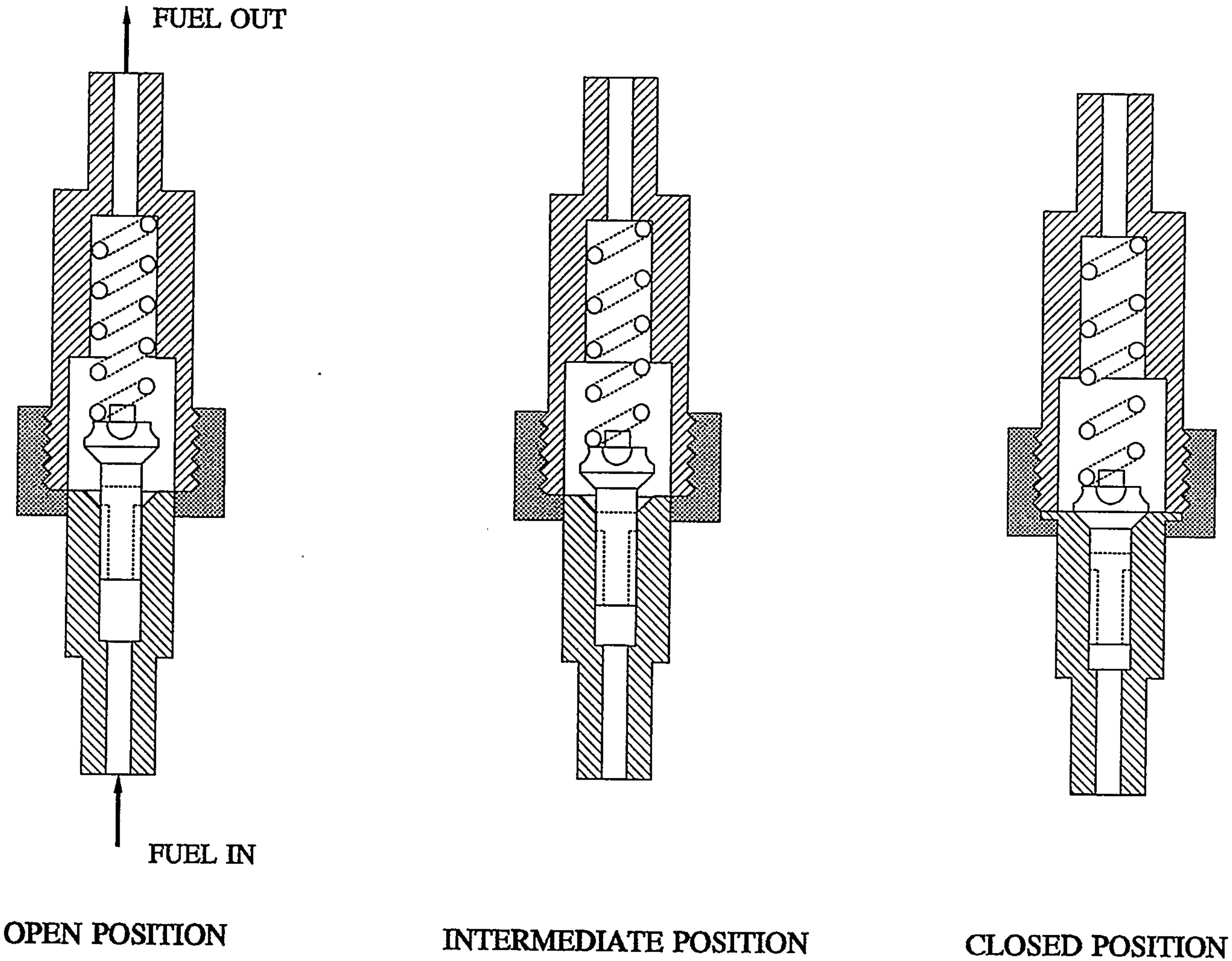

Figure 3.21: Working positions of delivery valve

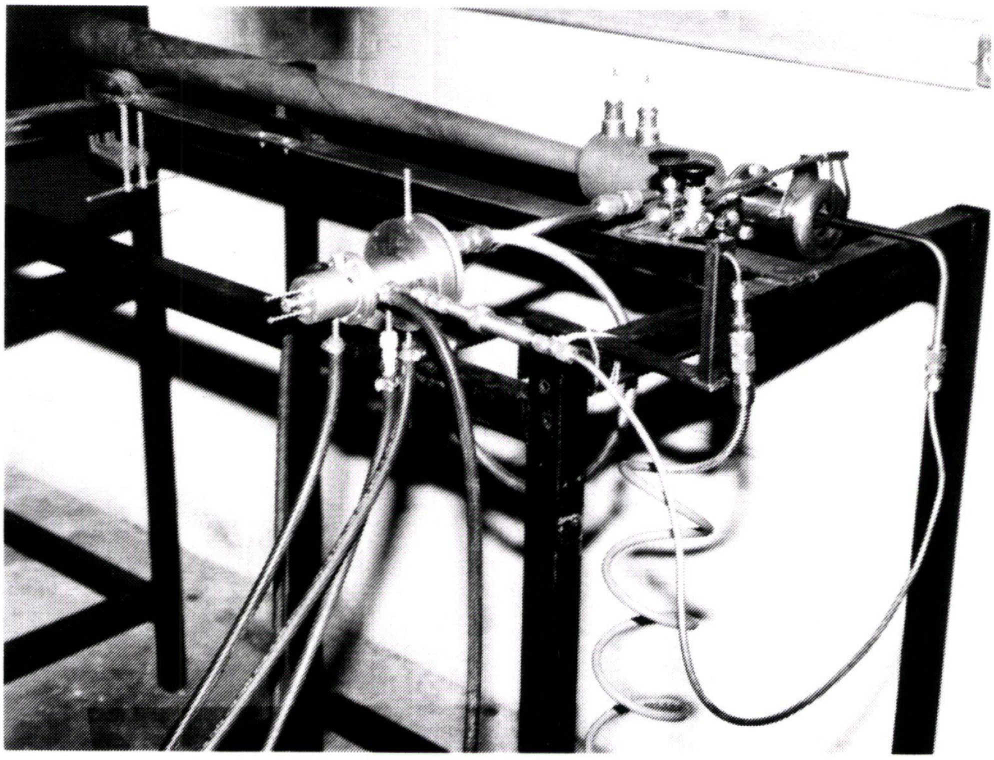

Figure 3.22: Mounting of the Mark 2 interrupter on the pulse combustor

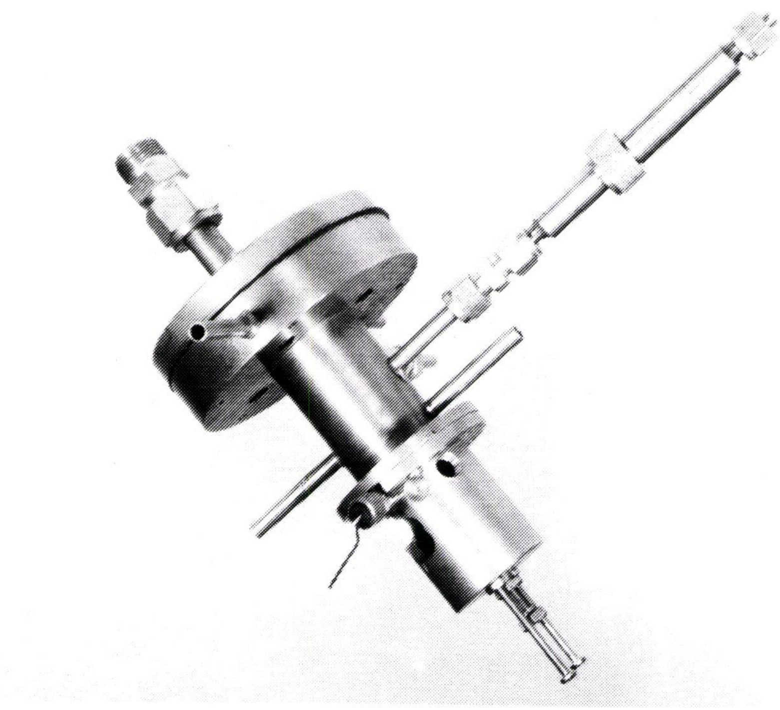

Figure 3.23: Mark 2 interrupter equipped with the delivery valve

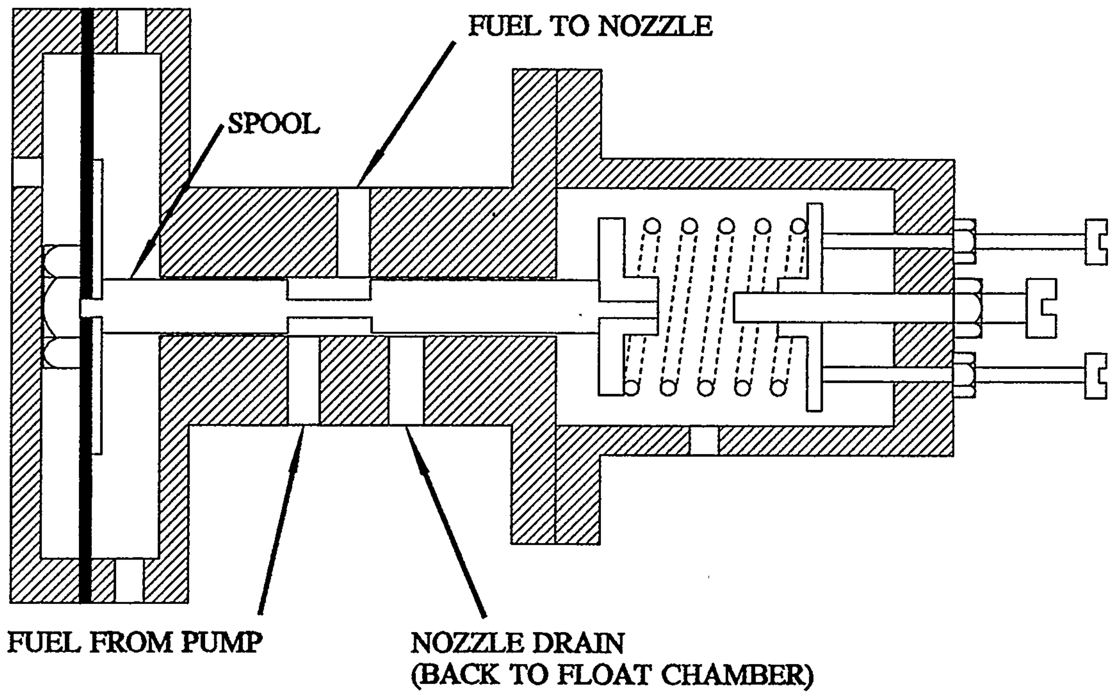

Figure 3.24: Cross section of Mark 3 interrupter

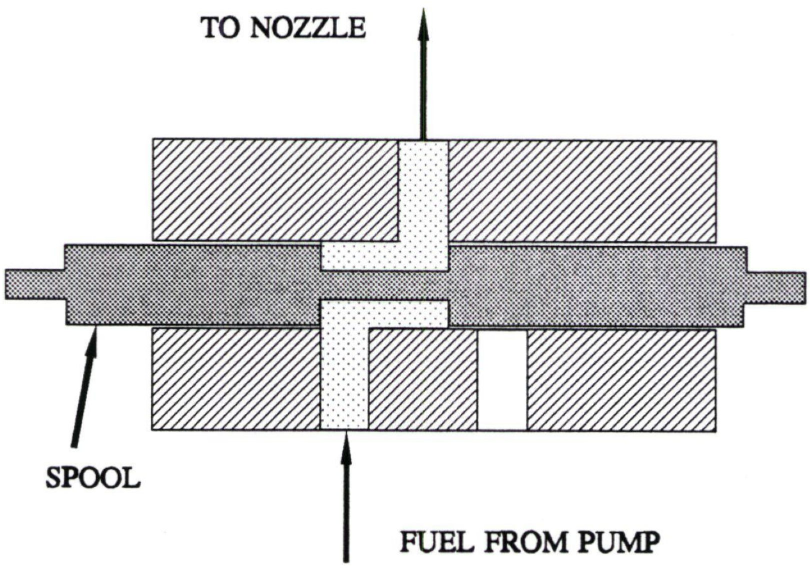

(a) Fuel from pump to fuel nozzle

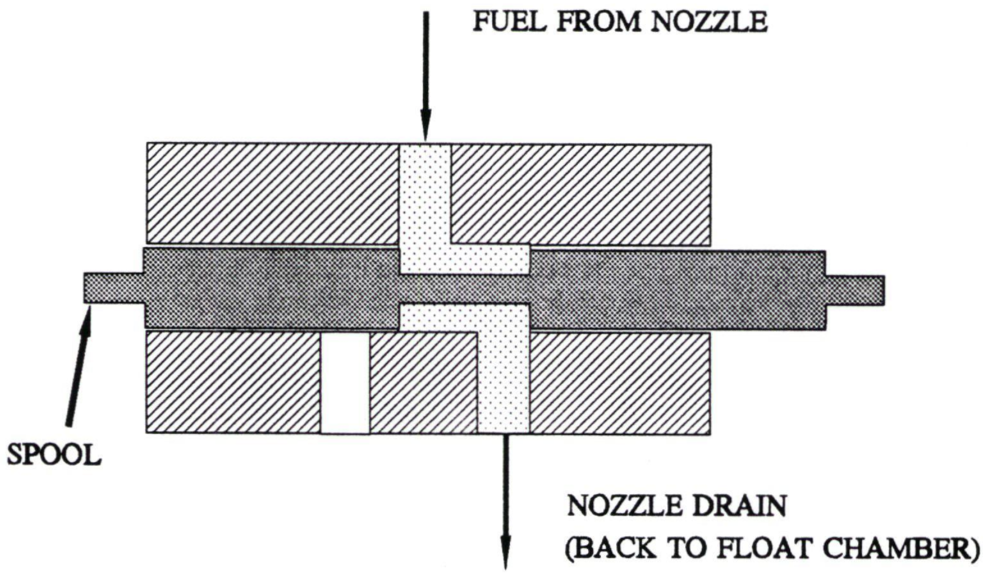

(b) Fuel from nozzle fuel line to float chamber

Figure 3.25: Working principle of Mark 3 interrupter

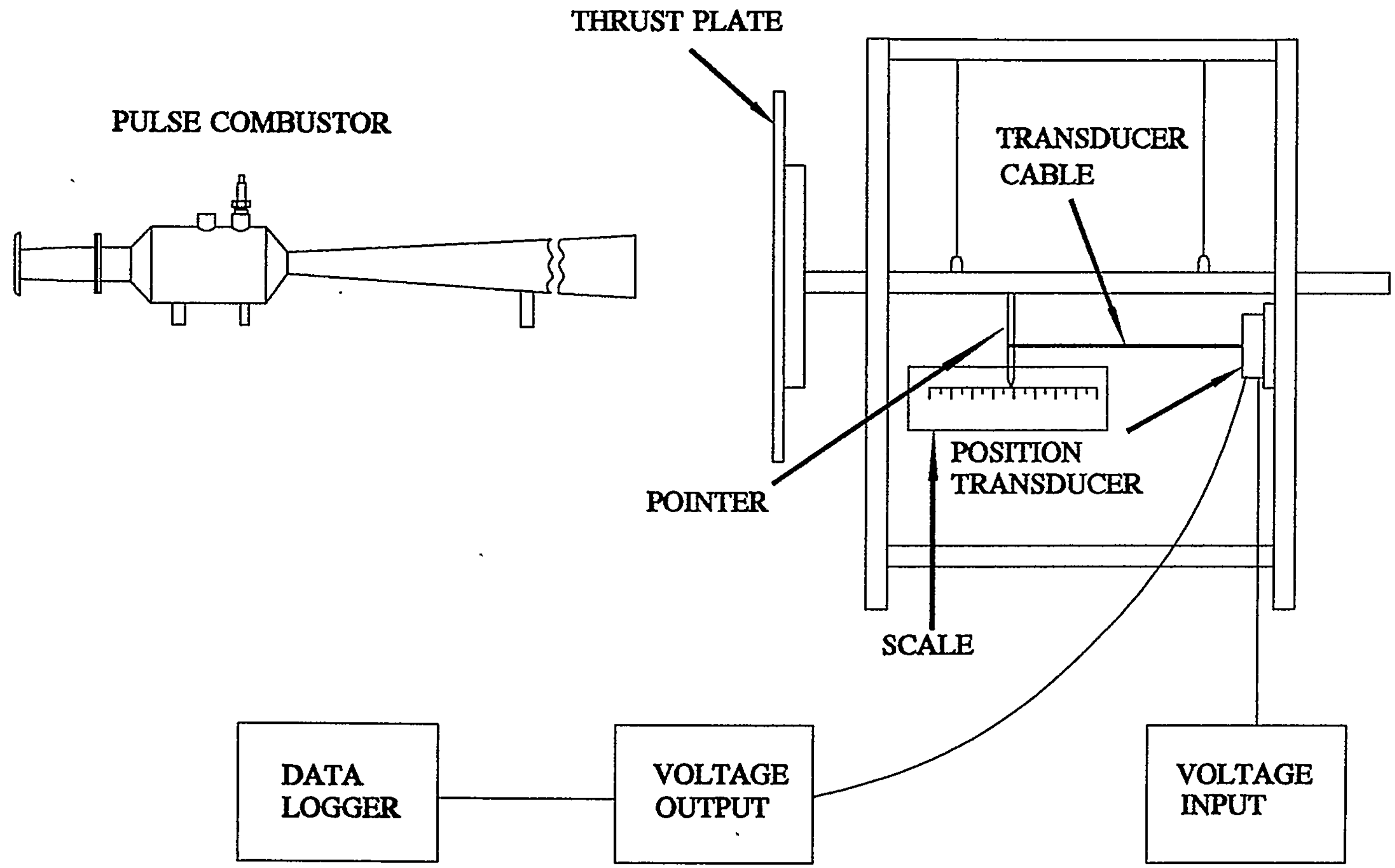

Figure 3.26: Schematic of the thrust measuring equipment

Figure 3.27: The Beckman Model 804 infrared and paramagnetic analysers

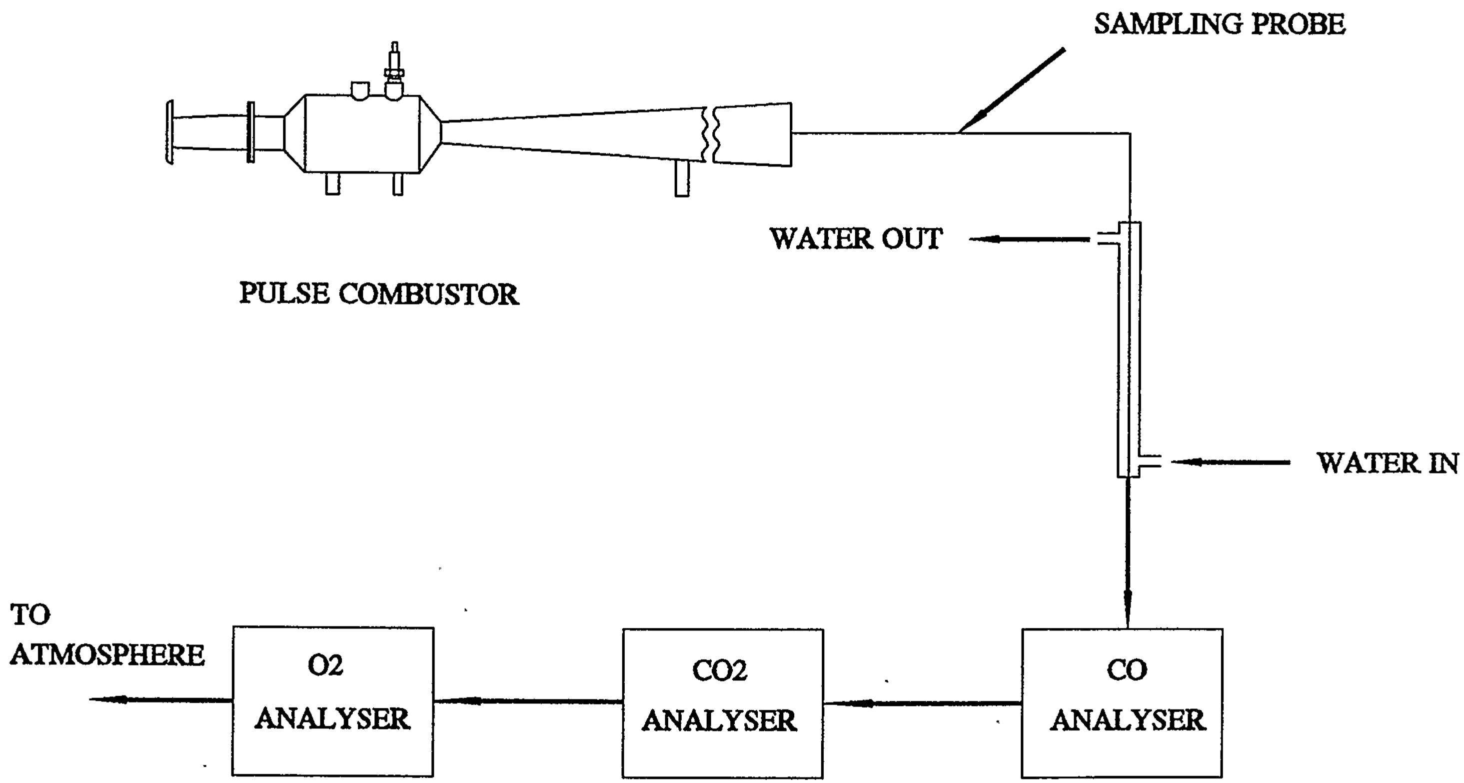

Figure 3.28: Schematic of exhaust gas analysis equipment

CHAPTER 4 DYNAMIC ANALYSIS OF CARBURETTOR AND MARK 1 INTERRUPTER FUEL SYSTEMS

4.1 CARBURETTOR

A simple dynamic analysis of the shim steel non-return valve was performed to ascertain whether enough pressure difference was available across the carburettor to move the non-return valve in the time available for valve travel. A similar analysis was performed by Ibrahim (12) for the mylar non-return valve. The valve lift (s) for the carburettors used , i.e. the distance travelled by the shim steel non-return valve, was fixed at 0.61 mm. The non-return valve opened during the recharging (phases 3 and 4 in Figure 1.4) and closed during the outflow (phases 1 and 2 in Figure 1.4) from the pulse combustor.

As can be seen from Figure 6.10, which shows the frequency vs the fuel flow rate of a pulse combustor similar to the one used with the carburettor, the frequency of the combustor was approximately 190 Hz. It was assumed that the time interval (t) permitted for the valve to move the required 0.61 mm distance was 10% of the inflow or the outflow process.

$$t = \frac{1}{2 \times 10 \times 190} = 2.6 \times 10^{-4} \quad s \ = 0.26 \quad ms$$

Assuming the acceleration (a) of the valve to be uniform

$$s = u \cdot t + \frac{1}{2} \cdot a \cdot t^2$$

where,

u = initial velocity of the non-return valve

at $\quad t = 0, \qquad u = 0$

therefore,

$$a = \frac{2 \cdot s}{t^2}$$

Let F be the force acting on the valve to produce this acceleration

$$F = m \cdot a = \Delta p \cdot A$$

$$m = \rho \cdot A \cdot x$$

where,

m = mass of the valve (kg)

Δp = pressure difference across the valve (Pa)

A = area of valve (m^2)

x = valve thickness (m)

ρ = density of valve material (kg/m^3)

therefore,

$$\Delta p = \frac{2 \cdot s \cdot x \cdot \rho}{t^2}$$

Taking the density (ρ) of the shim steel valve as 7500 kg/m^3 .

Hence evaluating Δp,

$$\Delta p \ = \ 1.35\times10^5 \cdot x \quad \text{kPa}$$

The pressure differences required across the carburettor for various valve thicknesses were calculated using the above equation. The calculated values are tabulated in Table 4.1. Also shown are the pressure differences required to drive the mylar non-return valves of various thicknesses. The mylar material used had the same density as that of water.

As can be observed from Table 4.1 the pressure difference required across the carburettor was much higher for the shim steel valve than for the mylar valve of the corresponding thickness because of the significant difference in the density of the two materials. Figure 4.1 shows a combustion chamber pressure vs time plot obtained using a 4.0, 70°A nozzle with high pressure steady flow fuel injection system. The pulse combustor used for this run was the same as that used with the carburettor fuel system. The plot is representative of the typical pressure variations found in this type of pulse combustor. Because of the temperature drift of the pressure transducer the atmospheric pressure line could not be plotted with certainty. As an approximation it was taken that 62% of the cycle time was spent below atmospheric pressure (10). It can be seen that the peak to peak pressure fluctuations was 74 kPa. The positive and negative pressure (above and below atmospheric pressure) available were 48 kPa and 26 kPa respectively. The pressure difference available across the carburettor was dictated by the minimum of the above two pressures i.e. the negative pressure.

When the negative pressure of 26 kPa is compared with the pressure difference required to drive the thicker shim steel valves (Table 4.1) it can be seen that the negative pressures available became gradually insufficient for the proper operation of the shim steel valve as its thickness was increased. This was probably the reason for the rough running of the pulse combustor as the shim steel valve thickness became greater than 0.0762 mm. This is discussed in detail in section 5.3.1 of Chapter 5.

4.2 Mark 1 Interrupter

The function of the interrupter system was to supply the fuel to the pulse combustor intermittently i.e. the fuel was to be injected when the combustion chamber pressure fell below atmospheric pressure and shut off when the pressure rose above atmospheric pressure. To meet this condition the phasing of the fuel supply with the combustion chamber pressure was of prime importance. The only parameter that could be varied to control the phasing of fuel injection was the length of the connector pipe joining the combustion chamber pulse combustor and the diaphragm of the interrupter. The pressure variation in the pulse combustor was sensed by the diaphragm via this connector pipe. By varying the length of the connector pipe the time required for the pressure pulse to travel from the combustion chamber to the diaphragm could be altered. The length of the connector pipe was chosen such that the interrupter worked on the pressure sensed from the cycle previous to the current operating cycle of the pulse combustor. The following calculations were made to determine the approximate connector pipe length required.

Let,

t_1 = time required for the pressure pulse to travel from the combustion chamber of pulse combustor to the diaphragm of the interrupter (ms)

t_2 = time required to displace the spool to open and close the fuel ports (ms)

t_3 = time required for the pressure pulse to travel in the fuel line from the interrupter to the nozzle tip (ms)

Figure 4.1 shows a combustion chamber pressure vs time plot for the high pressure steady flow fuel injections system (4.0, 70°A type fuel nozzle). This plot is representative of the pressure vs time variation in the pulse combustor used. The time period of one cycle was 5.2 ms and the positive and negative pressures were 48 kPa and 26 kPa respectively.

If the interrupter was to work on one cycle before the current operating cycle of the pulse combustor, then

$$t_1 + t_2 + t_3 = 5.2 \quad \text{ms} \qquad \text{.........} \ (4.2.1)$$

(a) Calculation of t_1:

T_1 = temperature of gas in combustion chamber = 1500 K

T_2 = ambient temperature = 300 K

T_{av} = average temperature of gas in the connector pipe = (1500+300)/2 = 900 K

a_1 = velocity of sound in the gas in the connector pipe = $(\gamma.R.T_{av})^{0.5}$ = 601 m/s

let,

x = length of connector pipe (m)

therefore,

$$t_1 = \frac{x}{a_1} = 1.66 \cdot x \quad \text{ms}$$

(b) Calculation of t_2:

m = net mass of moving parts in the interrupter = 35 g

This included the mass of the spool, washer, retaining nut and half the mass of the diaphragm and the return spring. The diameter of the diaphragm used was 76.2 mm.

A = area of the diaphragm = 4.56×10^{-3} m^2

As can be seen from Figure 4.1 the positive pressure (Δp) available for driving the interrupter was 48 kPa. The total displacement of the spool (S) was 10 mm and the spring constant (K) of the return spring was 700 N/m.

therefore,

F = net force on the spool = $\Delta p.A - S.K/2$ = 215.38 N

a = linear acceleration of spool = F/m = 6053.7 m/s^2

also,

$$S = u \cdot t_2 + \frac{1}{2} \cdot a \cdot t_2^2$$

u = initial velocity of the spool

at $\quad t_2 = 0, \qquad u = 0$

therefore,

$$t_2 = \sqrt{\frac{2 \cdot S}{a}} = 1.82 \quad \text{ms}$$

(c) Calculation of t_3:

The length of the fuel line (y) connecting the interrupter and the nozzle was 0.4 m. Assuming the velocity of sound (a_2) in kerosene to be 1500 m/s

$$t_3 = \frac{y}{a_2} = 0.26 \quad \text{ms}$$

hence, from equation 4.2.1

$$1.66 \cdot x + 1.82 + 0.26 = 5.2$$

therefore,

$$x = 1.87 \quad \text{m}$$

This was an approximate calculation as it was assumed that the positive pressure in the combustion chamber was applied to the spool instantaneously, whereas in reality it takes some finite time for the pressure to build up in the combustion chamber. Also the acceleration of the spool was taken to be linear and friction was neglected. This calculation served merely as a guideline for choosing the length of the connector pipe for the actual experiment.

VALVE THICKNESS x (mm)	Δp (kPa) FOR SHIM STEEL NON-RETURN VALVE	Δp (kPa) FOR MYLAR NON-RETURN VALVE
0.0254	3.43	0.46
0.0508	6.86	0.92
0.0762	10.29	1.37
0.1270	17.15	2.29
0.2540	34.29	4.57

Table 4.1: Pressure difference required across the carburettor for the shim steel and mylar non-return valve

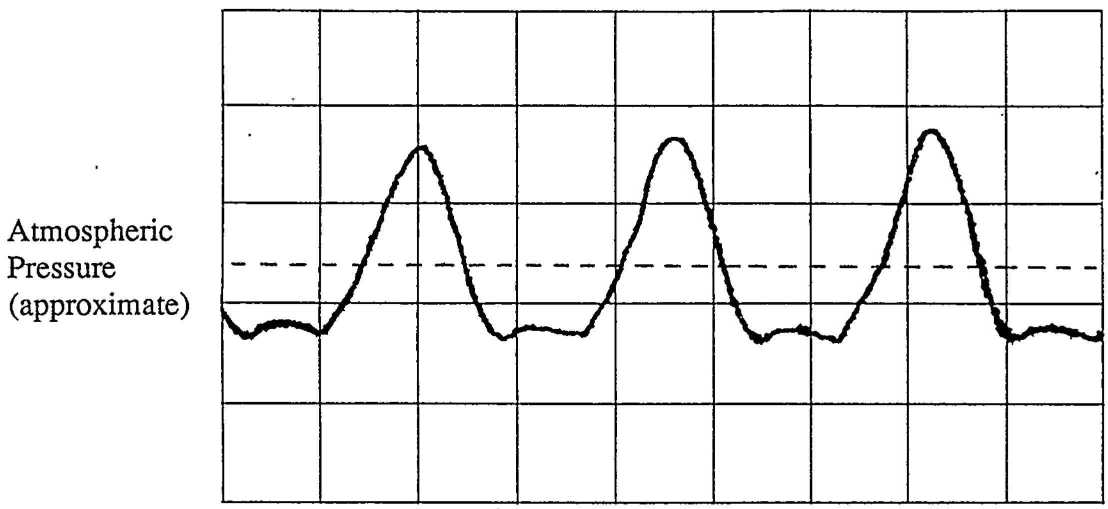

X axis: 2ms/div. Y axis: 34.47 kPa/div.

Fuel flow rate: 6.77 kg/h

Figure 4.1: Combustion chamber dynamic pressure for the high pressure steady flow fuel system

CHAPTER 5 CARBURETTOR FUEL SYSTEM: OPERATING PROCEDURE, OBSERVATIONS, RESULTS AND DISCUSSION

5.1 OPERATING PROCEDURE

The operating procedure followed for running the pulse combustor with the carburettor fuel system is described below.

5.1.1 Start Up

As a first step the spark plug ignition was turned on, followed by the opening of the compressed air supply valves. Finally the fuel supply was turned on by moving the needle valve out of the carburettor jet. This was done remotely with the help of a cable attached to the needle valve. The fuel flow was adjusted until ignition occurred in the combustion chamber. At the start the combustor behaved as a steady flow burner. After a warm up period of about one minute the combustor went into self sustained resonance. The compressed air supply and the spark plug ignition were then turned off.

5.1.2 Running

Once the pulse combustor went into self sustained resonance the inlet and tail pipe thrust readings were taken at different fuel flow rates. The fuel flow rate was varied by altering the position of the needle valve in the carburettor body and the amount of fuel going to the pulse combustor was metered with the help of a calibrated rotameter. Fuel rich blowout occurred when the fuel flow rate was increased above 8 kg/h and lean mixture blowout occurred once the fuel flow rate was decreased below 2 kg/h. Test data was compiled for several fuel flow rates to obtain a full operating range. The exhaust gas analyses for the tail pipe and the inlet could be made one at a time only. Determination of the composition of the exhaust gases at each fuel flow setting took 3 to 4 minutes. Because of the poor ventilation in the laboratory, the pulse combustor was switched off after each reading to allow time for the exhaust gases to clear off.

5.1.3 Shut Down

After obtaining all the data for a given test configuration the combustor was shut down by moving the needle valve to the close position in the carburettor body. Then the compressed air supply was switched on to cool the combustor. Finally the power supply to the transformer was switched off and control valve under the fuel float chamber was closed.

5.2 GENERAL OBSERVATIONS

(1) It was found that the running of the pulse combustor became rough as the thickness of the shim steel non-return valve was increased. For shim steel valves thicker

than 0.0762 mm back flow occurred from the air inlet of the carburettor. The problem of back flow of exhaust gases and gasoline became more severe with increasing valve thickness. This was attributed to the fact that the inertia and stiffness of the valve increased with an increase in its thickness.

(2) The sprayer in the fuel nozzle was attached to the main body by silver solder (Figure 3.4). A few times it was possible to melt the silver solder while running the carburettor with a thick shim steel non-return valve. When this happened the spokes of the sprayer were ejected from the tail pipe. It was suggested by Kentfield (54) that this occurred because of a back flow of hot gases through the carburettor when using thick shim steel non-return valves. The back flow of gases through the fuel nozzle caused an increase in its temperature. This was enough to melt the silver solder.

(3) The carburettor assembly had to be protected from the thermal radiation from the pulse combustor by using a thermal shield. This helped keep the temperature of the fuel in the carburettor down and prevented the fuel from vaporizing.

(4) The carburettor assembly had to be bolted tightly to the air inlet of the pulse combustor to prevent leakage of the fuel. It was observed that gas leakage through the flanges connecting the inlet pipe to the combustion chamber and the inlet to the non-return valve assembly caused a loss of suction. This adversely affected the thrust performance of the pulse combustor and also caused the concentration of CO in the exhaust gases to increase. CO concentrations were also found to increase with a crack or hole in the welds of the combustion chamber.

(5) The threads of the spark plug and the bolts connecting the combustion chamber to the air inlet were coated with "Never Seez". This was an anti-seize and lubricating compound that provided protection from extreme heat (up to 1000 ^{o}C), corrosion, rust, seizure and carbon fusion.

5.3 PERFORMANCE RESULTS AND DISCUSSION

5.3.1 Effect of Non-Return Valve Material on Performance

As a first step the pulse combustor was run with the carburettor equipped with the original 0.0508 mm thick mylar non-return valve taken from the hand held warm air blower. Because the long term objective of the program was to develop a fuel system that would allow the substitution of the pulse combustor for the conventional combustor in a gas turbine, attention was focused on the part most likely to fail under adverse operating conditions, namely the mylar non-return valve. Although the mylar valve showed no signs of wear and tear for the duration of the current tests (not more than 10 minutes at a time) it was deemed necessary to substitute it with a more rugged material like shim steel and compare the performance of the two.

Figure 5.1 shows the thrust produced by the pulse combustor with a 0.0508 mm thick mylar non-return valve. Other valve thicknesses were not tested as Ibrahim (12) reported that the pulse combustor performance did not change appreciably by varying the thickness of the valve. In addition to the total thrust the individual thrusts produced by the inlet and the tail pipe are also shown. On an average the tail pipe produced 65% of the total thrust.

The mylar non-return valve was replaced with a non-return valve made out of shim steel. The advantage of using shim steel over mylar was that it was less likely to fail under conditions of high temperature and pressure and long running periods likely to be encountered in a gas turbine. Figure 5.2 shows the total thrust produced by the pulse combustor using shim steel valve of various thicknesses. As can be observed there was no marked difference in the performance of the pulse combustor, although the total thrust showed a slight improvement with increasing thickness of the valve. When valves thicker than 0.0762 mm were tested it was found that the running of the combustor become rough. Also the back flow of gases from the inlet of the carburettor increased progressively with valve thickness.

Two reasons seemed to contribute to this behaviour. As the valve thickness increased beyond 0.0762 mm the pressure drop required across the carburettor to drive the valve increased (Table 4.1). Thus the actual pressure available from the combustor become insufficient to operate the valve properly as the valve thickness increased. This led to the back flow from the carburettor inlet resulting in rough running. The back flow of gases from the air inlet of the carburettor was also a result of the increase in the stiffness of the shim steel valve with an increase in its thickness. Hence, the thicker valves could not seal the fuel inlet holes of the valve seat (Figure 3.3) effectively when the pressure inside the combustion chamber increased above atmospheric pressure and this led to the back flow through the carburettor during phases 1 and 2 (Figure 1.4) of the combustor cycle.

Figure 5.3 compares the performance of the 0.0508 mm mylar valve with the performance of the 0.0762 mm thick shim steel valve. The pulse combustor produced slightly more thrust using the shim steel valve than the mylar valve. But in general both curves followed the same trend.

5.3.2 Exhaust gas analysis

Both the inlet and tail pipe exhaust gas compositions were ascertained for the full fuel flow range using the mylar non-return valve. The sampling probe was placed 70 mm inside the inlet and the tail pipe. Figures 5.4, 5.5 and 5.6 show the CO, CO_2 and O_2 concentrations in the exhaust gas of the inlet and the tail pipe.

CO concentration in the inlet and tail pipe followed opposite trends i.e. it decreased with fuel flow rate for the inlet and increased with the fuel flow rate for the tail pipe. The CO concentrations obtained by Rehman (55) for a four inlet gas fired pulse combustor are shown in Figure 5.7. The CO emissions for Rehman's pulse combustor increased with an increase in the fuel flow rate for both the inlet and tail pipe. It can be seen that the CO emissions in the inlet of the carburetted pulse combustor and the gas fired pulse combustor followed opposite trends. The reason for the decrease in CO concentrations in the inlet of the carburetted pulse combustor with increase in the fuel flow rate was that as the fuel flow rate increased more air was sucked through the carburettor inlet. This lead to a better mixing and atomization of the fuel and air in the carburettor. So the fuel air mixture that was injected into the combustor was well mixed and atomized at higher fuel flow rates. This contributed to a more efficient combustion and a decrease in CO concentration. Whereas, for the gas fired combustor the fuel was always injected in a gaseous state so atomization of fuel was not an influencing parameter. With an increase in the fuel flow rate the pressure at which the fuel was injected into the combustion chamber also increased and may have become more than the peak firing pressure of the pulse combustor. Thus the fuel was injected into the combustion chamber throughout the cycle and when back flow through the inlet occurred (phases 1 and 2 in Figure 1.4) the unburnt, or partially reacted, fuel was ejected out through the inlet leading to higher CO concentrations as the fuel flow rate increased. Another factor that could have contributed to the high CO emissions was that the four inlet pulse combustor was not an optimised design. Kentfield et al (56) found that for a well set up single inlet gas-fired pulse combustor the CO emissions were less than 5 ppm for the inlet (equipped with a flow rectifier device to turn the back flow) and approximately 30 ppm for the tail pipe.

The concentrations of CO_2 in the inlet and tail pipe (Figure 5.5) both decreased with an increase in the fuel flow rate. This could be attributed to the fact that as the fuel flow rate increased more fresh air was sucked in by the combustor and this diluted the exhaust gases flowing out of the inlet and the tail pipe. Another observation that could be made was that the concentrations of CO_2 in the tail pipe was 13 to 16 times the concentrations of CO_2 in the inlet. The reason for this was that the flow through the tail pipe consisted mainly of exhaust gases and to a lesser extent of fresh air. On the other hand, the flow through the inlet consisted mainly of fresh air and to a lesser extent of exhaust gases because during the recharging of the pulse combustor the inlet provided most of the fresh air and the tail pipe provided the products of combustion that helped in re-ignition. This was confirmed by comparing the concentration of O_2 in the inlet and tail pipe (Figure 5.6). The O_2 concentration in the inlet was approximately 20.5% showing that flow through the inlet consisted mainly of fresh air and some exhaust gases. On the other hand the concentration of O_2 in the tail pipe varied approximately from 10.6% to 13.8% showing that the tail pipe flow consisted largely of exhaust gases.

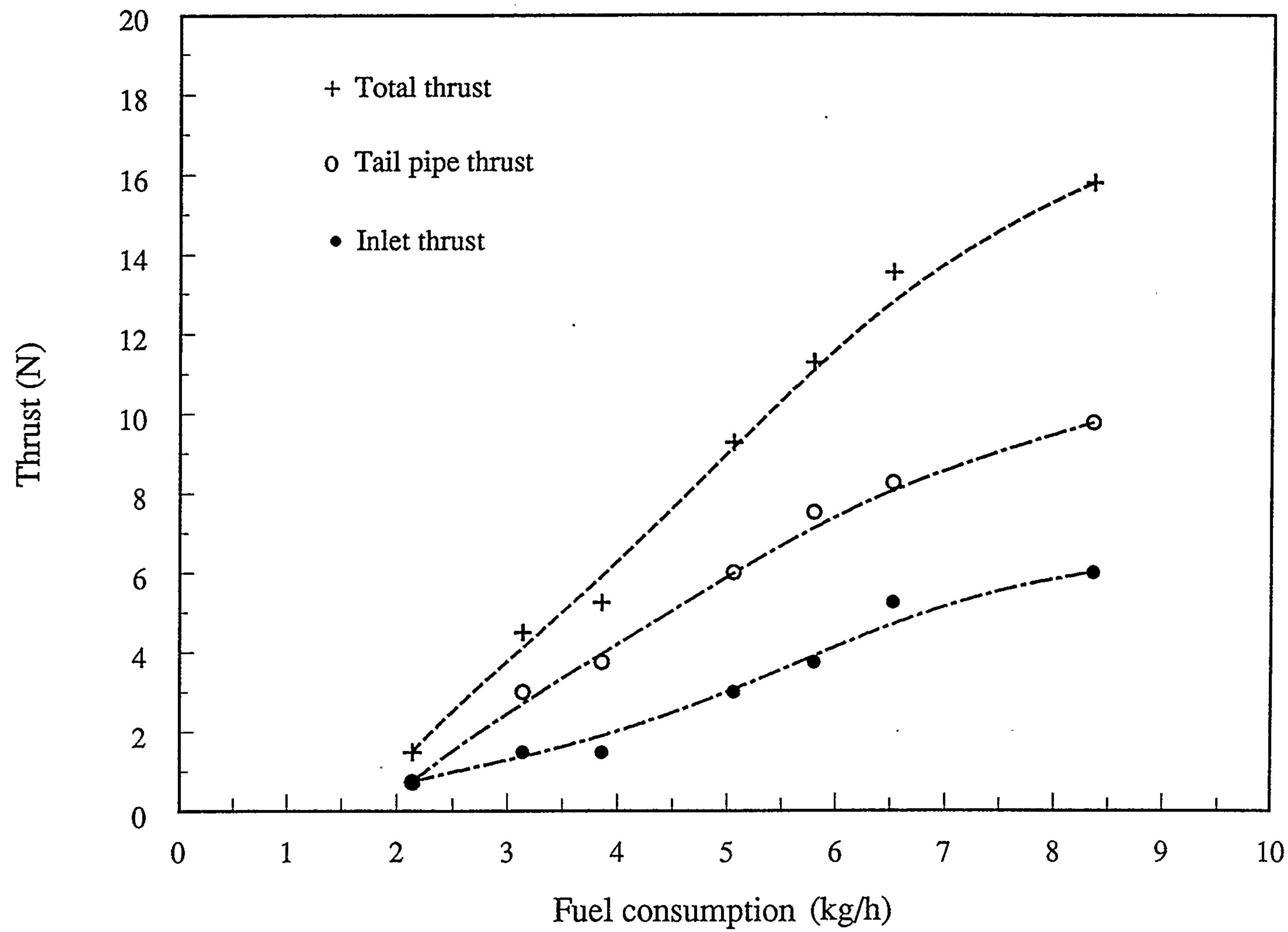

Figure 5.1: Total and individual thrusts produced by the pulse combustor using 0.0508 mm thick mylar non-return valve

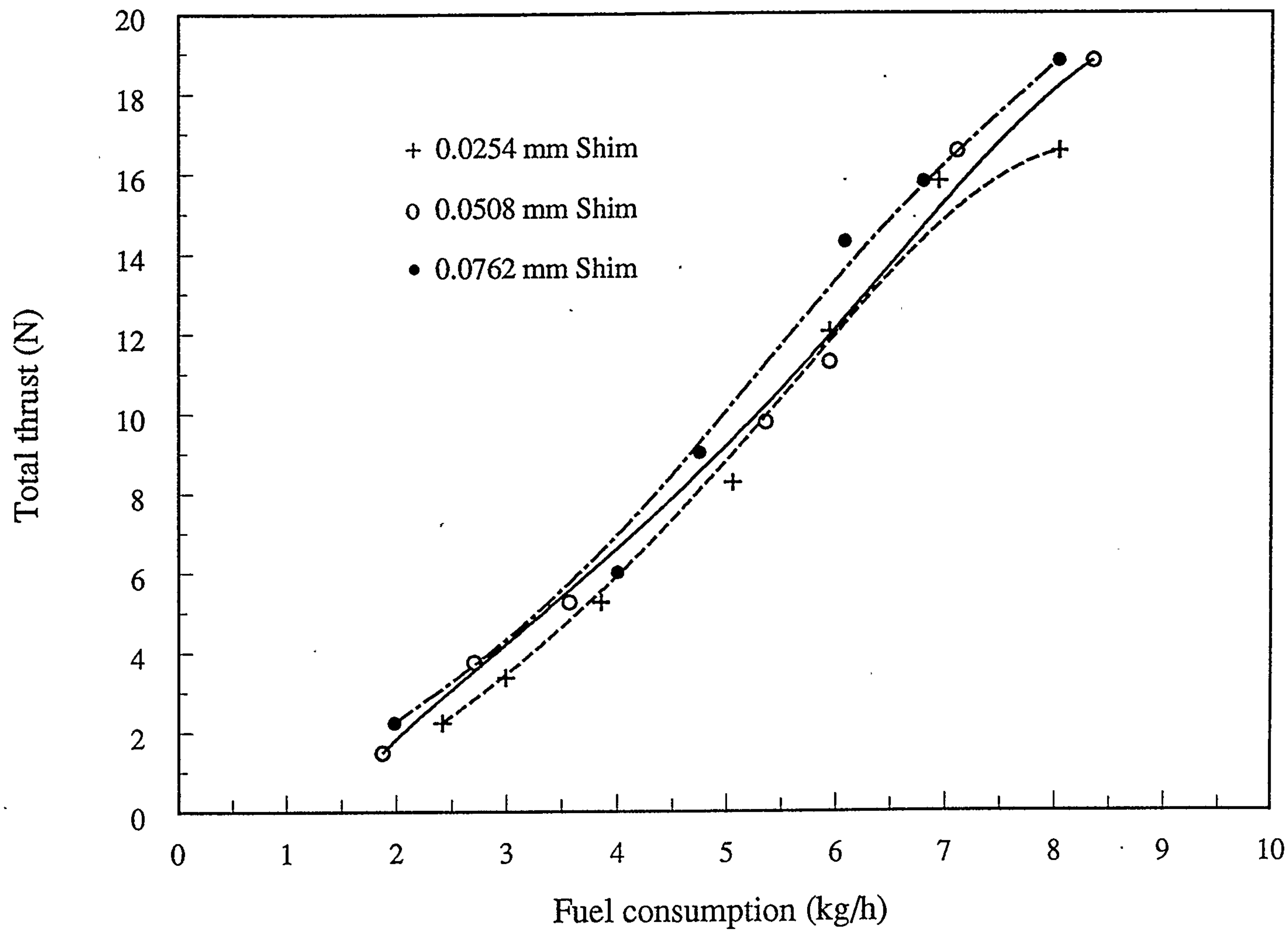

Figure 5.2: Performance of the pulse combustor using shim steel non-return valves of various thicknesses

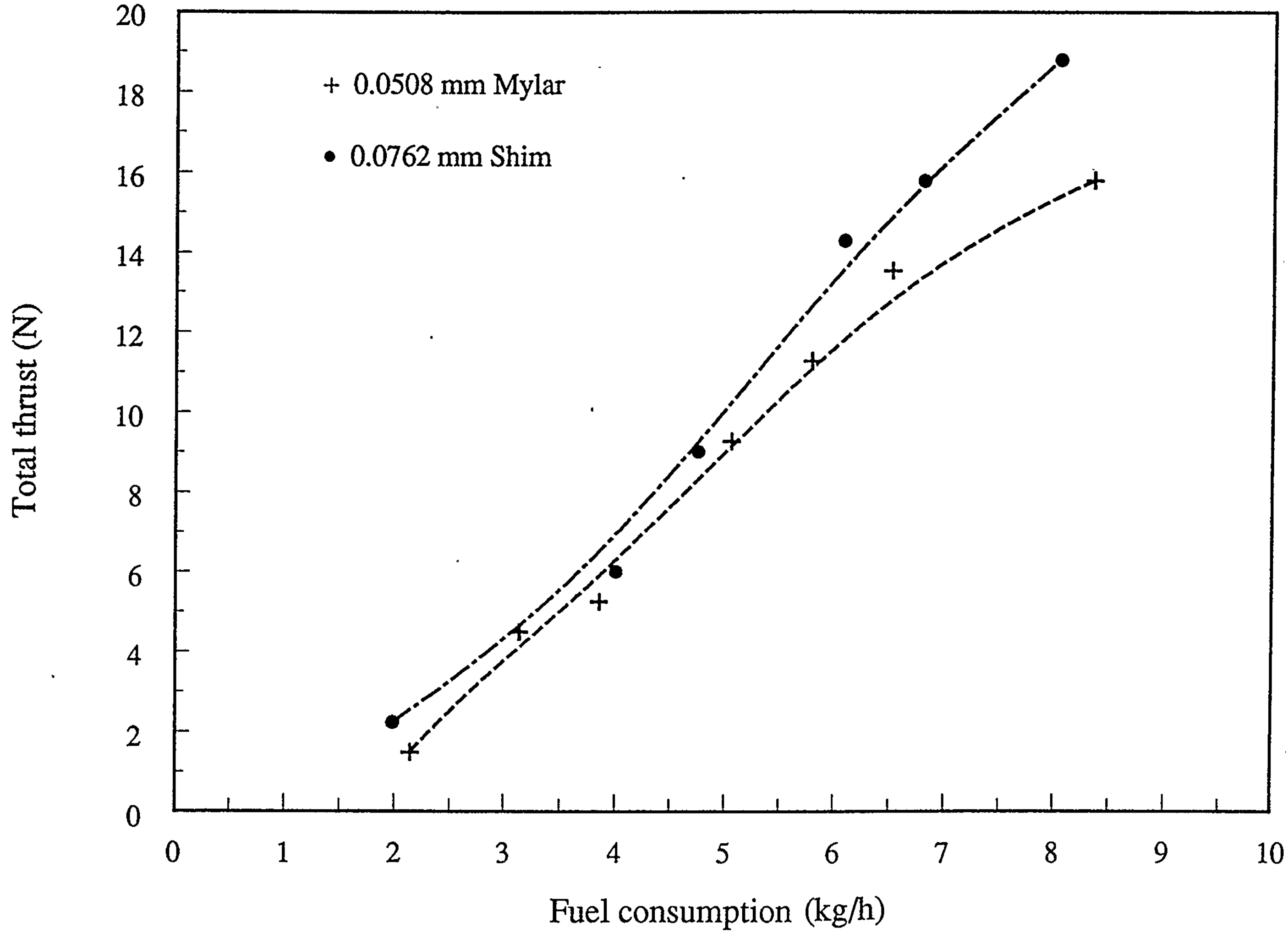

Figure 5.3: Comparison of the combustor performance using mylar and shim steel non-return valve

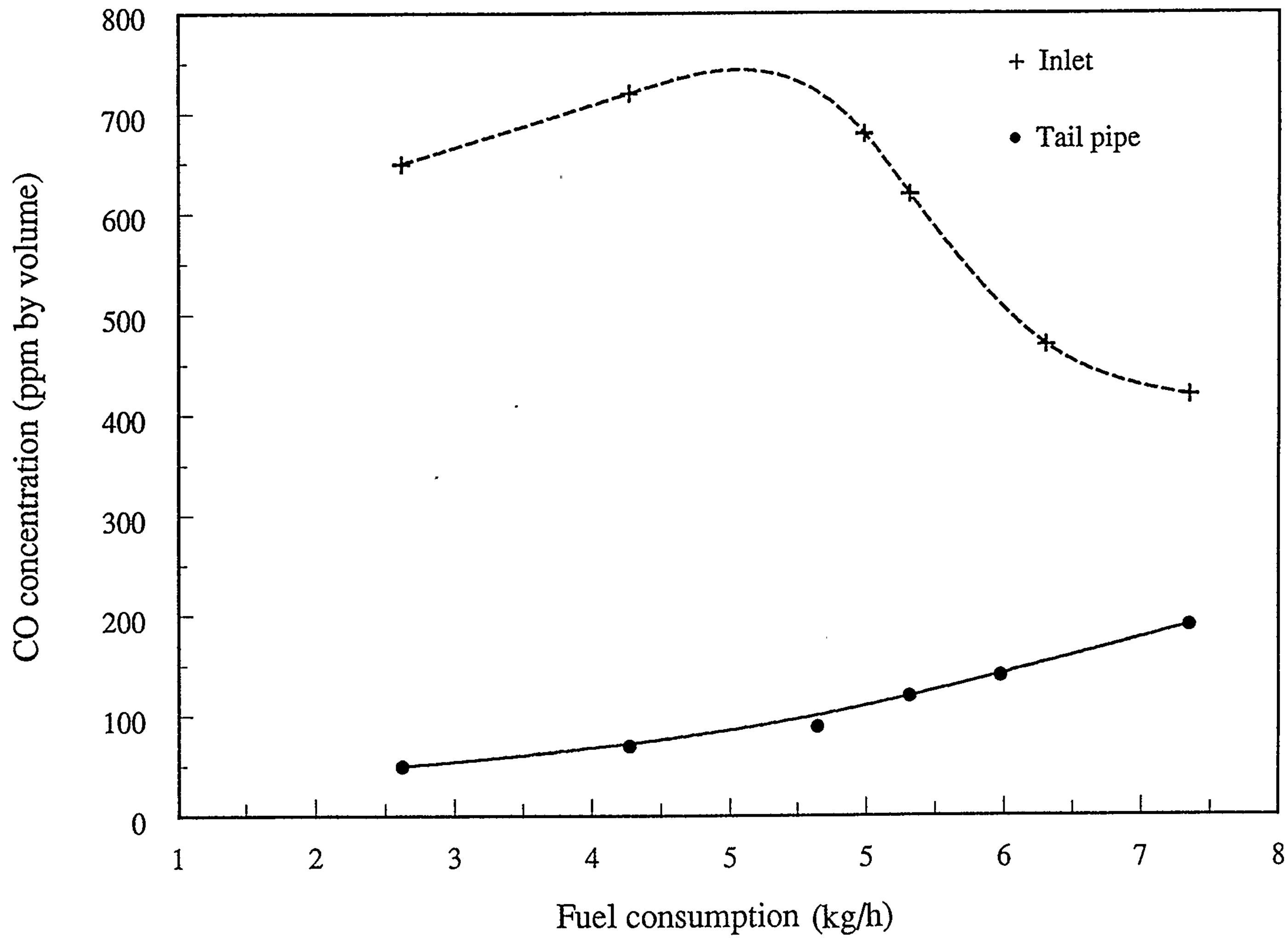

Figure 5.4: Concentration of CO in the inlet and tail pipe of the pulse combustor using a 0.0508 mm thick mylar non-return valve

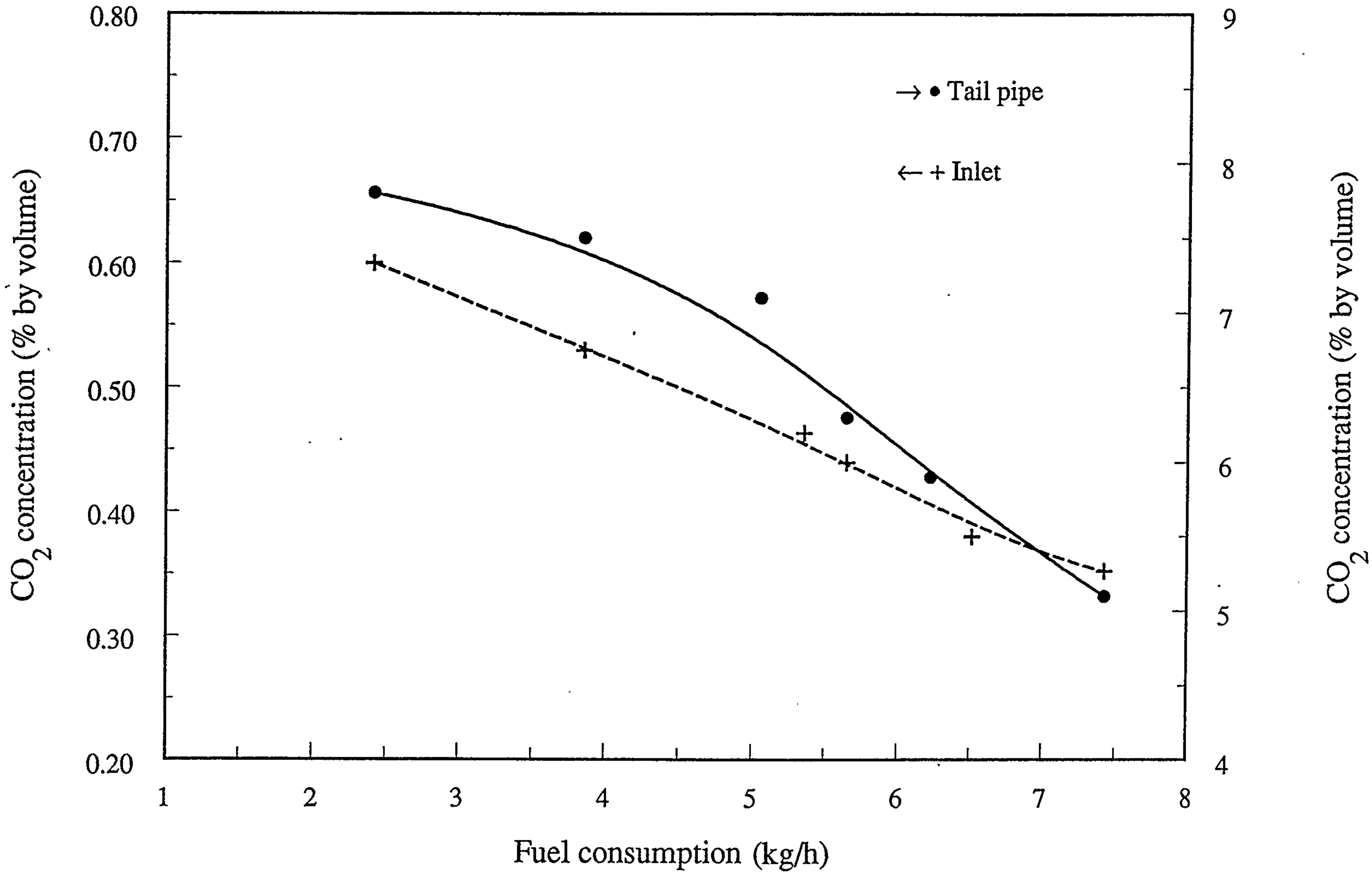

Figure 5.5: Concentration of CO_2 in the inlet and tail pipe of the pulse combustor using a 0.0508 mm thick mylar non-return valve

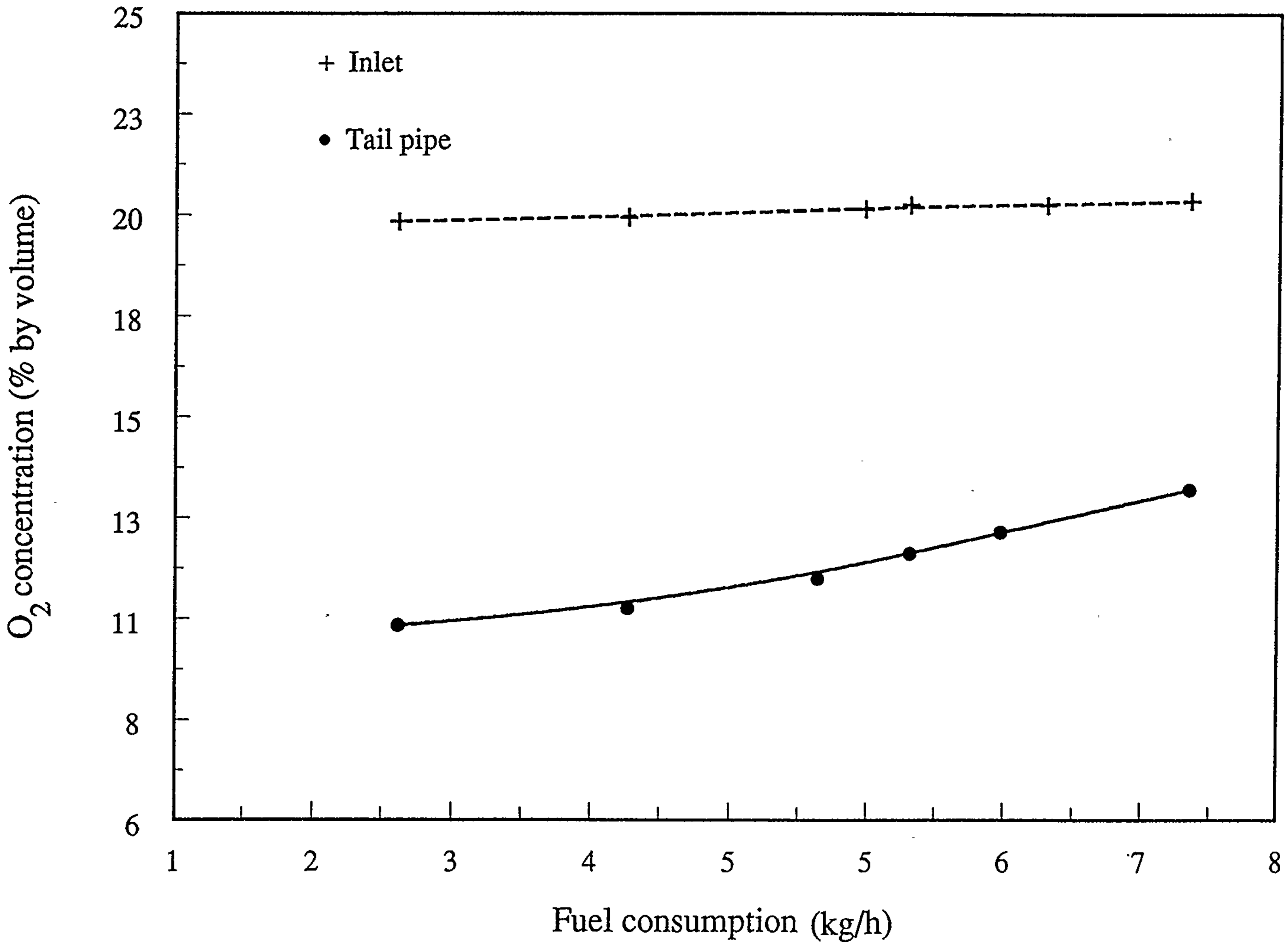

Figure 5.6: Concentration of O_2 in the inlet and tail pipe of the pulse combustor using a 0.0508 mm thick mylar non-return valve

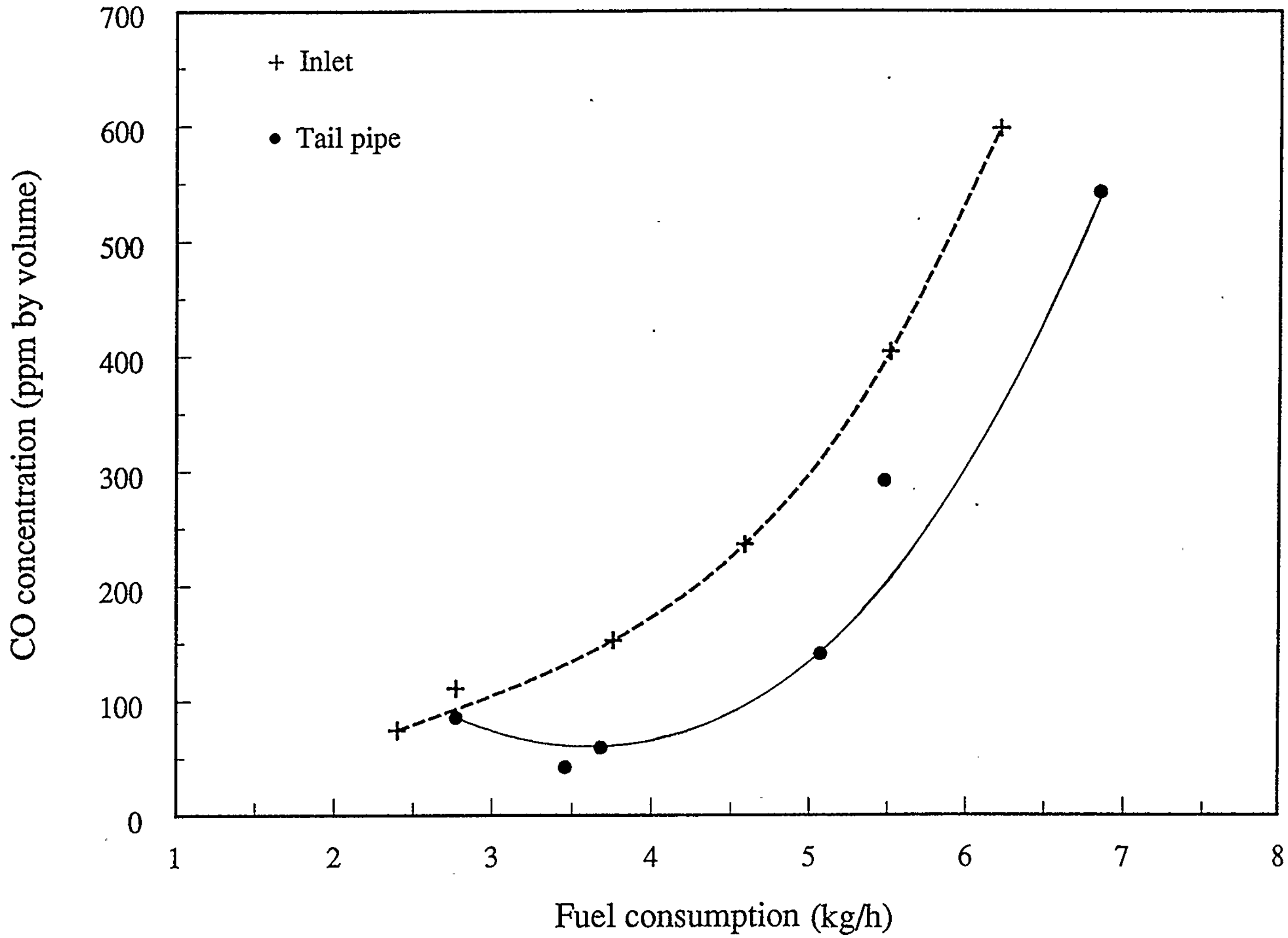

Figure 5.7: Concentration of CO in the exhaust gases for a four inlet gas fired valveless pulse combustor obtained by Rehman (55)

CHAPTER 6: HIGH PRESSURE AND LOW PRESSURE STEADY FLOW FUEL INJECTION SYSTEMS: PROCEDURE, OBSERVATIONS, RESULTS AND DISCUSSION

6.1 OPERATING PROCEDURE

6.1.1 Start Up

As for the carburettor fuel system, the ignition to the spark plug was switched on first, followed by the opening of the compressed air supply valves. Finally the electric motor that drove the fuel pump was switched on. Fuel flow was varied until the pulse combustor went into resonance. The initial warm up period was approximately one minute before resonance occurred. After that ignition to the spark plug and the compressed air supply were switched off.

6.1.2 Running

Once the pulse combustor went into self sustained resonance the inlet and tail pipe thrust readings were taken at different fuel flow rates. The fuel flow was varied by turning the pressure adjusting screw in the pump with the help of a screwdriver. For the high pressure steady flow fuel injection system the fuel pressure could be varied from 345 kPa gauge to 1034 kPa gauge. On the other hand, in the case of the low pressure steady flow fuel injection system the fuel pressure could be varied from 69 kPa gauge to 345 kPa gauge. Fuel flow rate was measured with the aid of a calibrated rotameter.

The exhaust gas analyses for the inlet and the tail pipe were made one at a time only and it took 3 to 4 minutes to determine the composition of the exhaust gases at each fuel flow setting. Because of the poor ventilation in the laboratory, the pulse combustor was switched off after each reading (inlet or tail pipe) to allow time for the exhaust gases to clear off.

6.1.3 Shut Down

The pulse combustor was shut down by switching off the electric motor that drove the fuel pump. The compressed air supply was then switched on to cool down the combustor. Finally the transformer was disconnected from the main power supply and the rotameter and fuel tank control valves were closed.

6.2 GENERAL OBSERVATIONS

(1) It was observed that when the fuel nozzles were changed or when the spring in the pressure regulating valve was changed to convert the fuel system from high pressure steady flow fuel injection system to the low pressure steady flow fuel injection system air bubbles got trapped in the fuel system. This prevented the pulse combustor from going into self sustained resonance. As soon as the compressed air supply was

switched off the combustor ceased to resonate. This was because of the disruption of the fuel spray in the combustion chamber as the trapped air bubbles in the fuel system were pumped out through the fuel nozzle. To avoid this problem, air trapped in the pump was released through the pump port connected to the pressure gauge. Air trapped in the fuel line connecting the pump and the fuel nozzle was purged out by spraying the fuel in open air (outside the pulse combustor) for a couple of minutes. This effectively removed the air trapped in the fuel system and led to the smooth running of the pulse combustor.

(2) When the pulse combustor was started it generated a lot of smoke from the inlet and tail pipe for both types of fuel systems. It was observed that the pulse combustor produced more smoke running with diesel than with kerosene. Smoke in the exhaust continued until the combustor went into resonance and after that the exhaust became smoke free. Although the exhaust became smoke free, after the pulse combustor went into resonance, yet it caused irritation in the throat and watering of the eyes. This was probably because of unburnt hydrocarbons in the exhaust gases from the pulse combustor.

(3) As the fuel nozzle and pipe were placed in the inlet of the combustor (Figure 3.12) the exhaust from the inlet passed around the nozzle assembly. After a test run when the uncooled fuel nozzle was removed from the combustor, it was found that the fuel nozzle and pipe were covered with soot deposits from the exhaust gases. The soot particles could be removed from the fuel pipe by rubbing.

For the case when a water cooled fuel nozzle was used (section 6.3.5) the nature of deposits on the fuel nozzle assembly was different. Water cooling seemed to cause the chilling of the products of combustion on the fuel pipe. The result was that the products of combustion were condensed and deposited on the fuel pipe in the form of brown flakes that were hard to remove.

(4) It was found that when the uncooled fuel nozzle was immediately removed from the pulse combustor after a test fuel vapour came out of the nozzle orifice. This continued for about a minute until the nozzle cooled down. This was because the nozzle pipe was immersed in the flame in the inlet of the pulse combustor, causing the nozzle pipe to heat up sufficiently to vaporise the fuel in it. This phenomenon was not observed with the water cooled nozzle (section 6.3.5) in which the fuel pipe was cooled by a continuous flow of cold water in a water jacket around it. The cooling water seemed to keep the temperature of the fuel sufficiently low to inhibit the vaporizing of the fuel.

6.3 PERFORMANCE RESULTS AND DISCUSSION

6.3.1 Effect of Nozzle Type

As outlined in section 3.3.2.2 of Chapter 3 three types of fuel nozzles were tested for both the high and low pressure steady flow fuel injection systems. The spray forms of the three types of nozzles are shown in Figure 3.10. Type A nozzle formed a hollow cone, type B formed a solid cone and type W generated a combination of both a hollow and a solid cone. When the combustor was run on the three types of nozzles it was found that the combustor went into self sustained resonance with the type A nozzle only. With nozzle types B and W the combustor ceased to resonate after the compressed air supply was switched off. This appeared to be due to a hollow cone inside the fuel spray of the

Type A nozzles that trapped the products of combustion from the previous cycle. This presumably helped in the mixing of fuel, fresh air and products of combustion with one another to form a combustible charge, an essential requirement for re-ignition and continuation of the combustor cycle. Conversely, for the nozzle types W and B there was no hollow space in the fuel spray to trap the products of combustion. Thus the fuel in the centre of the fuel spray did not combine with fresh air and products of combustion from the previous cycle to form a well mixed charge for the next cycle. Once the compressed air supply was switched off the improper mixing of the fuel with air and products of combustion caused the combustor to cease resonance.

6.3.2 Effect of Fuel Type

All the tests on the pulse combustor using the high and low pressure steady flow fuel injection systems were carried out with kerosene as the fuel. The gear pump used for injecting fuel was also recommended for diesel fuel in addition to kerosene. Thus, a single test run was made with diesel fuel to check the ability of the combustor to handle diesel fuel. Ibrahim (12) noted that his carburetted pulse combustor did not go into self sustained resonance with diesel fuel. The high pressure steady flow fuel injection system was used to inject the diesel fuel. Gasoline could not be tested with this fuel system because the gear pump used was not recommended for gasoline. This was because the pump had no separate lubricating system and relied on the lubrication provided by the fuel being used in it. Since gasoline does not have good lubrication properties, it was not feasible to use it in the present set up.

The combustor did not go into resonance with diesel fuel and a lot of smoke was generated (more than while running it with kerosene). The reason for this was, presumably, the low volatility of diesel. However, once the combustor was started on kerosene it was possible to switch to diesel without blowout. Figure 6.1 shows the total thrusts generated by the pulse combustor running on kerosene and diesel fuel. Both curves show a similar trend of increasing thrust with an increase in fuel flow rate. The slightly better performance of the pulse combustor with diesel could be because of higher heating value of diesel as compared to kerosene. Another reason for this could be the higher density of diesel resulting in less unburnt fuel to be expelled from the inlet during backflow through the inlet. The fuel nozzle used for kerosene was 4.0, 80^{o}A and for diesel 4.0, 70^{o}A. In both the cases high pressure fuel system was used.

6.3.3 Influence of Fuel Spray Cone Angle

Influence of fuel spray cone angle was investigated by running the combustor on Type A nozzles having different spray cone angles. Figure 6.2 shows the variation in the performance of the pulse combustor using fuel nozzles with different spray cone angles. As can be observed the spray cone angle did not have much influence on the performance of the combustor. The breakdown of the total thrust produced by the combustor into the inlet and tail pipe thrusts using a 4.0, 90 ^{o}A nozzle is shown in Figure 6.3. Almost 56% of the total thrust was produced by the tail pipe and the rest by the inlet pipe.

6.3.4 Effect of Fuel Pressure

Effect of fuel pressure on the performance of the pulse combustor was tested by using the high and low pressure steady flow fuel injection systems. For the high pressure system (variation of fuel pressure from 345 kPa gauge to 1034 kPa gauge) a 4.0, 70°A fuel nozzle was used and for the low pressure system (variation of fuel pressure from 69 kPa gauge to 345 kPa gauge) a 8.0, 70°A fuel nozzle was used. Figure 6.4 shows that the low pressure fuel system gave a better performance than the high pressure fuel system over the full fuel flow range. The reason for this could be that with the high pressure system the fuel was injected all through the cycle of the pulse combustor because the fuel pressure was much higher than the peak firing pressure in the combustion chamber of the combustor. Hence during the expansion process of the cycle when back flow occurred from the inlet, fuel being injected into the combustor was thrown out with the exhaust gases. This caused some fuel to be wasted and this tended to be confirmed by high CO emissions in the inlet.

However, with the low pressure fuel system fuel was injected at a much lower pressure than with the high pressure system. Thus the fuel supply was modulated by the firing pressure in the combustor to some extent. This supposition tended to be confirmed by inlet CO emissions that were lower than those in the first case. Specific fuel consumption (S.F.C.) of the pulse combustor running on high pressure diesel and high and low pressure kerosene is shown in Figure 6.5.

6.3.5. Effect of Water Cooling

The initial arrangement used to water cool the nozzle is shown in the top of Figure 6.6. In this set up a hole had to be drilled in the inlet pipe to accommodate the pipe through which the water entered. There was a slight clearance between this water pipe and the hole drilled in the inlet to accommodate it. It was found that this clearance resulted in the CO emission in the inlet of the combustor to increase substantially. Therefore, a second water cooling circuit was designed as shown in bottom of Figure 6.6. This arrangement did not require a hole to be drilled in the inlet pipe and consequently the CO emissions decreased.

The performance of the combustor using an uncooled and a cooled fuel nozzle with the low pressure steady flow fuel injection system is shown in Figure 6.4. The better performance of the uncooled fuel nozzle could be attributed to the vaporization of the fuel. With the uncooled nozzle the nozzle fuel line got sufficiently hot by coming in contact with the flame and this helped in the vaporization of the fuel, whereas for the cooled nozzle the cooling water kept the temperature of the fuel sufficiently low so as to inhibit it from vaporizing. The fuel in the second case was injected in the form of atomized liquid droplets and not as a vapour. Vapour seemed to mix more thoroughly with fresh air and the products of combustion than liquid droplets. This was confirmed by higher CO levels in the tail pipe for the cooled nozzle than for the uncooled nozzle (Figure 6.14) showing that more fuel was wasted using a cooled rather than an uncooled fuel nozzle.

6.3.6 Combustion Chamber Pressure

The dynamic pressure variation in the combustion chamber of the pulse combustor was measured with the help of the piezoelectric transducer for both the high and low pressure fuel systems. Figures 6.7 and 6.8 show the pressure variation for two fuel settings for the high and low pressure fuel systems respectively using the uncooled fuel nozzles. These plots show the amplitude of the pressure variation in the combustion chamber. The atmospheric pressure line could not be plotted because of the d.c. drift superimposed on the output signal from the pressure transducer. Due to this the absolute values of the maximum and minimum pressures reached in the combustion chamber could not be ascertained.

Maximum combustion chamber pressure variation for both the high and low pressure fuel systems is shown in Figure 6.9. The difference between the maximum and minimum pressures showed an increasing trend with an increase in the fuel flow rate. The reason for this was that as more fuel was injected into the combustion chamber the momentum of the outgoing exhaust gases during the expansion process increased. This contributed to an increase in the vacuum in the combustion chamber. Hence more fresh air got sucked in during the charging phase of the cycle leading to a higher peak pressure. From the pressure plots it was possible to calculate the frequency of operation of the pulse combustor at each fuel setting. This is shown in Figure 6.10 for both the high and low pressure fuel systems. For both the fuel systems the cyclic frequency showed a variation of 4 to 5 Hz over the full operating range.

6.3.7 Exhaust Gas Analysis

6.3.7.1 *High Pressure Fuel System*

Gas analysis of the exhaust gases for the high pressure fuel system was carried out using both the cooled and uncooled nozzle. The concentrations of CO, CO_2 and O_2 in the inlet and tail pipe for a 4.0, 70°A uncooled nozzle are tabulated in Tables 6.1 and 6.2. The same results for a 4.0, 70°A cooled nozzle are presented in Tables 6.3 and 6.4.

The CO values for the inlet pipe for the two nozzles are also plotted in Figure 6.11. As can be seen from the figure CO emissions in the inlet were reduced significantly by water cooling the nozzle. This could be explained on the basis of the fact that with the uncooled nozzle, the nozzle got heated up and this in turn helped vaporize the fuel. Thus the fuel that was sprayed into the combustion chamber was in a vaporized form for the uncooled nozzle. During back flow from the inlet it was possible for the exhaust gases to blow the vaporized fuel out of the inlet leading to high CO emissions. Conversely, with a water cooled nozzle the continuous flow of cold water around the fuel pipe prevented the fuel from vaporizing. Thus the fuel injected into the combustion chamber was in the form of finely atomized liquid droplets. During back flow from the inlet, because of the momentum of the liquid spray droplets, it was harder for the droplets to be blown out with the exhaust gases. This resulted in a much lower CO emissions for the cooled fuel nozzle than for the uncooled nozzle.

For the tail pipe the CO emissions for the cooled fuel nozzle were higher than those for the uncooled nozzle (Figure 6.12). This could be a result of better mixing of the vaporized fuel with air and products of combustion for the uncooled nozzle. In the case of the cooled nozzle the liquid spray droplets did not properly mix with the fresh air and products of combustion resulting in the expulsion of unburnt fuel from the tail pipe. In general for both cases CO emissions from the inlet were much higher than for the tail pipe because the fuel nozzle was situated in the inlet and back flow from the inlet, during the expansion process of the working cycle, caused unburnt fuel to be expelled from the inlet.

6.3.7.2 *Low Pressure Fuel System*

CO, CO_2 and O_2 concentrations in the inlet and tail pipe for a 8.0, 70° A uncooled nozzle are tabulated in Tables 6.5 and 6.6. The same results for a 8.0, 70° A cooled nozzle are represented in Tables 6.7 and 6.8.

Figure 6.13 shows the CO levels in the inlet using the two types of nozzles. It is interesting to note that with this fuel system cooling did not prove as beneficial as it did with the high pressure fuel system. Two causes probably contributed to this behaviour. [1] The pressure of the injected fuel with the low pressure fuel system was much lower than with the high pressure fuel system. This made it easier for the liquid droplets in the fuel spray to be blown out with the exhaust gases during back flow from the inlet. [2] Because of the low fuel pressure in the low pressure fuel system the atomization of the fuel was poor leading to poor mixing between the fuel, fresh air and products of combustion. Both these factors off-set the benefits of water cooling achieved with the high pressure fuel system for the inlet pipe.

As was the case with the high pressure fuel system, the CO emissions in the tail pipe with the low pressure system were higher for the cooled nozzle than for the uncooled nozzle (Figure 6.14). Again lower fuel pressure led to poor atomization and mixing of fuel with the air in the case of the water cooled nozzle. This resulted in high CO emissions from the tail pipe.

FUEL CONSUMPTION (kg/h)	CO CONC. (PPM BY VOLUME)	CO_2 CONC. (%AGE BY VOLUME)	O_2 CONC. (%AGE BY VOLUME)
6.77	1800	0.480	20.7
7.17	1740	0.440	20.6
8.49	1410	0.376	20.4
9.93	1290	0.336	20.4
10.72	1260	0.352	20.4
11.87	1230	0.352	20.4

Table 6.1: Exhaust gas composition in inlet pipe at different fuel flow rates for high pressure steady flow fuel injection system with uncooled fuel nozzle.

FUEL CONSUMPTION (kg/h)	CO CONC. (PPM BY VOLUME)	CO_2 CONC. (%AGE BY VOLUME)	O_2 CONC. (%AGE BY VOLUME)
6.77	50	5.8	13.8
7.17	70	5.6	14.0
8.49	90	5.0	14.5
9.93	140	4.6	14.8
10.72	180	4.2	15.2
11.87	240	3.8	15.7

Table 6.2: Exhaust gas composition in tail pipe at different fuel flow rates for high pressure steady flow fuel injection system with uncooled fuel nozzle.

FUEL CONSUMPTION (kg/h)	CO CONC. (PPM BY VOLUME)	CO_2 CONC. (%AGE BY VOLUME)	O_2 CONC. (%AGE BY VOLUME)
7.04	720	0.340	20.8
8.23	510	0.272	20.8
9.28	450	0.272	20.8
10.72	420	0.236	20.7
11.74	400	0.216	20.4
12.38	400	0.240	20.4

Table 6.3: Exhaust gas composition in inlet pipe at different fuel flow rates for high pressure steady flow fuel injection system with water cooled nozzle.

FUEL CONSUMPTION (kg/h)	CO CONC. (PPM BY VOLUME)	CO_2 CONC. (%AGE BY VOLUME)	O_2 CONC. (%AGE BY VOLUME)
7.04	80	7.10	11.3
8.23	100	7.10	12.1
9.28	150	6.90	12.2
10.72	220	6.70	12.3
11.74	320	6.30	12.3
12.38	500	5.70	13.1

Table 6.4: Exhaust gas composition in tail pipe at different fuel flow rates for high pressure steady flow fuel injection system with water cooled nozzle.

FUEL CONSUMPTION (kg/h)	CO CONC. (PPM BY VOLUME)	CO_2 CONC. (%AGE BY VOLUME)	O_2 CONC. (%AGE BY VOLUME)
6.77	1500	0.432	20.3
7.83	1100	0.352	20.4
8.62	850	0.300	20.4
9.80	730	0.295	20.6
11.47	750	0.290	20.6
12.00	740	0.290	20.7

Table 6.5: Exhaust gas composition in inlet pipe at different fuel flow rates for low pressure steady flow fuel injection system with uncooled fuel nozzle.

FUEL CONSUMPTION (kg/h)	CO CONC. (PPM BY VOLUME)	CO_2 CONC. (%AGE BY VOLUME)	O_2 CONC. (%AGE BY VOLUME)
7.04	70	5.05	13.6
7.83	80	4.60	14.5
8.50	90	4.20	15.1
9.54	120	3.75	15.6
10.72	150	3.50	16.1
12.13	230	3.20	16.5

Table 6.6: Exhaust gas composition in tail pipe at different fuel flow rates for low pressure steady flow fuel injection system with uncooled fuel nozzle.

FUEL CONSUMPTION (kg/h)	CO CONC. (PPM BY VOLUME)	CO_2 CONC. (%AGE BY VOLUME)	O_2 CONC. (%AGE BY VOLUME)
6.77	1170	0.416	20.4
7.83	950	0.340	20.4
8.76	900	0.340	20.4
9.80	750	0.316	20.5
10.72	730	0.308	20.5
12.00	730	0.324	20.5

Table 6.7: Exhaust gas composition in inlet pipe at different fuel flow rates for low pressure steady flow fuel injection system with water cooled fuel nozzle.

FUEL CONSUMPTION (kg/h)	CO CONC. (PPM BY VOLUME)	CO_2 CONC. (%AGE BY VOLUME)	O_2 CONC. (%AGE BY VOLUME)
6.77	180	4.80	14.4
7.44	190	4.80	14.4
8.62	290	4.35	14.9
9.41	420	4.35	14.9
10.72	770	4.60	14.7
12.00	1300	4.60	14.5

Table 6.8: Exhaust gas composition in tail pipe at different fuel flow rates for low pressure steady flow fuel injection system with water cooled nozzle.

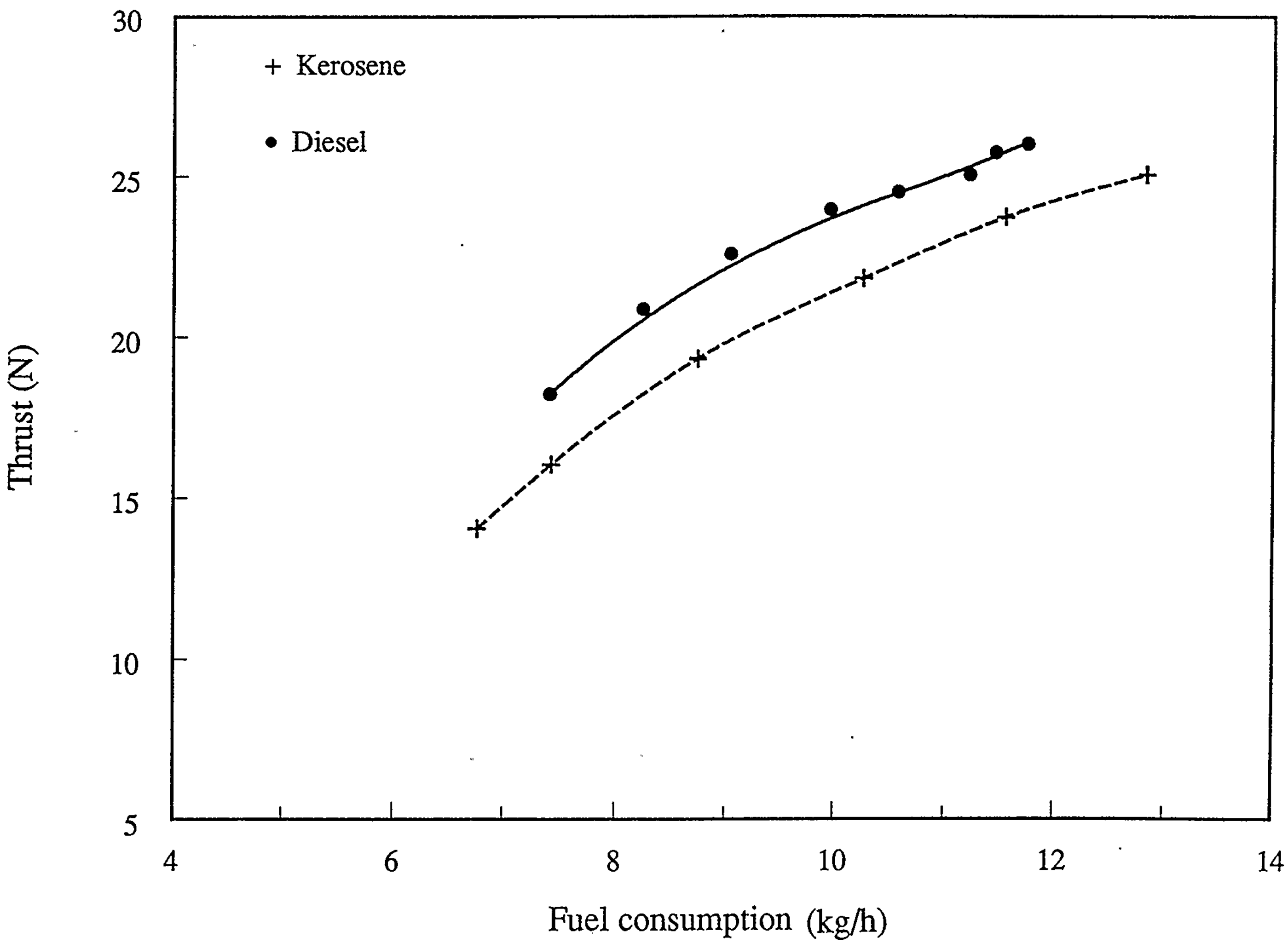

Figure 6.1: Performance of pulse combustor running on kerosene and diesel

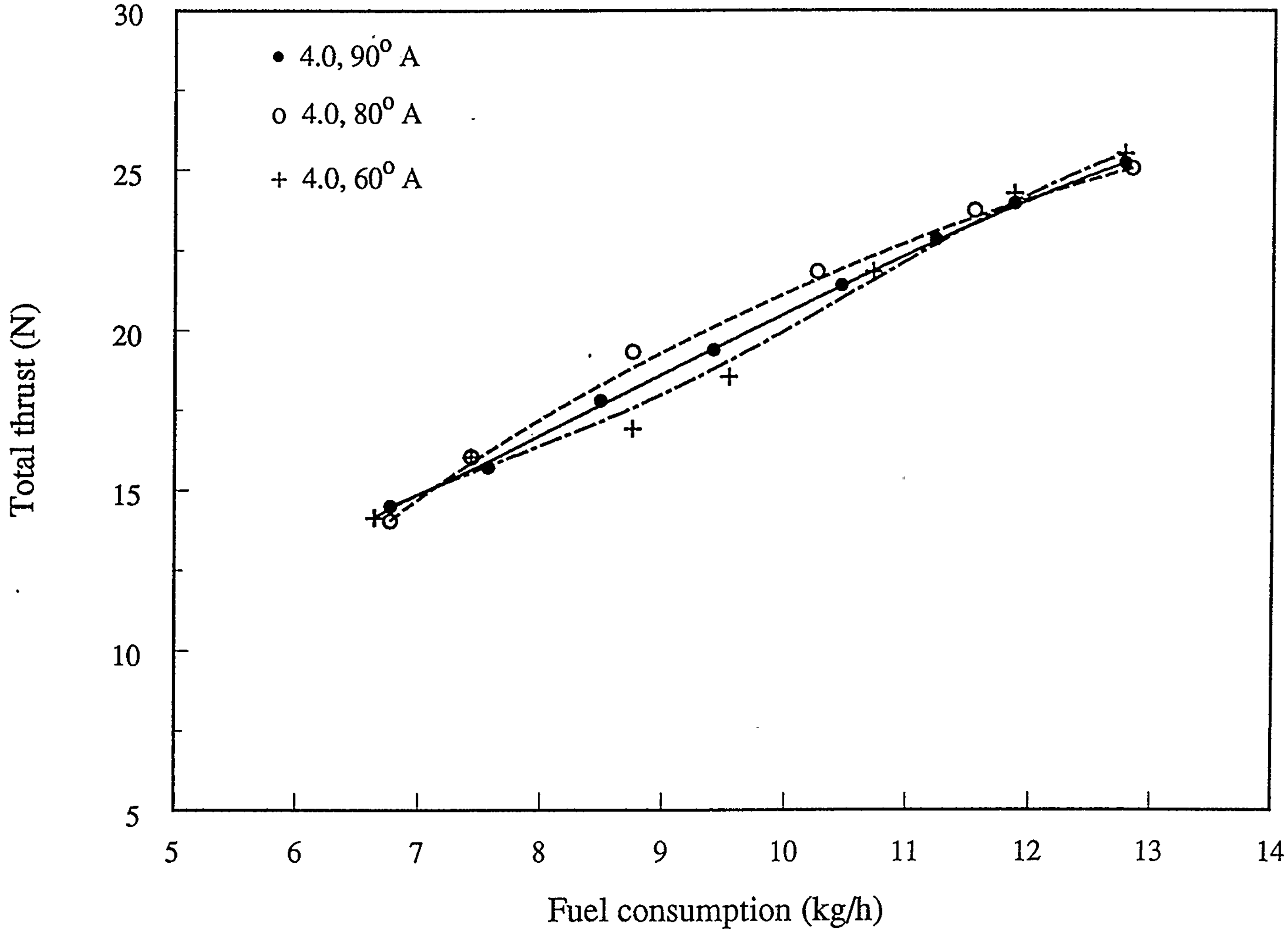

Figure 6.2: Performance of pulse combustor using fuel nozzles with different spray cone angles

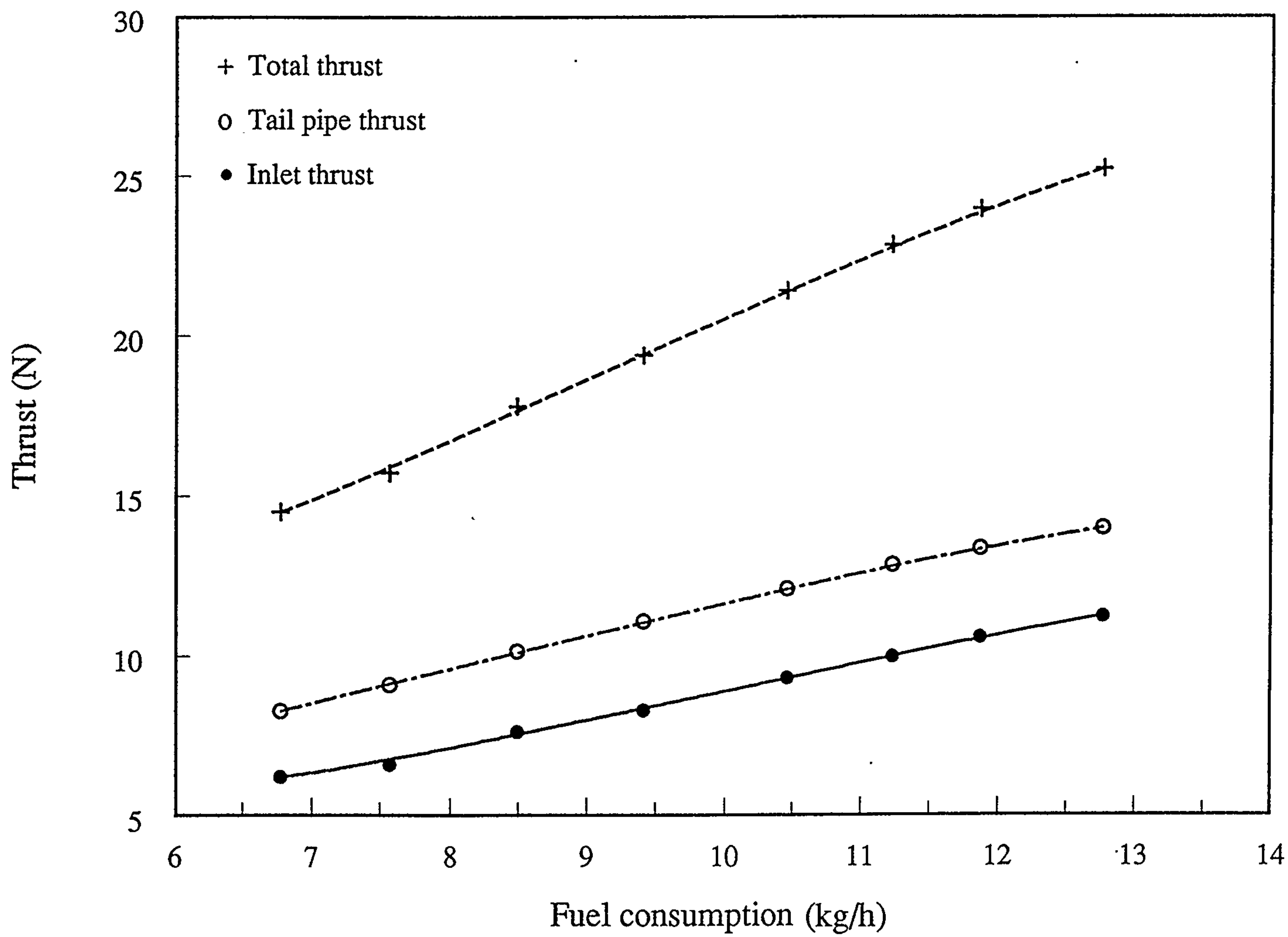

Figure 6.3: Total and individual thrusts produced by the pulse combustor using a 4.0, 90° A fuel nozzle

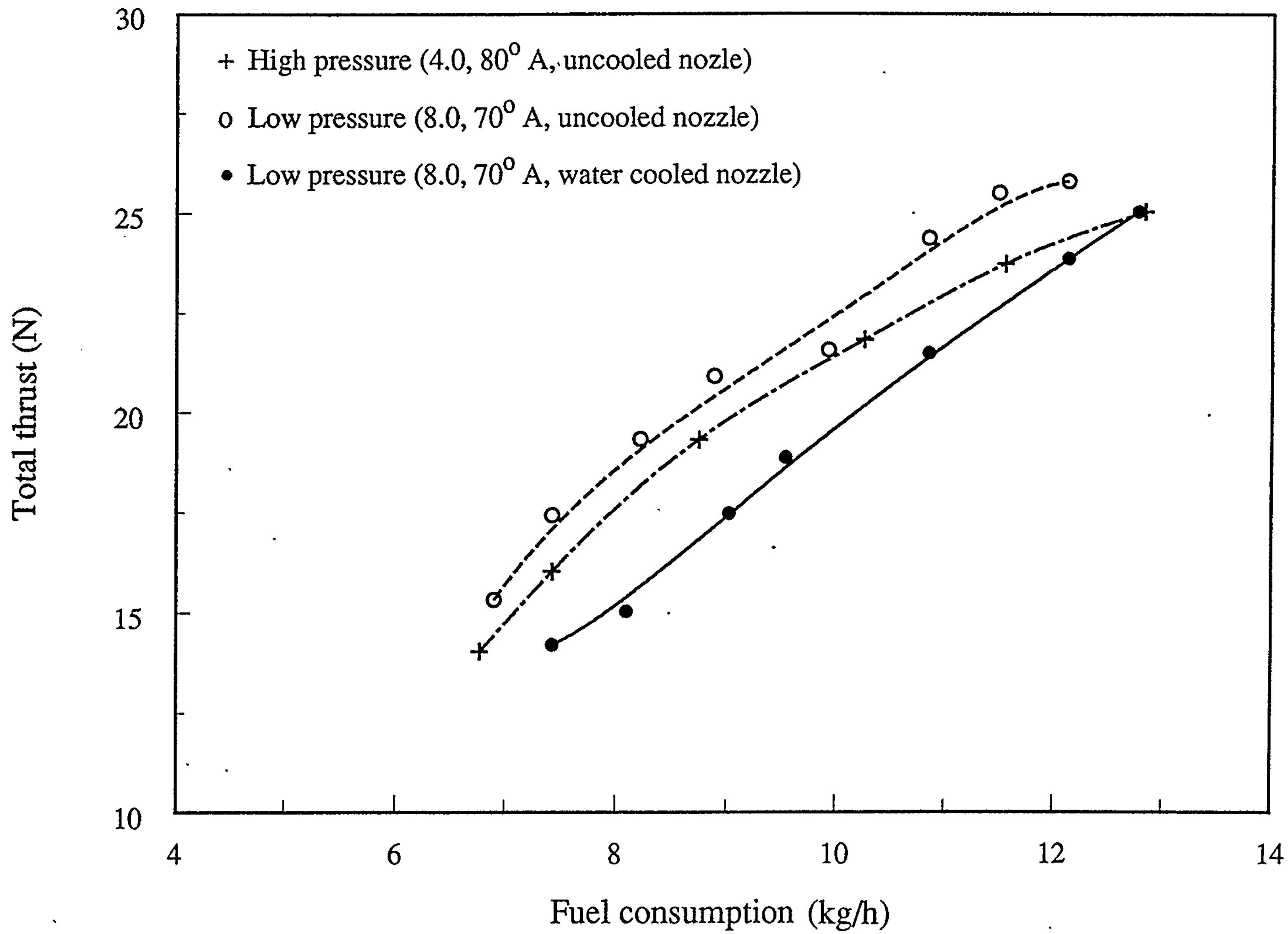

Figure 6.4: Effect of fuel pressure and water cooling on performance of the pulse combustor

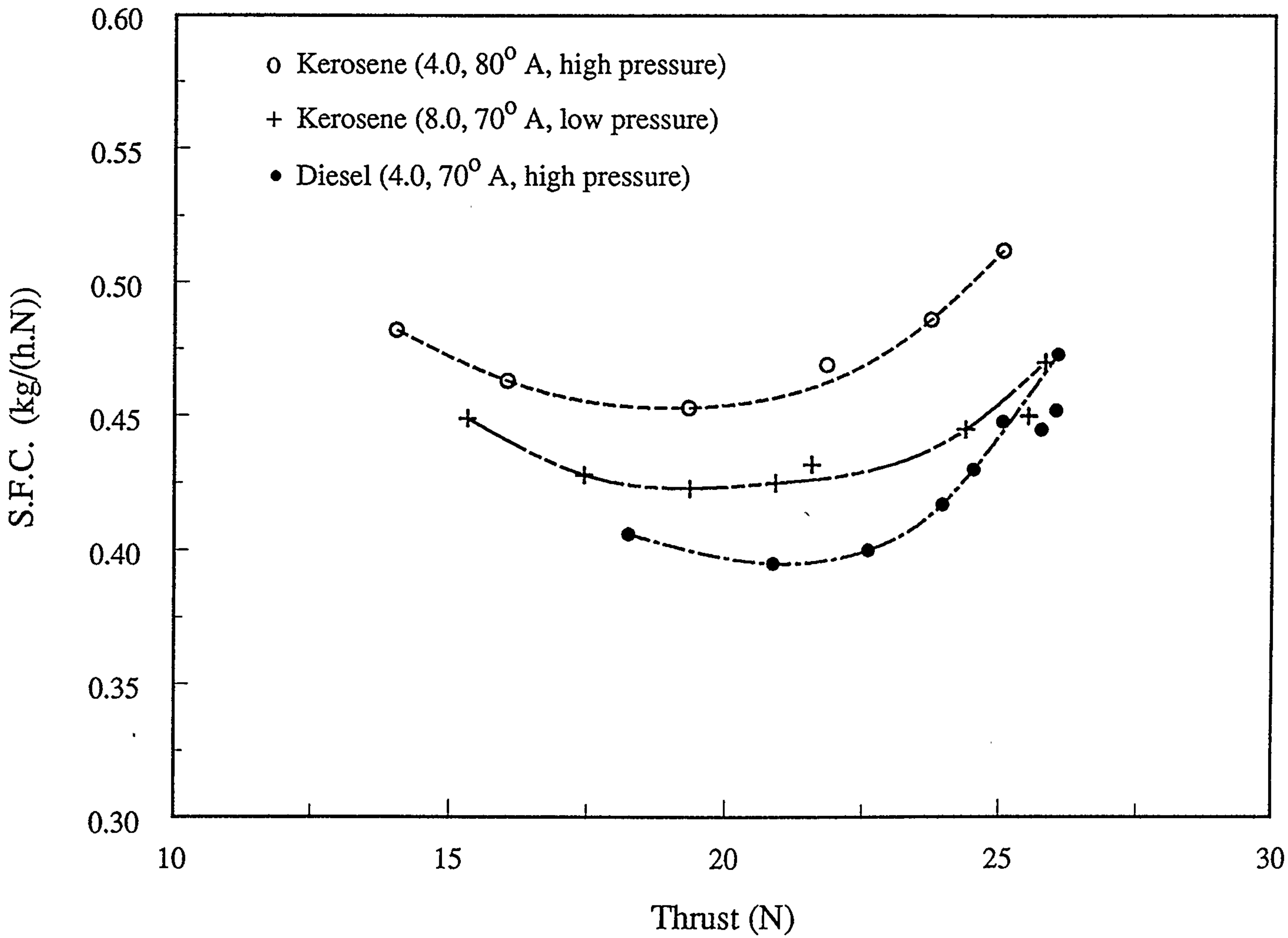

Figure 6.5: Specific fuel consumption of pulse combustor running on high pressure diesel and high and low pressure kerosene

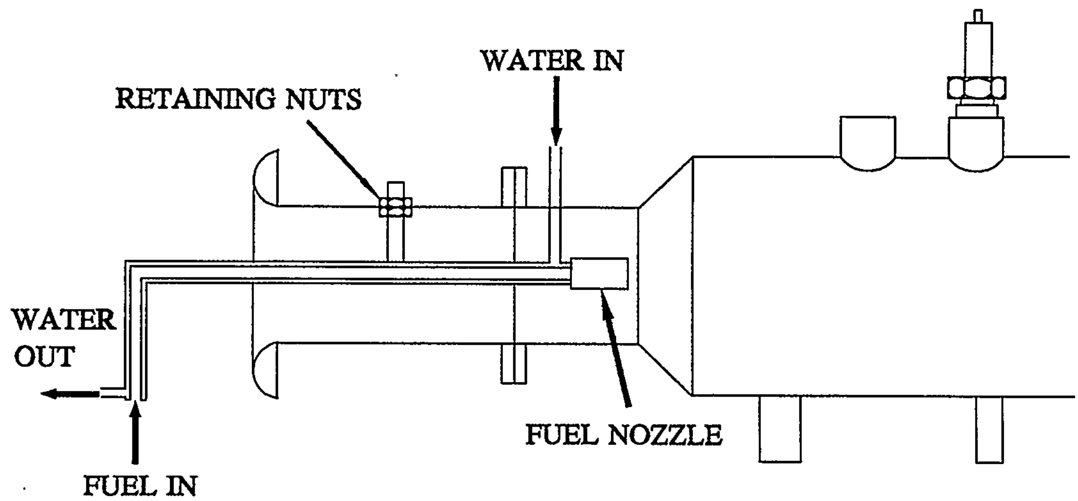

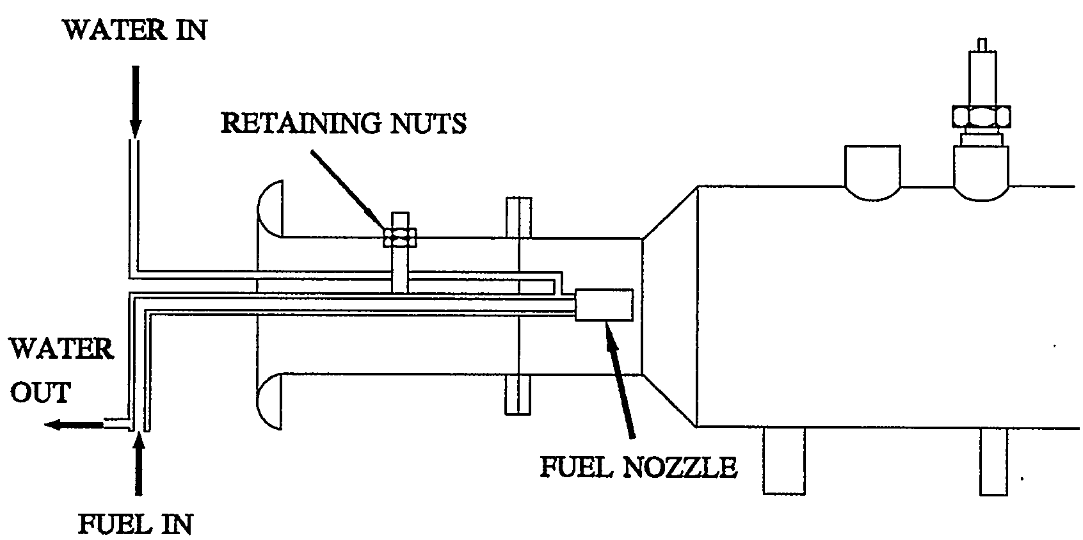

Figure 6.6: Water cooling circuits for the fuel nozzle

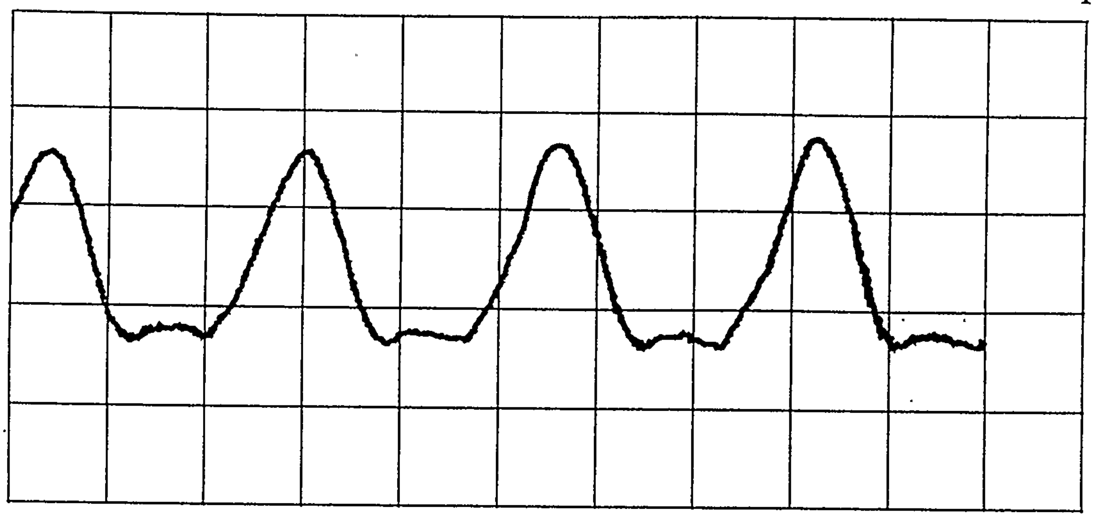

X axis: 2ms/div. Y axis: 34.47 kPa/div.

Fuel flow rate: 6.77 kg/h

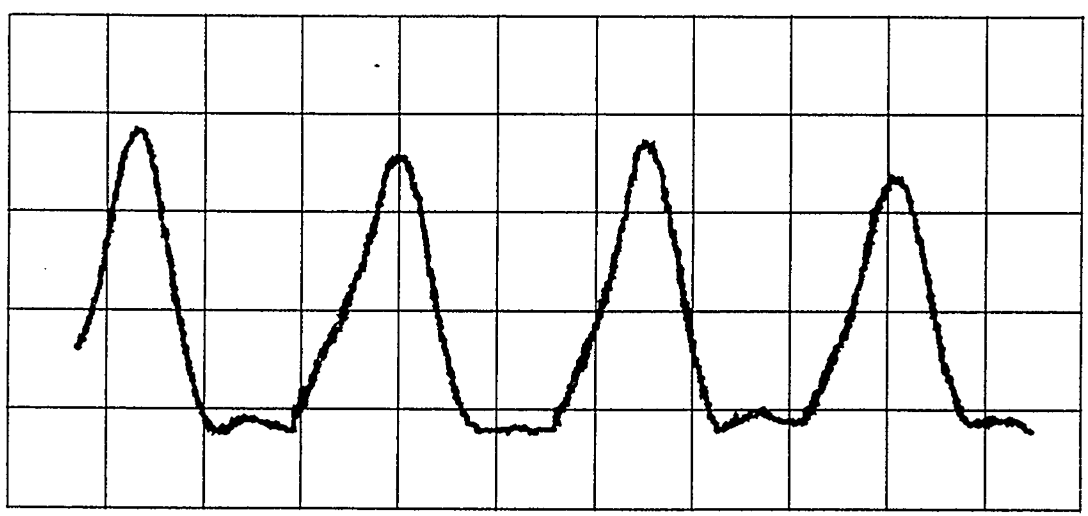

X axis: 2ms/div. Y axis: 34.47 kPa/div.

Fuel flow rate: 11.87 kg/h

Figure 6.7: Combustion chamber dynamic pressure for the high pressure steady flow fuel injection system using an uncooled fuel nozzle

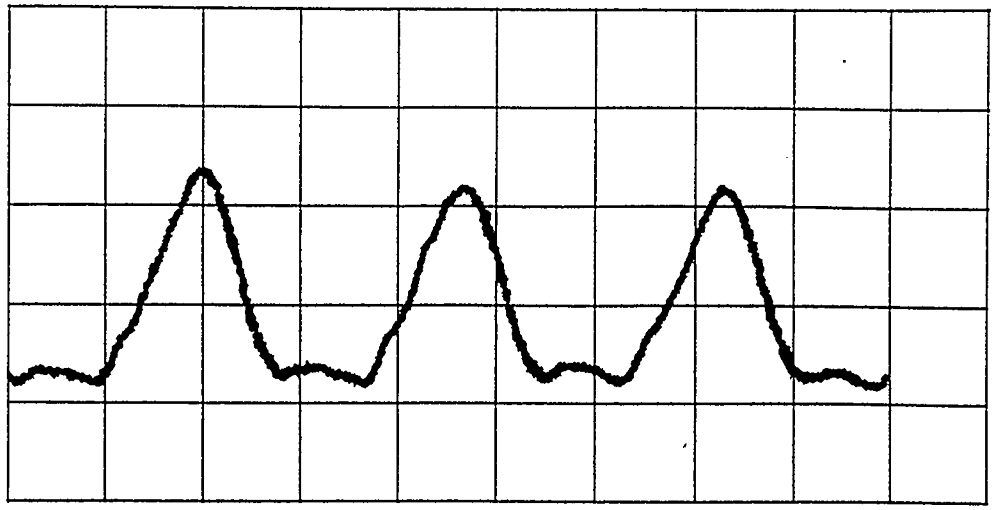

X axis: 2ms/div. Y axis: 34.47 kPa/div.

Fuel flow rate: 6.09 kg/h

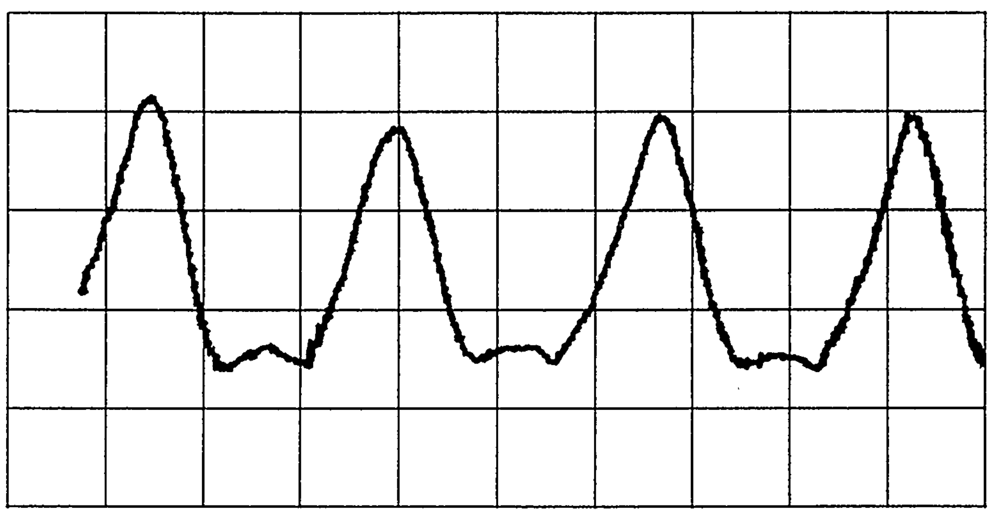

X axis: 2ms/div. Y axis: 34.47 kPa/div.

Fuel flow rate: 9.28 kg/h

Figure 6.8: Combustion chamber dynamic pressure for the low pressure steady flow fuel injection system using an uncooled fuel nozzle

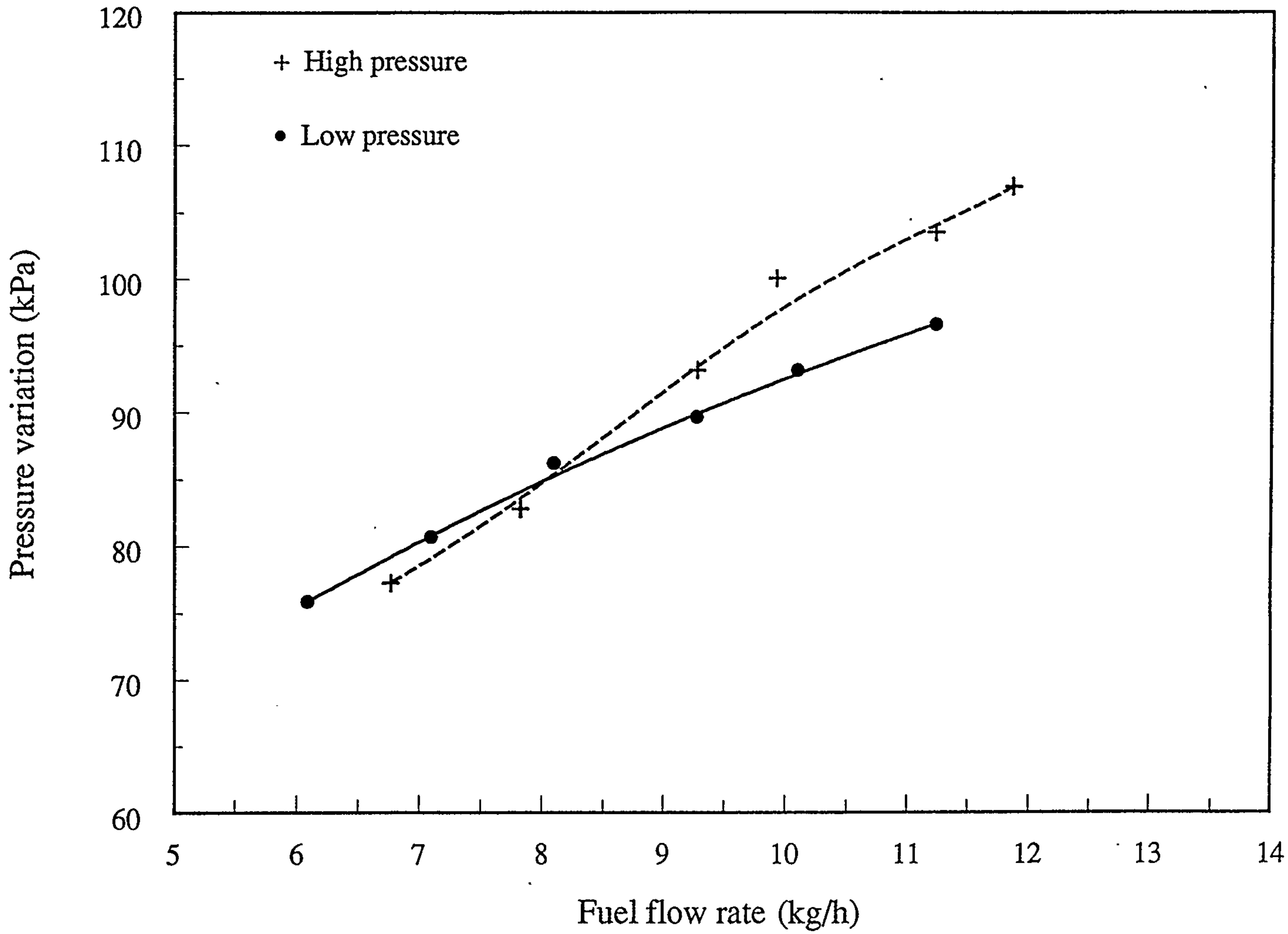

Figure 6.9: Maximum combustion pressure variation at different fuel flow rates for the high and low pressure steady flow fuel injection systems using uncooled fuel nozzles

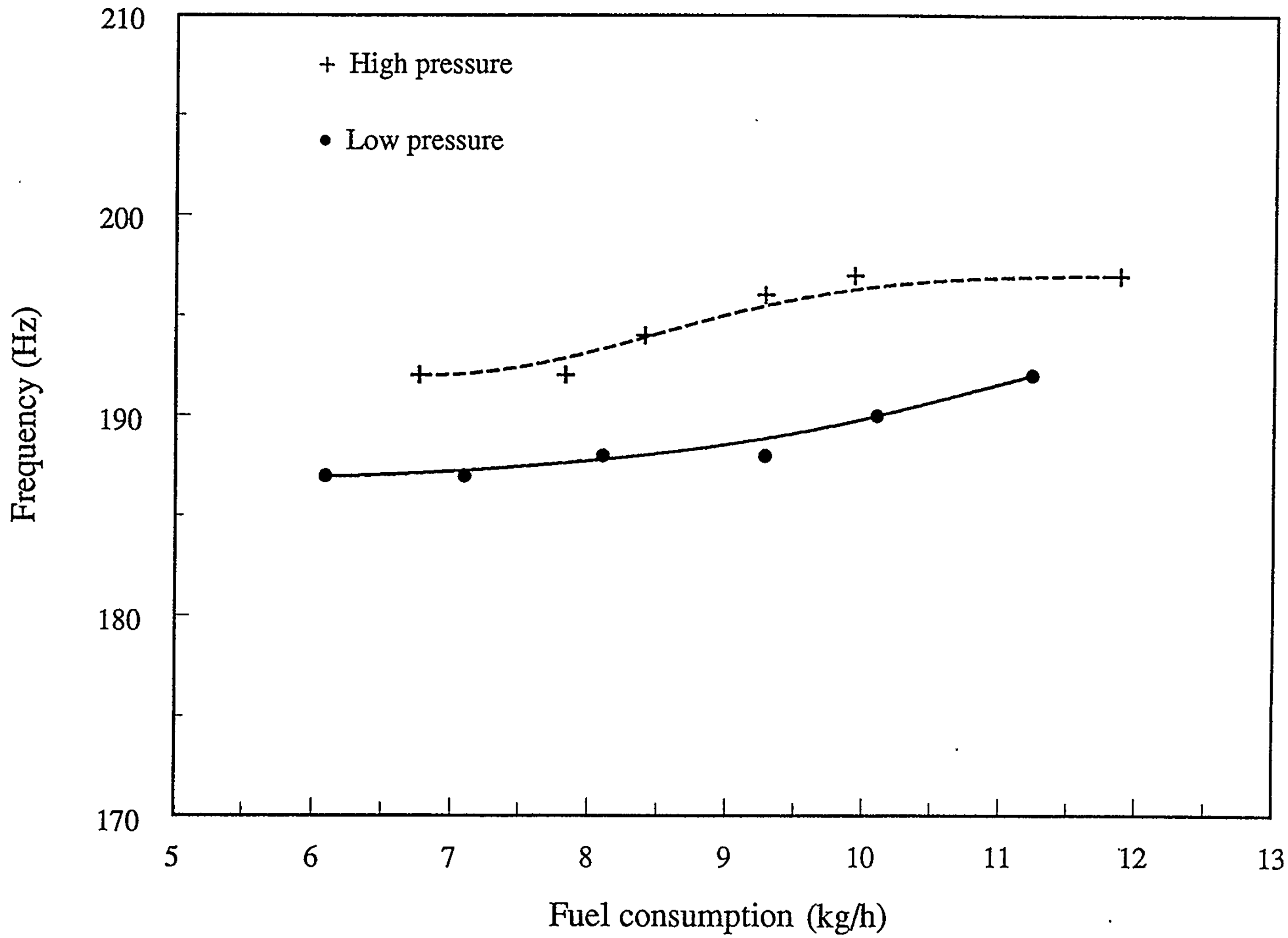

Figure 6.10: Variation of combustor frequency with fuel flow rate for the high and low pressure steady flow fuel injection systems using uncooled fuel nozzles

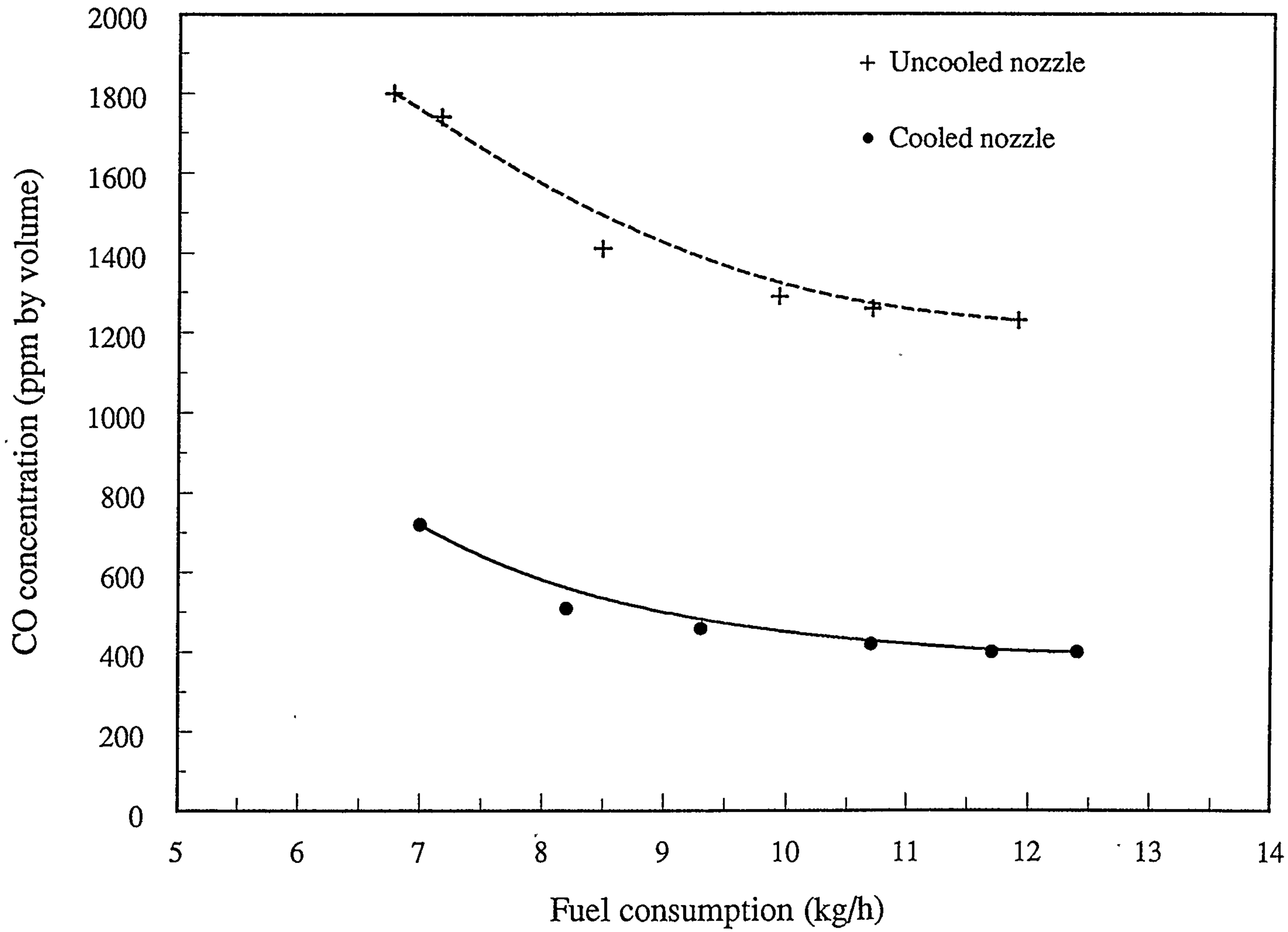

Figure 6.11: Concentration of CO in inlet of pulse combustor using high pressure steady flow fuel injection system

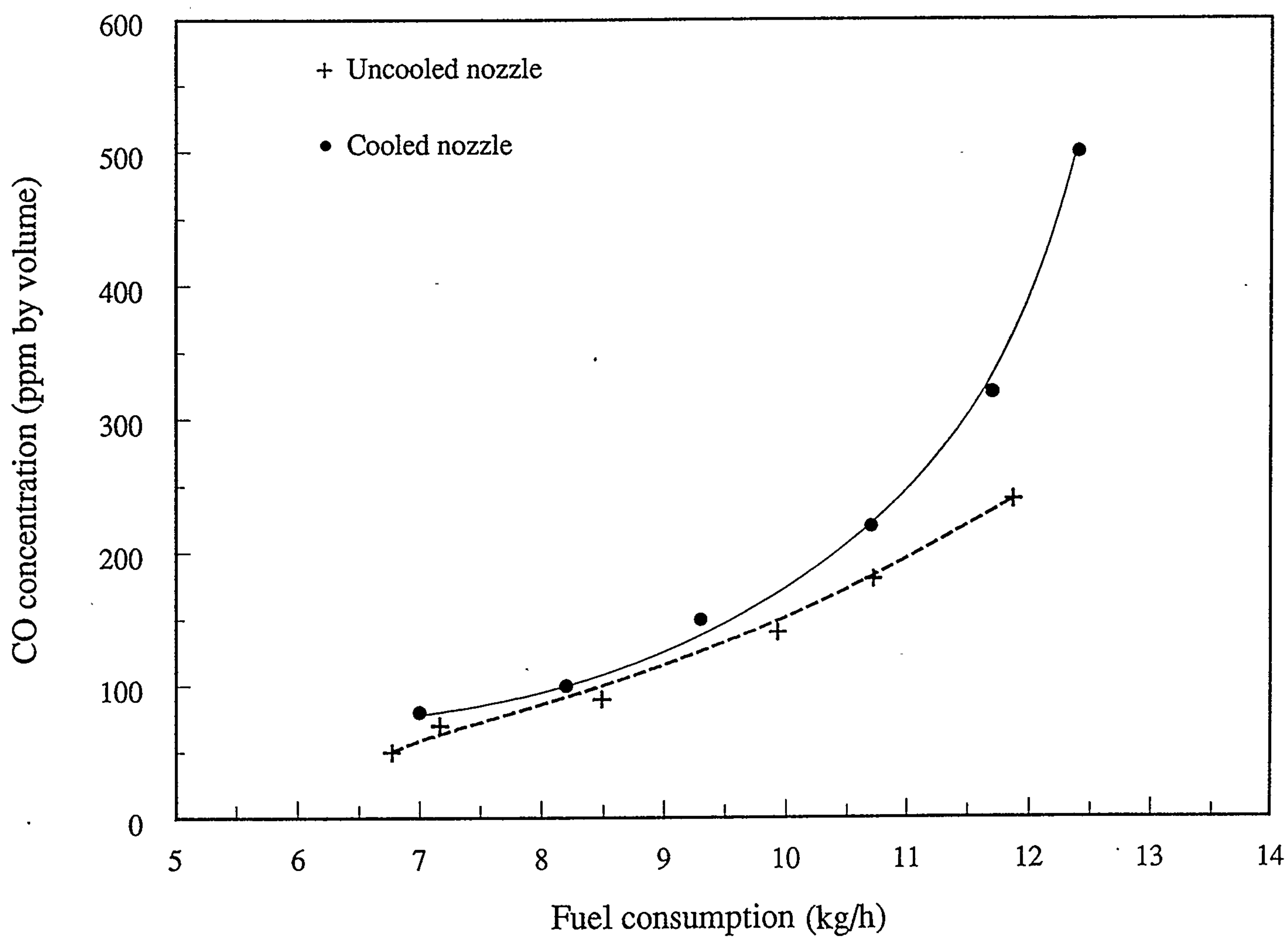

Figure 6.12: Concentration of CO in the tail pipe of pulse combustor using high pressure steady flow fuel injection system

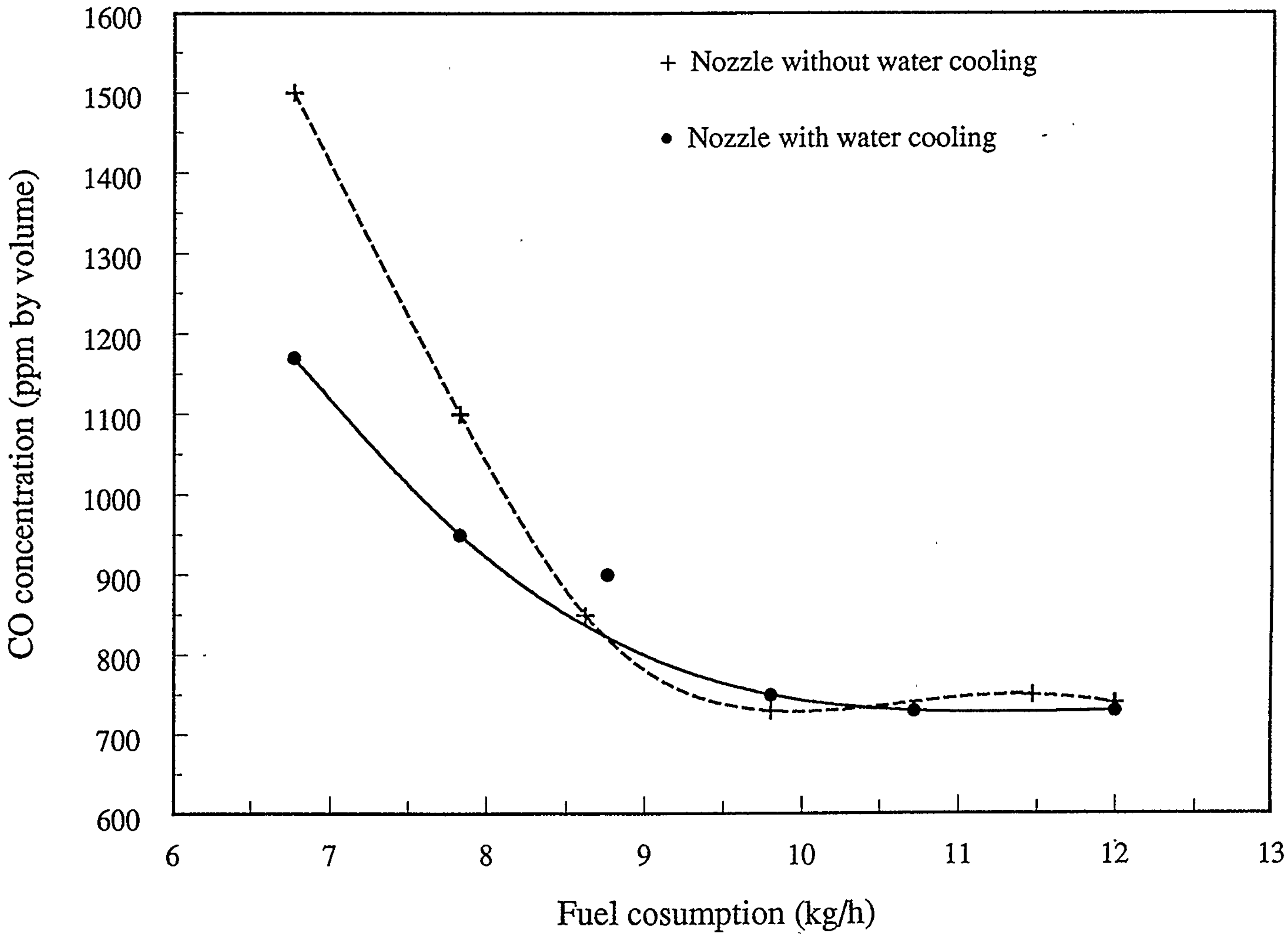

Figure 6.13: Concentration of CO in inlet of pulse combustor using low pressure steady flow fuel injection system

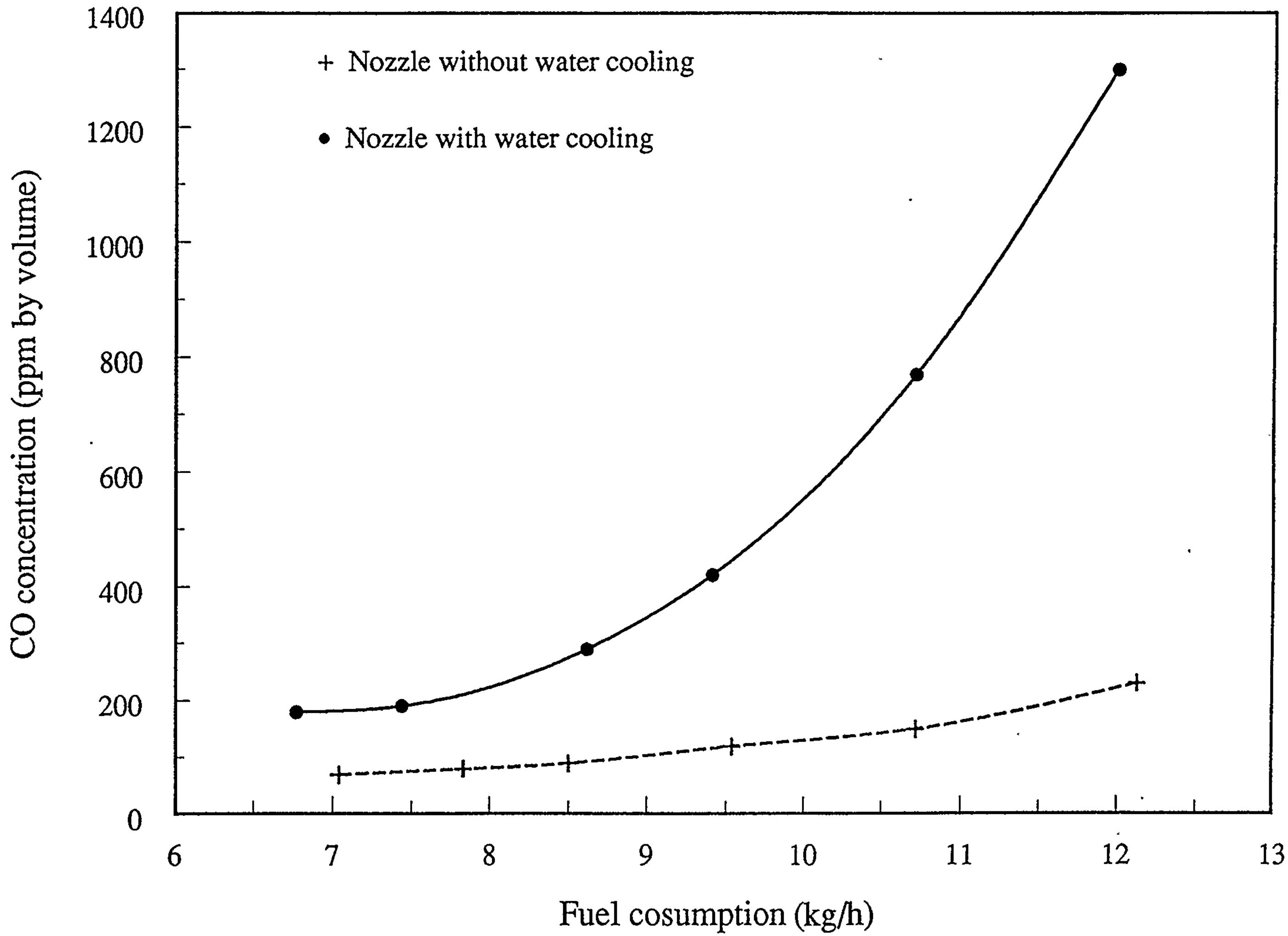

Figure 6.14: Concentration of CO in tail pipe of pulse combustor using low pressure steady flow fuel injection system

CHAPTER 7 HIGH PRESSURE FUEL INTERRUPTER SYSTEM: PROCEDURE, OBSERVATION, RESULTS AND DISCUSSION

7.1 OPERATING PROCEDURE

The procedure followed for starting, running and switching off the pulse combustor equipped with the fuel interrupter system was the same as that followed for the high and low pressure steady flow fuel injection systems (section 6.1).

7.2 GENERAL OBSERVATIONS

(1) After the initial test run with the Mark 1 fuel interrupter system it was found that the retaining hexagon nut that held the diaphragm and the spool together came off during the running of the pulse combustor. This was due to the mechanical vibrations of the pulse combustor, as the fuel interrupter was mounted on the same frame as the pulse combustor. The problem was solved by replacing the stainless steel nut with a plastic (nylatron) nut. Another advantage of the nylatron nut was that it was lighter than the stainless steel nut and this reduced the inertia of the moving parts.

(2) It was observed that after four to five test runs the diaphragm, cut out of a neoprene sheet, warped because of swelling. Thus the diaphragm had to be changed frequently. The swelling was caused by the neoprene material coming in contact with kerosene that leaked from the clearance between the spool and the interrupter body. This disrupted the proper working of the interrupter.

(3) On occasions the neoprene diaphragm material got sheared around the periphery of the aluminum washer at its back (Figure 3.12). This was caused by the pushing of the diaphragm by the combustion chamber pressure against the washer. Rounding off the outer edge of the washer seemed to reduce the risk of shearing.

(4) As shown in Figure 3.1 a hole had to be cut in the middle of the diaphragm to accommodate the spool. The two were locked together by a retaining nut. There was always a possibility that pressurized air on the combustion chamber side of the diaphragm could escape around the threads of the spool to the other side of the diaphragm. If this was to happen sufficient force may not be available to move the spool.

To check the possibility of leakage the interrupter was immersed in water and a static pressure was applied to the combustion chamber side of the diaphragm. It was observed that air bubbles came out from the other side of the diaphragm at a static pressure of approximately 20 kPa gauge. This was below the peak firing pressure of the pulse combustor. To stop the leakage of air, a silicone sealant material was applied on the threads of the spool and the retaining nut. The static pressure required to lead to leakage around the threads of the spool in this case was about 125 kPa gauge. This was substantially higher than the peak firing pressure of the pulse combustor. Another benefit of using the silicone sealant was that it did not form a strong bond between the spool and the nut. Thus the nut could be easily unfastened to replace the diaphragm.

(5) The return spring, used in the interrupter to bring back the spool to its original position once the combustion chamber pressure fell below atmospheric pressure, was chosen by trial and error. It was found that a weak spring did not have enough tension to force the spool back to its original position. While, too strong a spring did not allow the spool to move the full distance with the build up of pressure in the combustion chamber. After a few trials an appropriate spring was found that allowed the spool to move its full distance and returned it to its original position once the pressure in the combustion chamber fell below atmospheric pressure.

(6) For the proper functioning of the delivery valve, used with the Mark 2 and 3 interrupters, air from the nozzle fuel line had to be purged. It was found that with air trapped in the fuel line the delivery valve did not produce a sharp cut off of the fuel spray. Once the air in the fuel line was purged by spraying the fuel in open air for a couple of minutes, the delivery valve gave a sharp cut off of fuel from the fuel nozzle.

(7) The pulse combustor took more time to go into resonance with the interrupter system than it did with the high and low pressure fuel injection fuel systems.

7.3 MARK 1 INTERRUPTER: RESULTS AND DISCUSSION

A 430 mm long connector pipe having an inner diameter of 7.6 mm was used to transmit the pressure signal from the combustion chamber of the pulse combustor to the diaphragm of the interrupter. The connector pipe was water cooled to protect the diaphragm from the hot combustion gases.

The combustor went into resonance and smooth running was achieved. Exhaust gases from both the inlet and tail pipe were analyzed to determine the concentration of CO. Figure 7.1 shows the concentration of CO in the tail pipe of the combustor using a 4.0, 90°A uncooled nozzle. As would be expected the concentration of CO increased with fuel flow rate. On the whole CO emissions from the tail pipe were low. However, when the concentration of CO in the inlet exhaust gases was evaluated, it was found to be quite high. At a fuel flow rate of 9.2 kg/h CO emissions in inlet gases were 1500 ppm.

It was suspected that this could be due to the improper phasing of the fuel supply with the pressure variation in the combustion chamber of the pulse combustor. Therefore, an approximate calculation (section 4.2 of Chapter 4) was made to evaluate the length of connector pipe required for correct phasing of the pulse combustor. It was assumed that the interrupter worked on pressure sensed from the cycle previous to the current operating cycle of the pulse combustor. Accordingly, the correct length of the connector pipe was estimated to be around 1.87 m.

Different connector pipe lengths were tested and the concentrations of CO, CO_2 and O_2 in the inlet and tail pipe for the various connector pipes are shown in Tables 7.1 and 7.2 respectively. The fuel flow rate was set at 9.2 kg/h. Variations of CO concentrations in the inlet and tail pipe are also plotted in Figure 7.2. It can be observed from the plot that there was no significant variation in the CO emissions in the inlet with different connector pipe lengths. This can be explained along the following lines. As outlined in section 3.3.4.2 of Chapter 3, when the spool for the Mark 1 interrupter was moved by hand to the fuel cut-off position it took the fuel spray 3 to 5 seconds to die down. For the proper functioning of the interrupter the spray cut-off had to take place in a time less than 10% (approximately) of the time for one cycle of the pulse combustor (cycle time = 5.2 ms). Clearly this was not being achieved and the combustor was still receiving a continuous supply of fuel all through the cycle in spite of using the interrupter system. From Figure 6.11 it can be seen that at a fuel flow rate of 9.2 kg/h for the high pressure steady flow fuel injection system the concentration of CO in the inlet was around 1400 ppm. This is comparable to the CO emission values in the inlet using the Mark 1 interrupter at the same fuel flow rate (Figure 7.2). This further lends credence to the hypothesis that in spite of using an interrupter the combustor received a continuous supply of fuel through the cycle because of fuel dribbling from the nozzle.

7.4 MARK 2 INTERRUPTER: RESULTS AND DISCUSSION

7.4.1 Effect of Connector Length

The Mark 2 interrupter was equipped with a delivery valve to give a sharp cut-off of the fuel spray. It was found by spraying fuel in open air that the delivery valve did drastically cut down dribbling of the fuel nozzle as compared to the Mark 1 interrupter.

To determine the optimum length of the connector pipe for correct phasing of the fuel supply with the combustion chamber pressure, different lengths of connector pipes ranging from 0.30 m to 2.05 m were tested. Tables 7.3 and 7.4 show the exhaust gas composition, using different lengths of connector pipes, for the inlet and tail pipe of the pulse combustor with the Mark 2 interrupter for a fuel flow rate of 8.8 kg/h. A 4.0, 70^0 A uncooled fuel nozzle was used. Concentrations of CO for the two cases are plotted in Figure 7.3. CO concentrations in the tail pipe did not show appreciable variations with different connector pipe lengths, whereas for the inlet a sharp reduction in CO emissions was detected for a connector pipe length of 710 mm.

So the exhaust gas compositions for the inlet and tail pipe were analyzed for the 710 mm connector over the full fuel flow range. These values are tabulated in Tables 7.5 and 7.6. The values of the concentration of CO for the inlet and tail pipe are plotted in Figure 7.4. Also shown in the figure are CO emissions in the inlet and tail pipe for the high pressure steady flow fuel injection system using an uncooled fuel nozzle. On comparing the two fuel systems it can be observed that the CO emission levels in the tail pipe for the two cases were very similar. It was for the inlet pipe of the pulse combustor that the interrupter fuel system showed a marked improvement over the high pressure steady flow fuel system. Thus it would seem that the Mark 2 interrupter was somewhat successful in bringing down the CO emission in the inlet as compared to the Mark 1 interrupter, although the CO emissions from the inlet were still high.

7.4.2 Influence of Air Swirlers

According to Kentfield (57) the use of air swirlers in lightly loaded pulse combustors had previously resulted in a better mixing of fuel with fresh air and products of combustion. This was attributed to the swirl provided to the incoming air during recharging. So to investigate the effect of air swirl on the CO emission from the inlet, a set of three swirlers was soldered longitudinally to the nozzle fuel line in the inlet pipe. The air swirlers were 25 mm long and 0.79 mm thick. The angle of the swirlers varied from 10° to 40°. The concentration of CO in the inlet for each configuration of the swirler is shown in Table 7.7. The fuel flow rate was set at 9.0 kg/h and 4.0, 60°A uncooled fuel nozzle was used. The length of connector pipe was 710 mm. Variations of CO emissions in the inlet are also plotted in Figure 7.5. As can be seen there was no marked difference in the CO levels. While running the tests it was observed that for the 30° and 40° swirlers operation of the pulse combustor became rough. This was thought to be due to either a disruption of the fuel spray by the large swirl in the incoming air during recharging or the increased blockage of the inlet passage by the swirlers as the angle of the swirlers was increased. As the swirlers did not prove beneficial they were not used for the subsequent tests.

7.4.3 Effect of the Position of Fuel Nozzle in the Inlet of Pulse Combustor

Positioning of the fuel nozzle in the inlet of the pulse combustor is shown in Figure 3.11. In this set up the tip of the nozzle was approximately 10 mm from the start of the conical section that jointed the inlet to the combustion chamber. All the tests described till now were with the fuel nozzle in this position. The fuel nozzle was gradually moved towards the combustion chamber to investigate the variation in CO emission levels with the position of the fuel nozzle. The fuel setting, connector pipe and fuel nozzle were the same as in section 7.4.2.

When the nozzle was moved flush with the conical frustum it was found the CO emission dropped from 910 ppm (for the original setting) to 710 ppm, though the running became worse in the latter configuration. Moving the fuel nozzle 10 mm further towards the combustion chamber caused the pulse combustor to cease resonance. The reason for this may have been that the fuel nozzle was engulfed in the eddies in the conical frustum of the combustion chamber and this disrupted the fuel spray leading to the blowout in the pulse combustor.

7.4.4 Effect of Fuel Spray Cone Angle

Another variable on which the CO emissions from the pulse combustor could depend was the fuel spray cone angle. The commercial fuel nozzles used for injecting fuel were available with spray cone angles ranging from 45° to 90°. Table 7.8 shows the CO emissions in the inlet of the pulse combustor for different fuel spray cone angles using the Mark 2 interrupter and a 0.71 m connector pipe. The fuel flow rate was set at 9.1 kg/h. The variation of CO emissions is also plotted in Figure 7.5. CO emissions did not show an appreciable variation with the different fuel nozzles. However, the running of the combustor was smoother with the 90° fuel nozzle than with the 45° fuel nozzle. This could have been caused by the better distribution of fuel in the combustion chamber for the former fuel nozzle, leading to a better mixing of fuel and fresh air.

7.4.5 Effect of Water Cooling

As mentioned in section 6.3.5, water cooling the fuel nozzle for the high pressure steady state fuel injection system decreased the CO emissions in the inlet by a factor of

2 to 3. Hence, this warranted the use of water cooling for the fuel nozzle with the interrupter system also. The water circuit used was the same as before. Values of the CO, CO_2 and O_2 concentrations in the inlet and tail pipe are tabulated in Tables 7.9 and 7.10 respectively. The variation of CO emissions in the inlet for the cooled and uncooled fuel nozzles is plotted in Figure 7.6. The same is done for the tail pipe in Figure 7.7. CO emissions in the inlet decreased with water cooling of the fuel nozzle. This was because, in the cooled fuel nozzle, fuel was injected in the form of well atomized liquid droplets that were harder to blow back with the back flow of exhaust gases from the inlet. This was unlike the case with the uncooled fuel nozzle in which fuel was injected in vaporized form.

Two reasons led to the decrease in inlet CO emissions with fuel flow rate for the cooled fuel nozzle. With an increase in fuel flow rate, the pressure at which the fuel was injected into the combustion chamber increased. This led to [1] a better atomization of the fuel spray resulting in a better mixing of the fuel with fresh air and [2] an increase in the velocity of the fuel droplets making it harder for them to be blown out of the inlet during back flow.

7.4.6 Design Errors and Modifications

(A) Spool Movement

As indicated in section 3.3.4.2 the working of the Mark 2 interrupter was contingent on the full travel (5 mm) of the spool at the natural frequency of the pulse combustor so that the appropriate fuel ports were opened or closed. Till now there was no quantitative proof that the spool was travelling the full distance at the correct frequency.

To determine the frequency of the spool a hole was drilled in the back hub of the interrupter to accommodate a magnetic pickup as shown in Figure 3.23. The voltage output from the magnetic pickup was fed to a storage type oscilloscope. From the voltage plot obtained on the screen of the oscilloscope the frequency of the spool could be determined.

The principle behind the working of a magnetic pickup is that as ferrous metal passes through a magnetic field of the magnet in the magnetic pickup, it causes a change in the magnetic field. This induces a change in the output voltage from the magnetic pickup, from which the frequency of the moving part can be determined.

To determine the travel of the spool a small window was machined in the hub at the back of the interrupter. The two extremities of the spool travel were judged approximately by the contact of the spool with metal stops.

When the Mark 2 interrupter was run in the same configuration as in section 7.4.5 two interesting facts were revealed. [1] The frequency at which the spool oscillated was 190 Hz. As can be confirmed from Figure 6.10 this was also the natural frequency of the pulse combustor. [2] The travel distance of the spool was half of the total travel distance required for the interrupter to work properly. Thus although the spool was moving at the correct frequency, yet its travel was not enough to fully cut off the fuel supply to the nozzle i.e. till now fuel was being supplied to the pulse combustor all through the cycle. Instead of giving a sharp cut-off of the fuel supply when the pressure in the pulse combustor rose above atmospheric pressure, the interrupter just modulated the fuel supply. Fuel modulations did help reduce the CO emissions from the pulse combustor to some extent but did not provide the desired results.

There were several causes for the inadequate displacement of the spool. By applying a static pressure on the combustor side of the interrupter it was found that the original configuration of the spool, diaphragm and the return spring required a static pressure of 35 kPa gauge for the spool to undergo the full displacement of 5 mm. The dynamic pressure available from the combustion chamber was approximately of the same magnitude. Therefore, the force available from the pulse combustor seemed inadequate to move the spool over the full stroke. Primarily most of the force required was being taken up to move the 1.59 mm thick neoprene diaphragm. To reduce the required force the original diaphragm was replaced with a new 0.79 mm thick neoprene diaphragm. The static pressure required to move the spool with this diaphragm was reduced to 20 kPa gauge. This was a significant improvement over the old configuration.

Another reason for the inadequate spool displacement in the Mark 2 interrupter was that the holes through which the diaphragm communicated with the combustion chamber and the atmosphere (Figure 3.16) were too small. The diameter of the hole for the pressure tapping from the pulse combustor was 7.62 mm and for the vent to atmosphere was 5.08 mm. For the proper working of the interrupter it was calculated that the required velocity of air passing through the former was 347 m/s and the latter was 433 m/s. Thus the openings on both sides of the diaphragm were inadequate. The atmospheric vent opening acted as an effective damper to inhibit the movement of the diaphragm and the spool. To circumvent this problem the diameter of the hole for the pressure tapping was increased to 10.16 mm. On the other side of the diaphragm (open to atmosphere) three more holes were drilled to give a combined opening equivalent to a single 20.32 mm diameter hole. Also the dead volume in front of the diaphragm was reduced from 18090 mm^3 to 3620 mm^3 by machining off the flange. These measures brought the air velocities in the pressure tapping hole to 88 m/s and in the atmosphere vent holes to 20 m/s. Thus the diaphragm and spool assembly was now more free to move.

When the pulse combustor was run with these modifications it was observed that modifications did have the desired result and the spool displacement increased to 5 mm. This was sufficient for the proper working of the interrupter. Another observation that was made while running the pulse combustor using the modified Mark 2 interrupter was that the pulse combustor ran only with the uncooled fuel nozzle. Water cooling the fuel nozzle caused the combustor to cease resonance. It was suspected that this had to do with the working of the delivery valve. So attention was focused on the design and working of the delivery valve.

(B) Delivery Valve

The delivery valve used with the Mark 2 interrupter is shown in Figure 3.19. The piston of the delivery valve was fabricated out of stainless steel and weighed 6.03 g. The fuel holes in this piston were 11 mm below the valve seat. The amount of fuel going into the pulse combustor for one cycle was compared with the draw back volume of fuel of the delivery valve. Taking the density of kerosene as 800 kg/m^3 and the frequency of the combustor as 190 Hz.

Fuel going into the pulse combustor for one cycle at a fuel consumption rate of 8 kg/h = (8/3600).190 = 11.7 mg

Fuel draw back volume in the delivery valve for one cycle = $(\pi/4)(9)^2$ 11 = 699.7 mm^3 = 0.559 g.

Comparing the two values it can be seen that the fuel draw back by the delivery valve was 48 times the fuel going to the pulse combustor for one cycle. This presumably led to cavitation spaces in the nozzle fuel line. This seemed to explain why the modified Mark 2 interrupter worked with the uncooled nozzle and not with the cooled nozzle. With the uncooled fuel nozzle the fuel tended to vaporize in the fuel line and the fuel vapours occupied the empty space available. On the other hand, for the cooled nozzle, the fuel in the nozzle line was kept in liquid form by the action of the cooling water and the empty space in the fuel line led to the disruption of the fuel spray and consequently the running of the pulse combustor.

So a new delivery valve was fabricated out of aluminium as shown in Figure 7.8. Circular grooves were cut on the circumference of the piston to reduce viscous drag. The aluminium valve had the same dimensions as the old stainless steel valve except that the fuel holes in the new valve were 1.5 mm below the valve seat. This reduced the fuel draw back by the delivery valve to 0.076 g/cycle. Aluminium was chosen for the delivery valve material as it is much lighter than stainless steel. This reduced the mass of the valve from 6.03 g for the stainless steel version to 1.7 g for the aluminum item. Thus another advantage of aluminum was a reduced valve inertia. Using the aluminum delivery valve the modified Mark 2 interrupter did go into resonance with the water cooled fuel nozzle.

7.4.7 Dynamic Analysis of Modified Mark 2 Interrupter with Aluminium Delivery Valve

A dynamic analysis of the modified Mark 2 Interrupter with the aluminium delivery valve was carried out to calculate the length of connector pipe required for correct phasing of the fuel supply. This was similar to the analysis made for the Mark 1 interrupter as presented section 4.2. The only difference was that the time taken to open the delivery valve had to be taken into consideration also.

t_1 = time required for the pressure pulse to travel from the combustion chamber of pulse combustor to the diaphragm of the interrupter = 1.66x ms

t_2 = time required to move the spool by 0.005 m = 1.28 ms

t_3 = time required for the pressure pulse to travel in the fuel line from the interrupter to the nozzle tip = 0.6 ms

t_4 = time required to open the delivery valve (ms).

Where x is the length of the connector pipe length. The opening of the delivery valve was brought about by the fuel pressure working against return spring which was in compression.

Displacement of spool (S) = 0.5 mm

Area of piston (A) = 63 mm^2

Fuel pressure (P) = 500 kPa (gauge)

Spring constant (K) = 720 N/m

Mass of aluminum valve (m_1) = 1.7 g

Initial compression of spring (y) = 25.4 mm

Piston displacement required to open the fuel holes (z) = 2 mm

Mass of spring (m_2) = 2.07 g

Preload on the aluminium piston = K.y N

Force acting on the aluminum piston because of fuel pressure = P.A N

Net force acting on the aluminium piston (F) = PA - Ky - Kz/2 = 12.49 N

Considering half of the spring mass in the moving mass

a = linear acceleration of piston

$$= \frac{F}{m_1 + \frac{m_2}{2}} = 4567.45 \text{ m/s}^2$$

therefore,

$$t_4 = \sqrt{2 \cdot \frac{z}{a}} = 0.94 \text{ ms}$$

For the interrupter to work on the pressure sensed from the cycle preceding the current operating cycle of the pulse combustor, the sum of t_1, t_2, t_3 and t_4 should equal 5.2 ms (time for one cycle).

therefore,

x = 1.43 m.

Thus the approximate length of the connector pipe for the modified Mark 2 interrupter with the aluminium delivery valve at a fuel pressure of 500 kPa gauge was 1.43 m.

Using different connector pipe lengths the combustor was run on the modified interrupter and the new delivery valve. The inlet exhaust gases were analyzed for the concentrations of CO, CO_2, O_2. The test results are shown in Table 7.11. The values of CO emissions from these tables are plotted in Figure 7.9. The CO emission reached a minimum for the connector pipe length of 1.23 m. This value was close to the 1.43 m length of connector pipe calculated theoretically for the proper phasing of the fuel supply to the combustor.

With the 1.23 m long connector pipe the pulse combustor was run over the full fuel flow range. The concentration of the exhaust gases for the inlet and tail pipe are presented in Tables 7.12 and 7.13. The values of CO emission are also plotted in Figure 7.10. CO emissions for the inlet first decreased with fuel flow rate, reached a minimum at a fuel flow rate of 7.7 kg/h (fuel pressure of 500 kPa gauge) and then increased with increasing fuel flow rate. The apparent cause for this was that the phasing of the fuel supply was dependent on the fuel flow rate. With increasing fuel flow rate the amplitude of pressure variations in the pulse combustor increased (Figure 6.9). This increased the force exerted on the diaphragm, thereby altering the phasing of the system by affecting t_2. Another effect of increasing the fuel flow rate was that the fuel pressure also increased. As the opening of the delivery valve depended on the fuel pressure, time t_4 decreased with an increase in fuel pressure. This again upset the phasing of the system at the fuel flow changed. Thus a minimum in CO emissions was reached at a particular fuel flow rate. An increase or decrease of fuel flow rate (or fuel pressure) from this point altered the phasing of the system leading to an increase in CO emissions.

Such a behaviour was not encountered with the original Mark 2 interrupter because spool movement was not adequate for the proper operation of the combustor.

7.5 MARK 3 INTERRUPTER: RESULTS AND DISCUSSION

Not much success was achieved with running the pulse combustor using the Mark 3 interrupter. It was found that, with the initial return spring used, the spool stayed in the nozzle cut-off position for a very long time. This was because the spool displacement required for this interrupter was only 2 mm compared to 5 mm for the Mark 2 interrupter. This resulted in fuel being injected into the combustion chamber for a small fraction of the total working cycle.

When this return spring was substituted with a stronger spring the aluminium washer at the back of the diaphragm failed. This was because the strong spring resisted the combustion chamber pressure on the diaphragm resulting in the failure of the washer.

No thrust readings were obtained for any of the three interrupter systems tested since the performance of these systems was not good.

LENGTH OF CONNECTOR PIPE (mm)	CO CONC. (PPM BY VOLUME)	CO_2 CONC. (%AGE BY VOLUME)	O_2 CONC. (%AGE BY VOLUME)
300	1440	0.380	20.5
710	1220	0.380	20.5
1040	1320	0.376	20.5
1330	1380	0.364	20.4
1590	1380	0.380	20.5
2050	1470	0.380	20.5

Table 7.1: Exhaust gas composition in inlet pipe using different length connector pipes for Mark 1 interrupter at a fuel flow rate of 9.2 kg/h

LENGTH OF CONNECTOR PIPE (mm)	CO CONC. (PPM BY VOLUME)	CO_2 CONC. (%AGE BY VOLUME)	O_2 CONC. (%AGE BY VOLUME)
300	100	3.40	16.2
710	150	3.95	16.2
1040	110	3.25	16.3
1330	110	3.45	16.6
1590	80	3.45	15.5
2050	90	3.45	15.8

Table 7.2: Exhaust gas composition in tail pipe using different length connector pipes for Mark 1 interrupter at a fuel flow rate of 9.2 kg/h

LENGTH OF CONNECTOR PIPE (mm)	CO CONC. (PPM BY VOLUME)	CO_2 CONC. (%AGE BY VOLUME)	O_2 CONC. (%AGE BY VOLUME)
300	1330	0.35	20.4
710	960	0.30	20.5
1040	1500	0.30	20.5
1330	1560	0.30	20.5
1590	1150	0.35	20.4
2050	1200	0.30	20.5

Table 7.3: Exhaust gas composition in inlet pipe using different length connector pipes for Mark 2 interrupter at a fuel flow rate of 8.8 kg/h

LENGTH OF CONNECTOR PIPE (mm)	CO CONC. (PPM BY VOLUME)	CO_2 CONC. (%AGE BY VOLUME)	O_2 CONC. (%AGE BY VOLUME)
300	80	3.65	16.3
710	80	3.65	16.1
1040	80	3.55	15.7
1330	70	3.95	15.7
1590	70	3.95	15.7
2050	80	3.85	15.8

Table 7.4: Exhaust gas composition in tail pipe using different length connector pipes for Mark 2 interrupter at a fuel flow rate of 8.8 kg/h

FUEL CONSUMPTION (kg/h)	CO CONC. (PPM BY VOLUME)	CO_2 CONC. (%AGE BY VOLUME)	O_2 CONC. (%AGE BY VOLUME)
6.1	1000	0.30	20.6
7.5	1000	0.30	20.5
8.8	1000	0.30	20.5
9.7	1000	0.30	20.5
10.2	960	0.25	20.6
10.7	930	0.25	20.6

Table 7.5: Exhaust gas composition in inlet pipe using 710 mm long connector pipe at different fuel flow rates for Mark 2 interrupter.

FUEL CONSUMPTION (kg/h)	CO CONC. (PPM BY VOLUME)	CO_2 CONC. (%AGE BY VOLUME)	O_2 CONC. (%AGE BY VOLUME)
6.1	50	3.60	16.2
7.2	70	3.65	16.1
8.8	80	3.70	16.1
9.5	120	3.60	16.1
10.7	160	3.70	15.9
10.98	210	3.65	16.2

Table 7.6: Exhaust gas composition in tail pipe using 710 mm long connector pipe at different fuel flow rates for Mark 2 interrupter.

ANGLE OF SWIRLER (DEGREE)	CO CONC. (PPM BY VOLUME)	CO_2 CONC. (%AGE BY VOLUME)	O_2 CONC. (%AGE BY VOLUME)
10	1050	0.400	20.4
20	1050	0.396	20.4
30	1030	0.380	20.5
40	990	0.365	20.5

Table 7.7: Exhaust gas composition in inlet pipe using different angle air swirlers with the Mark 2 interrupter and a 710 mm long connector pipe at a fuel flow rate of 9.0 kg/h

SPRAY ANGLE (DEGREE)	CO CONC. (PPM BY VOLUME)	CO_2 CONC. (%AGE BY VOLUME)	O_2 CONC. (%AGE BY VOLUME)
45	910	0.296	20.6
60	900	0.292	20.6
70	890	0.288	20.6
80	940	0.352	20.6
90	870	0.336	20.6

Table 7.8: Exhaust gas composition in inlet pipe using different spray angle nozzles with the Mark 2 interrupter and a 710 mm long connector pipe at a fuel flow rate of 9.1 kg/h

FUEL FLOW RATE (kg/h)	CO CONC. (PPM BY VOLUME)	CO_2 CONC. (%AGE BY VOLUME)	O_2 CONC. (%AGE BY VOLUME)
6.1	830	0.388	20.4
7.4	750	0.364	20.5
8.0	700	0.340	20.6
9.2	630	0.304	20.6
10.5	470	0.288	20.6
11.3	430	0.276	20.6

Table 7.9: Exhaust gas composition in inlet pipe using a 4.0, 90° A water cooled nozzle, Mark 2 interrupter and a 710 mm long connector pipe

FUEL FLOW RATE (kg/h)	CO CONC. (PPM BY VOLUME)	CO_2 CONC. (%AGE BY VOLUME)	O_2 CONC. (%AGE BY VOLUME)
6.1	50	3.05	16.3
7.4	60	3.00	16.3
8.4	80	3.05	16.3
9.2	90	3.00	16.3
10.4	170	2.95	16.4
11.2	190	3.00	16.5

Table 7.10: Exhaust gas composition in tail pipe using a 4.0, 90° A water cooled nozzle and Mark 2 Interrupter and a 710 mm long connector pipe

LENGTH OF CONNECTOR PIPE (cm)	CO CONC. (PPM BY VOLUME)	CO_2 CONC. (%AGE BY VOLUME)	O_2 CONC. (%AGE BY VOLUME)
60	1310	0.150	20.5
92	1230	0.140	20.5
123	960	0.132	20.5
152	1080	0.140	20.5
182	1050	0.140	20.5
214	1310	0.152	20.4

Table 7.11: Exhaust gas composition in inlet pipe using different length connector pipes for Mark 2 interrupter (Aluminium delivery valve) at a fuel flow rate of 7.4 kg/h

FUEL FLOW RATE (kg/h)	CO CONC. (PPM BY VOLUME)	CO_2 CONC. (%AGE BY VOLUME)	O_2 CONC. (%AGE BY VOLUME)
6.0	1410	0.412	20.4
6.4	1200	0.340	20.5
7.7	780	0.272	20.6
8.4	840	0.290	20.6
9.0	880	0.308	20.6
9.9	1050	0.336	20.5

Table 7.12: Exhaust gas composition in inlet pipe using 1230 mm connector pipe and Mark 2 interrupter (Aluminium delivery valve).

FUEL FLOW RATE (kg/h)	CO CONC. (PPM BY VOLUME)	CO_2 CONC. (%AGE BY VOLUME)	O_2 CONC. (%AGE BY VOLUME)
6.0	50	4.9	14.3
6.4	70	4.9	14.3
7.7	140	5.0	14.0
8.8	210	5.5	13.6
9.5	240	5.2	14.0
10.6	270	4.8	14.9

Table 7.13: Exhaust gas composition in tail pipe using 1230 mm connector pipe and Mark 2 interrupter (Aluminium delivery valve).

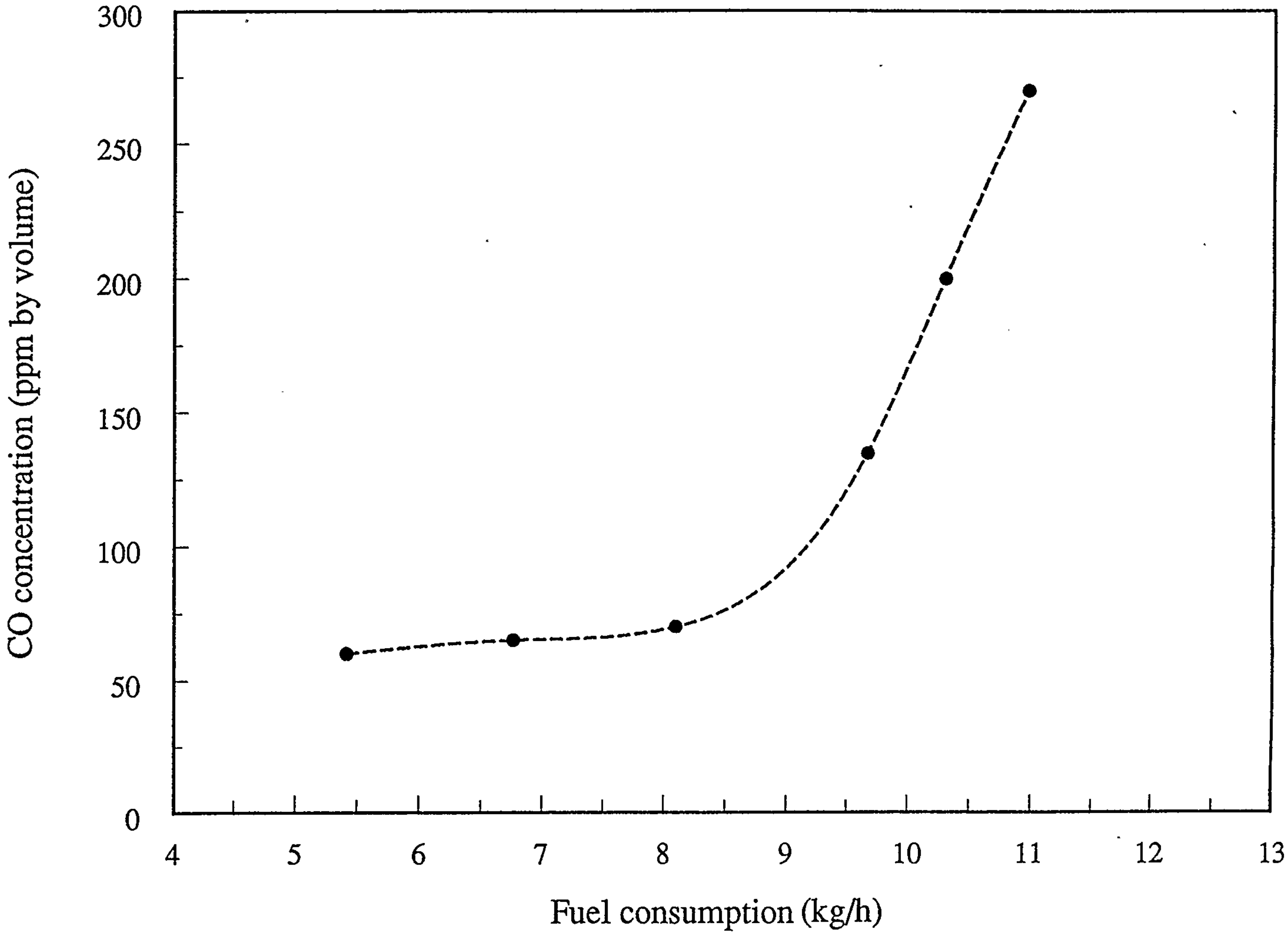

Figure 7.1: Concentration of CO in the tail pipe of pulse combustor using Mark 1 interrupter

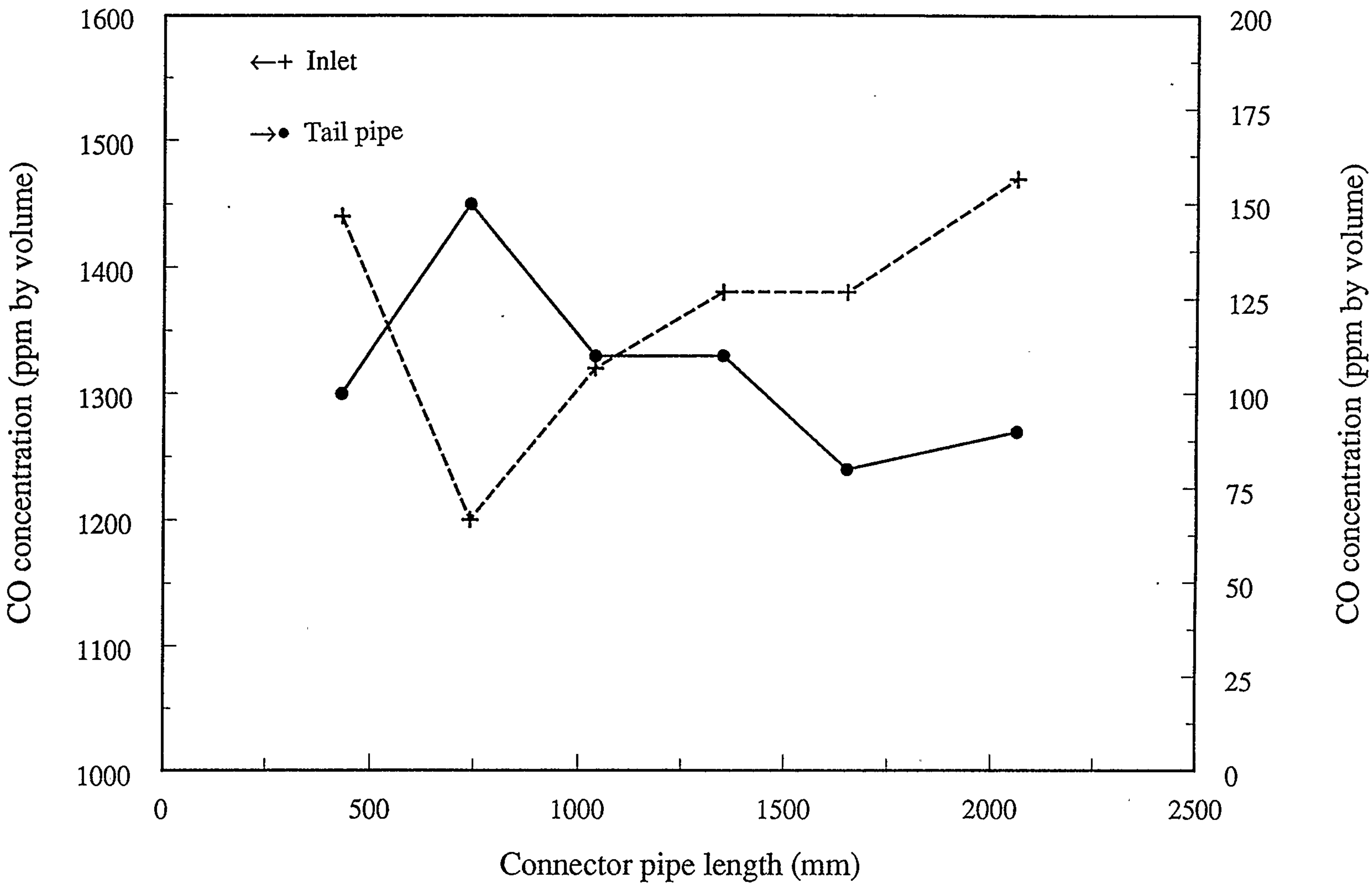

Figure 7.2: Variation in concentration of CO with connector pipe length in the inlet and tail pipe of the pulse combustor with Mark 1 interrupter for a fuel flow rate of 9.2 kg/h

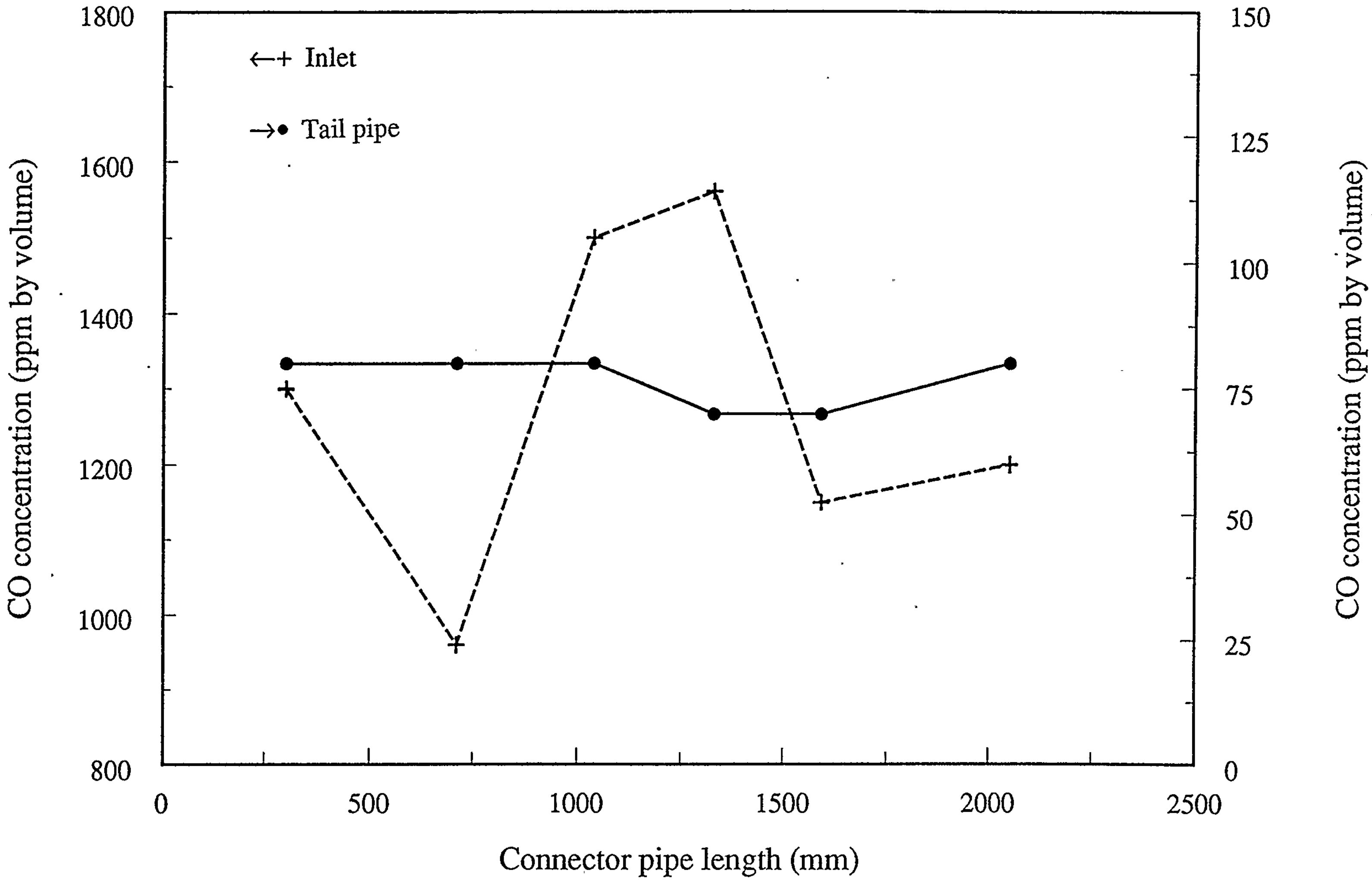

Figure 7.3: Variation in concentration of CO with connector pipe length in the inlet and tail pipe of the pulse combustor with Mark 2 interrupter for a fuel flow rate of 8.8 kg/h

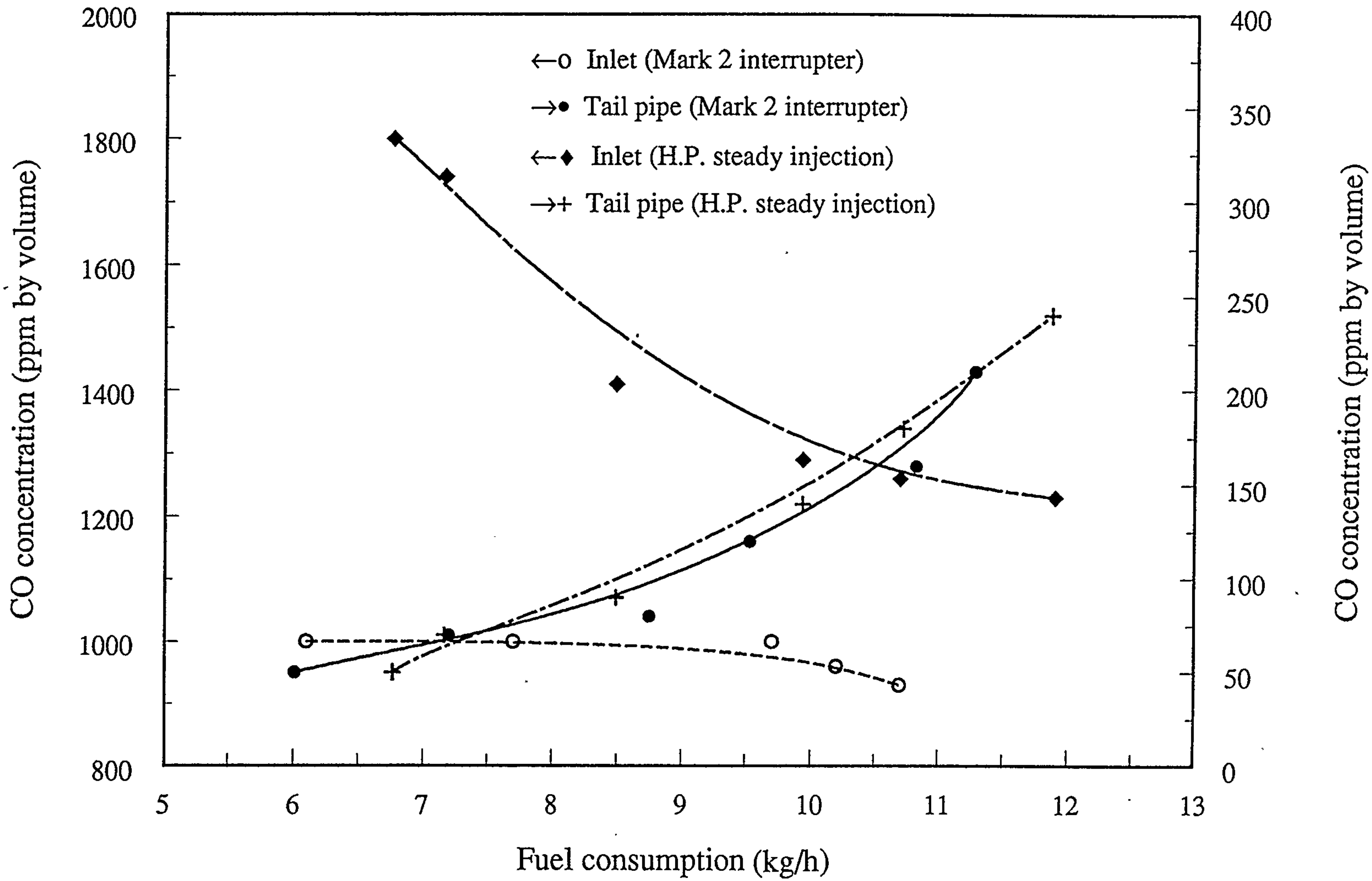

Figure 7.4: Concentration of CO in the inlet and tail pipe of the pulse combustor using Mark 2 interrupter and high pressure steady flow fuel injection fuel systems

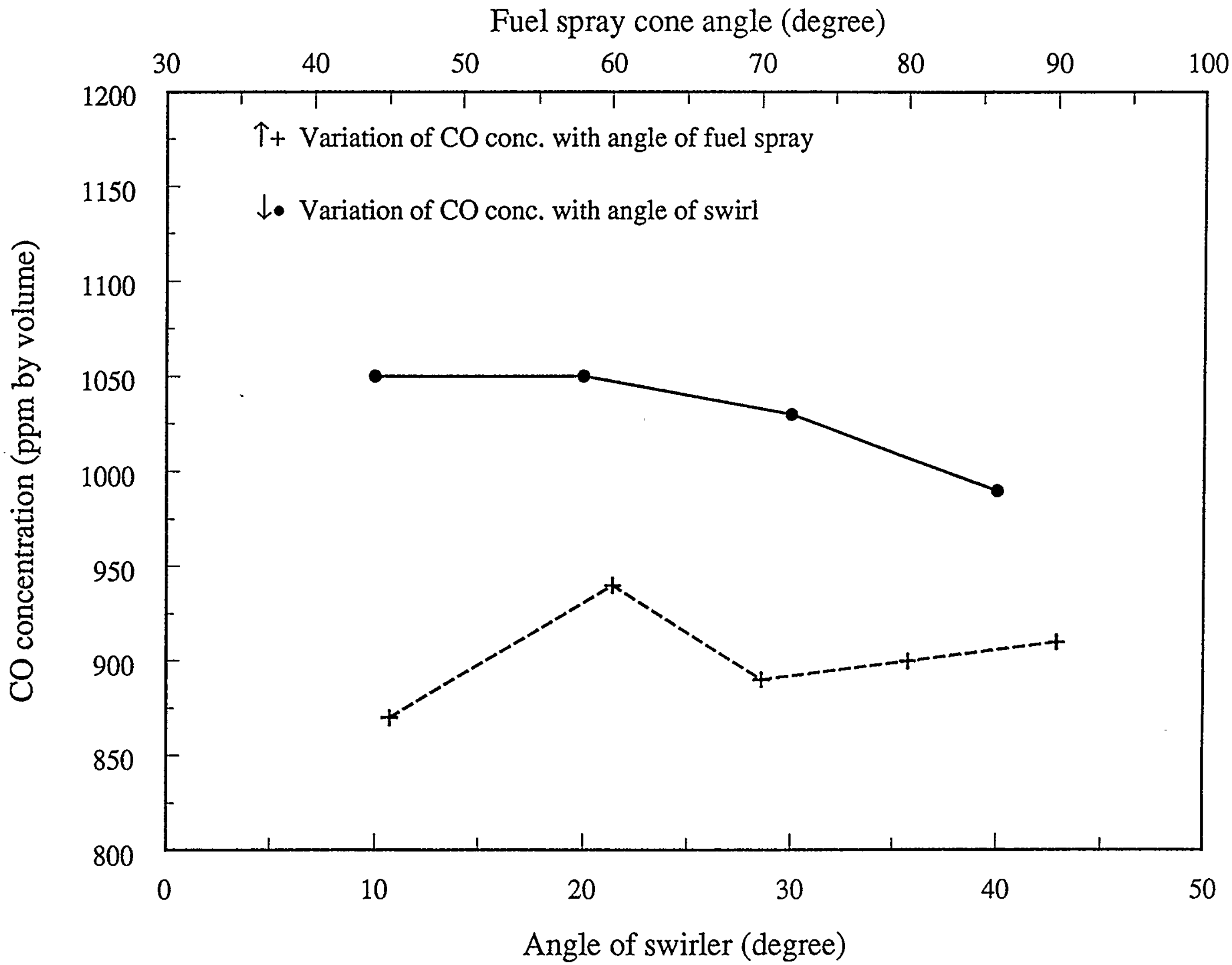

Figure 7.5: Variation in the concentration of CO in the inlet of the pulse combustor with angles of swirler and fuel spray for Mark 2 interrupter at a fuel flow rate of 9.0 kg/hr

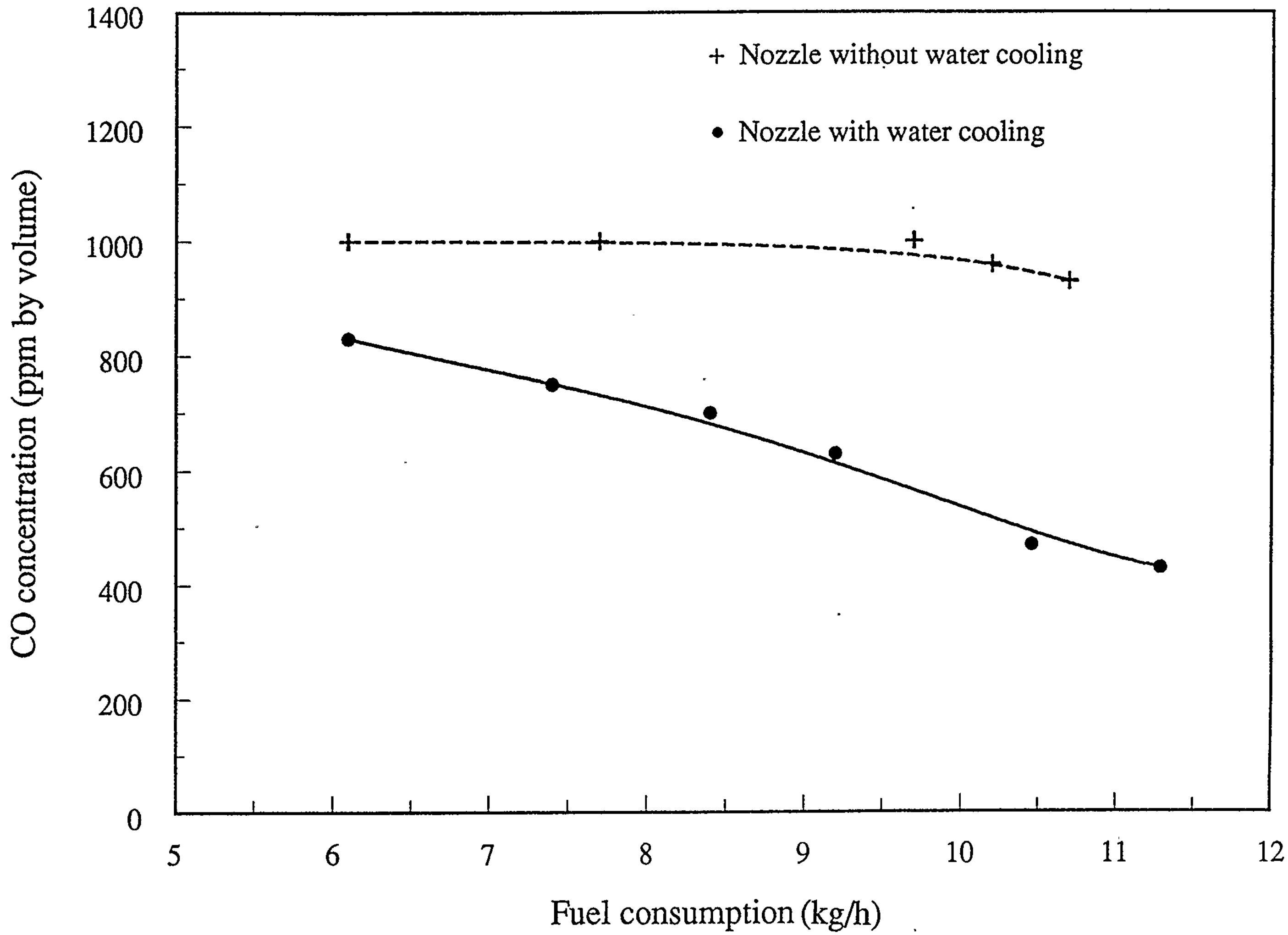

Figure 7.6: Variation in concentration of CO in the inlet for a cooled and uncooled fuel nozzle using Mark 2 interrupter and a 710 mm connector

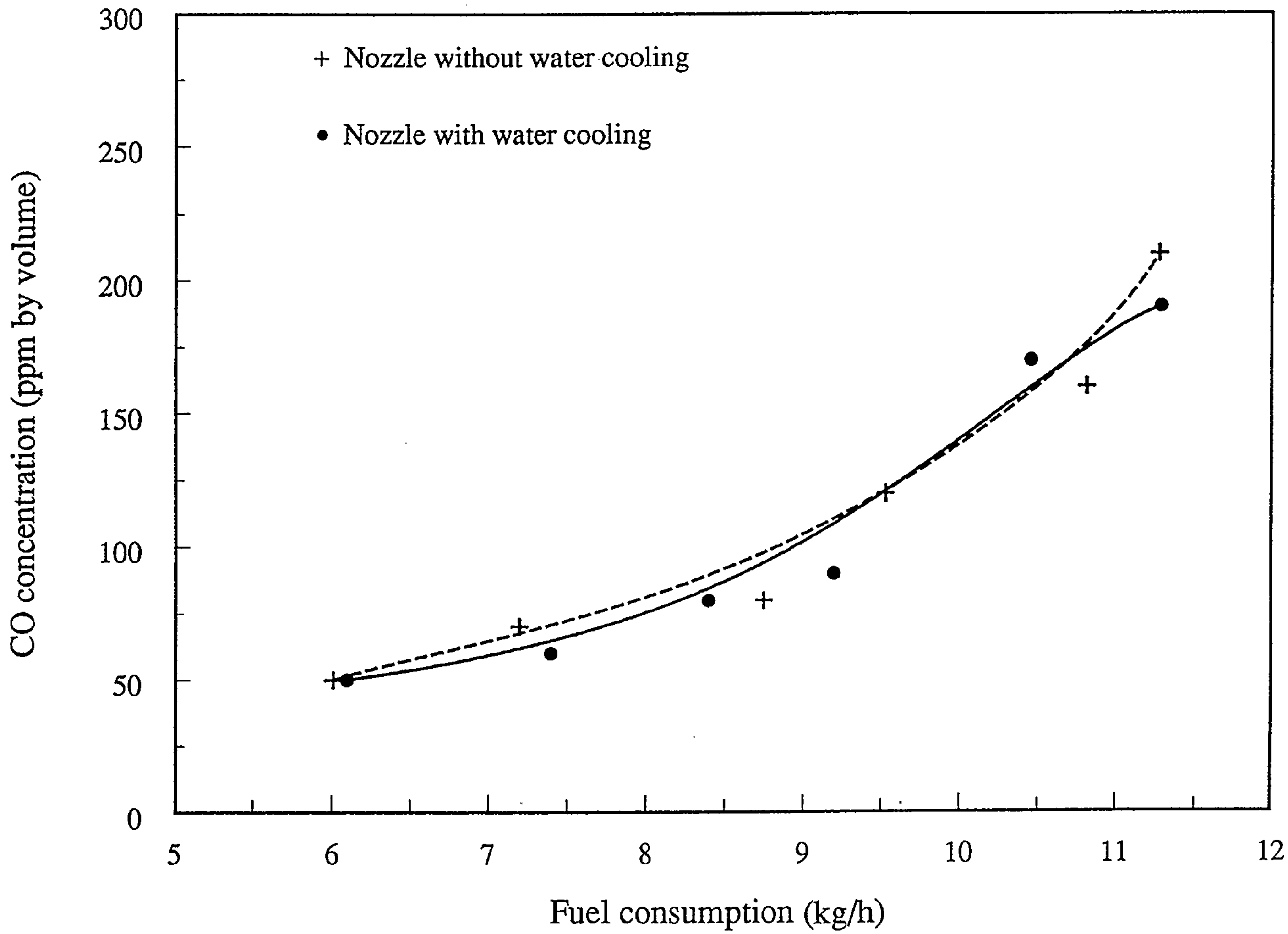

Figure 7.7: Variation in concentration of CO in the tail pipe for a cooled and uncooled fuel nozzle using Mark 2 interrupter and a 710 mm connector

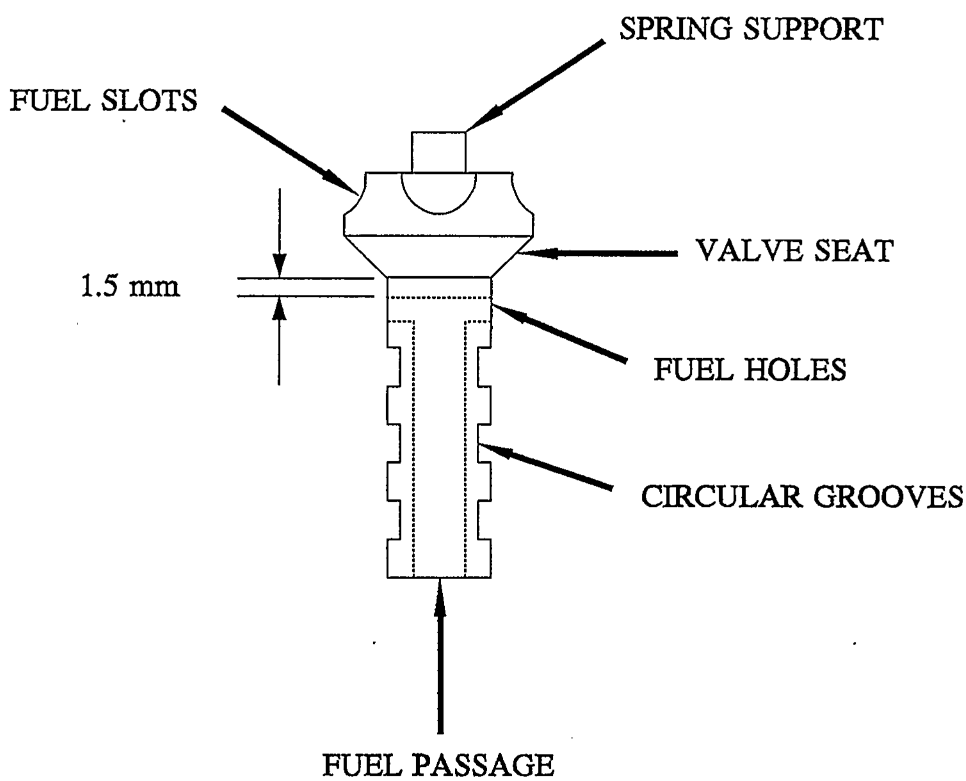

Figure 7.8: Aluminium delivery valve

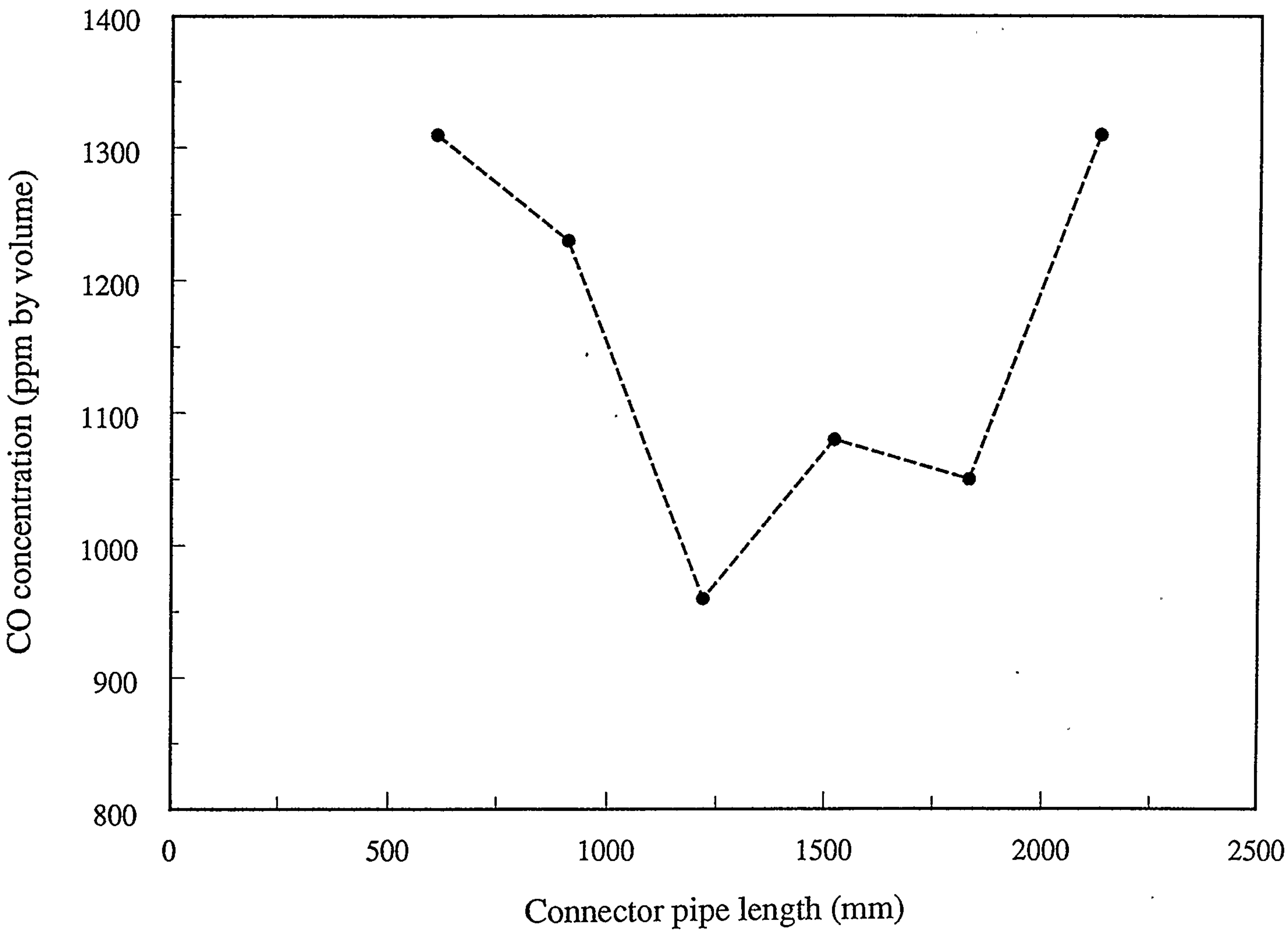

Figure 7.9: Variation in the concentration of CO in the inlet of the pulse combustor with different connector pipe lengths using modified Mark 2 interrupter and Aluminium delivery valve.

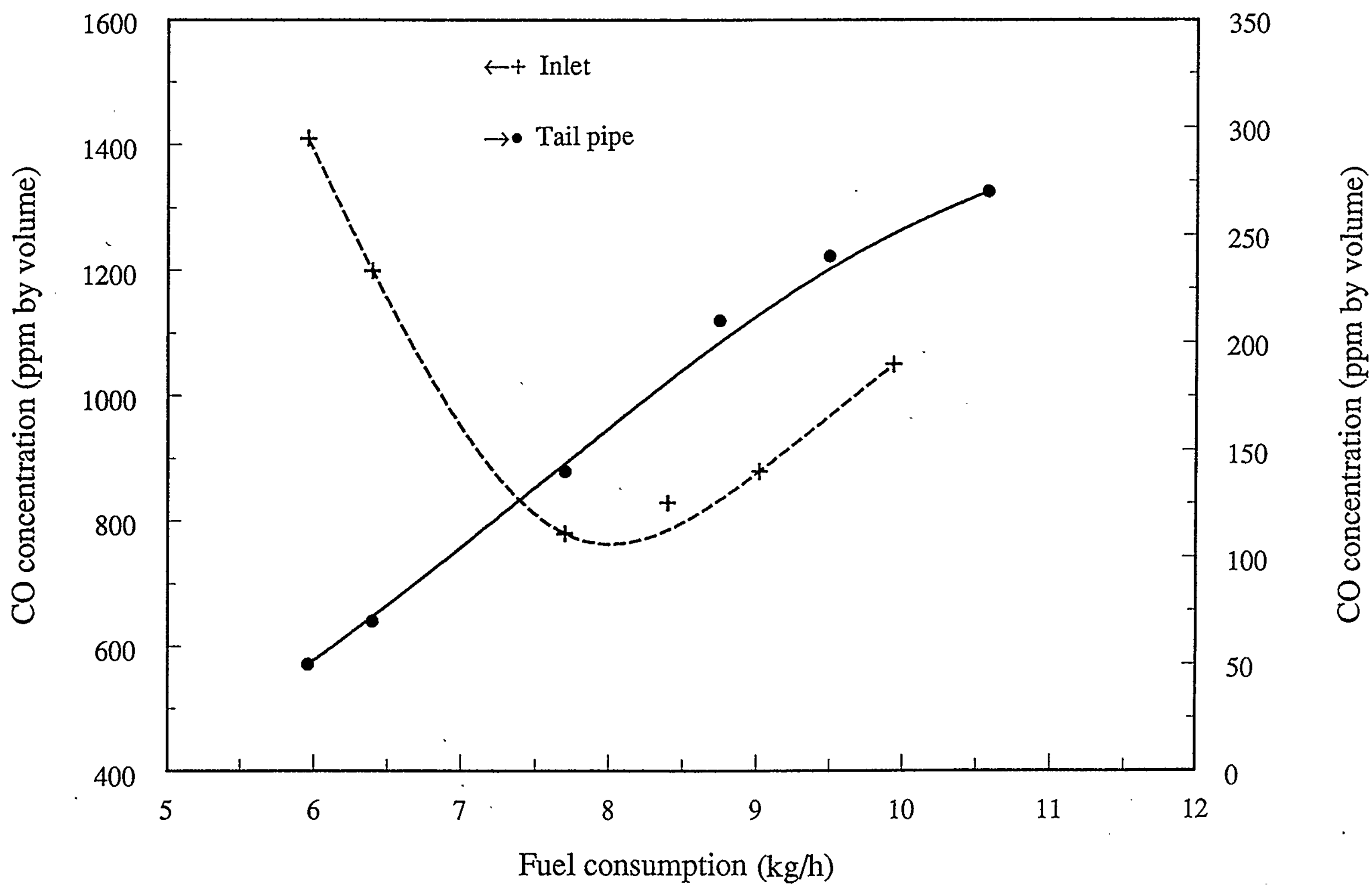

Figure 7.10: Concentration of CO in the inlet and tail pipe of pulse combustor using modified Mark 2 interrupter (Aluminium delivery valve) and 1230 mm connector pipe

CHAPTER 8 CONCLUSIONS AND RECOMMENDATIONS FOR FUTURE WORK.

8.1 CONCLUSIONS

The following conclusions for the different fuel systems tested could be drawn from the present work.

(a) CARBURETTOR:

1. The pulse combustor equipped with a carburettor operated equally well using a mylar or a thin shim steel non-return valve. The advantage of using shim steel over mylar for the valve material was that the former could withstand the adverse conditions of pressure and temperature in the gas turbine if a carburetted pulse combustor was to be used in a gas turbine.

2. The operation of the pulse combustor became rough as the thickness of the shim steel non-return valve increased. With an increase in the thickness of the non-return valve the pressure difference available across the pulse combustor became insufficient leading to rough running and back flow from the inlet of the carburettor.

3. Levels of CO emissions in the exhaust gases for the inlet were much higher

than for the tail pipe. Concentrations of CO_2 and O_2 in the exhaust confirmed that flow in the inlet consisted mainly of fresh air, whereas in the tail pipe it comprised mainly of exhaust gases.

(b) HIGH AND LOW PRESSURE STEADY FLOW FUEL INJECTION SYSTEMS:

1. The pulse combustor was sensitive to the location of the fuel nozzle and the distribution of fuel in the combustion chamber.

2. Self-sustained resonance of the pulse combustor was only achieved with a hollow fuel spray. With a solid or a semi-solid fuel spray the combustor ceased resonance once the compressed air supply was switched off.

3. The pulse combustor had the capability of operating on fuel pressures ranging from 69 kPa gauge to 1034 kPa gauge. The upper limit was set by the type of pump used. There was no indication that fuel pressures higher than this could not be handled by the pulse combustor.

4. Fuel selectivity was not a problem as the system operated on kerosene as well as on diesel fuel. Gasoline could not be tested because the pump used was not suitable for pumping this fuel.

5. The amplitude of pressure variation in the combustion chamber increased with an increase in fuel flow rates for both systems. The natural frequency of the machine did not show an appreciable change with fuel flow rates. It varied by approximately 4 Hz over the full operating range (i.e. about a 2% variation).

6. CO emissions from the inlet using both fuel systems were high (700 ppm to 1800 ppm). Compared to this CO levels in the tail pipe were significantly lower (50 ppm to 250 ppm). It seems that a reason for the high inlet emissions was that the fuel nozzle was situated in the inlet of the combustor and back flow from the inlet, during the expansion process of the working cycle, caused an expelling of unburnt fuel. Water cooling of the fuel nozzle in the case of the high pressure system was slightly beneficial in reducing the CO levels in the exhaust gases.

(c) HIGH PRESSURE FUEL INTERRUPTER SYSTEM

1. It was possible to modulate the fuel supply so that the fuel was supplied to the combustor only during phases 3 & 4 of the working cycle (Figure 1.4). A sharp cut-off of the fuel spray was required to ensure that fuel was supplied to the pulse combustor truly intermittently.

2. The intermittent supply of the fuel to the combustor depended on the magnitude of pressure variation in the combustion chamber and the fuel pressure. These two factors seemed to upset the phasing of the fuel system.

8.2 RECOMMENDATIONS FOR FUTURE WORK

The work described here is essentially a screening test to identify the most suitable approach for running the pulse combustor on liquid fuel. Most of the associated thinking was from the viewpoint of installing a pulse combustor on a gas turbine. The designs studied are far from optimized fuel systems primarily because of the high CO levels in the exhaust gases. Some future work that may be carried out to further this research is listed below:

(1) All the fuel systems that were investigated in the present work ran on atmospheric air. As the combustor in a gas turbine handles compressed air there is a need to investigate the ability of these fuel systems to run on compressed air. This may be done by running the pulse combustor in an enclosed compressed air plenum chamber or directly on a gas turbine.

(2) To reduce the concentration of CO in the exhaust gases to acceptable limits some device like an after-burner could be designed and tested.

(3) The use of more sophisticated gas analysing equipment could help evaluate, in addition to the levels of CO, CO_2 and O_2, the concentration of NO_x, unburnt hydrocarbons and other products of combustion. This would provide a better insight into the combustion process taking place in the combustor and may help reduce the high emissions of CO.

(4) The interrupter system investigated in the present work did not provide the desired results primarily, it appears, because the phasing of the fuel system was upset by changes in both fuel pressure and the amplitude of pressure variation in the combustion chamber. Therefore, if the fuel was to be supplied intermittently, a fuel system similar to a diesel engine fuel system may have to be designed. Just as in a diesel engine, where fuel is supplied for only a fraction of the total cycle, this system would supply fuel to the pulse combustor only when the pressure in the combustion chamber fell below atmospheric pressure. This would require a fuel shut off valve in the nozzle tip to give

instantaneous cut-off of the fuel spray. Instead of a gear pump a piston pump could be used. Such a pump would run at the natural frequency of the pulse combustor and inject fuel according to the pressure variation in the combustion chamber. For the correct phasing a feedback mechanism from the pulse combustor would be required to ensure that fuel was supplied at the correct frequency and cycle phasing.

REFERENCES

1. Higgins, B., 'On the Sound Produced by Current of Hydrogen Gas Passing Through a Tube', (edited by Nicholson), J. Nat. Phil. Chem. and the Arts, 1802, p. 129.

2. Lord Rayleigh, 'The Theory of Sound', Dover, Vol. 2, New York, 1945.

3. Keller, J.O., Bramlette, T.T. , Dec, J.E. and Westbrook, C.K., 'Pulse Combustion: The Importance of Characteristic Times', Combustion and Flame , Vol. 75, 1989, pp. 33-44.

4. Keller, J.O., and Westbrook, C.K., 'Response of a Pulse Combustor to Changes in Fuel Composition', Twenty-first Symposium (International) on Combustion, 1986, pp. 547-555.

5. Putman, A.A., Belles, F.E., and Kentfield, J.A.C., 'Pulse Combustion', Prog. Energy Combustion and Science, 1986, Vol. 12, pp. 43-79.

6. Markstein, G.H. (Editor), 'Non-steady Flame Propagation ', Pergamon Press, 1964, p. 188.

7. Putnam, A.A., 'General Survey of Pulse Combustion', First International Symposium on Pulsating Combustion, University of Sheffield, 1971.

8. International Symposium on Pulsating Combustion, Monterey, California, U.S.A., 1991.

9. Lindholm, A., Naslund, A., Klingmann, J., and Nilsson, U., 'Measurements of Experimental Pulse Combustors at Lund Institute of Technology', International Symposium on Pulsating Combustion, Monterey, California, U.S.A., 1991.

10. Speirs, B.C., 'An Optimal Multiple Inlet Pulse Combustor', M.Sc. Thesis, The University of Calgary, 1989.

11. Fernandes, L.C.V., 'Pulse Combustor Secondary Duct Flow', Ph.D. Thesis, The University of Calgary, 1989.

12. Ibrahim, G.M.S., 'Carburetted Liquid Fuelled Pulsed Combustor', M.Sc. Thesis, The University of Calgary, 1979.

13. Rehman, A., 'Performance of Scaled Pulsed Combustors', M.Sc. Thesis, The University of Calgary, 1978.

14. Huber, L.H., 'Swingfire Operated Heating Units for Commercial Vehicles', ATZ Technical Review of the Automotive Industry. Vol. 66, No. 2, 1964, pp. 31-37.

15. Lockwood, R.M., 'Summary Report on Investigation Miniature Valveless Pulse-Jets, Report No. ARD-307, Hiller Aircraft Company , Palo Alta, California, 1962.

16. Pearson, R.D. and Harley, R., 'Pulse Combustors for Helicopter Gas Turbines and their Computer Assisted Development', First International Symposium on Pulsating Combustion, University of Sheffield, 1971.

17. Carvalho, J.A., Miller, N., Daniel, B.R., and Zinn, B.T., 'Combustion Characteristics of Unpulverized Coal Under Pulsating and Non-pulsating Conditions', Fuel, Vol. 66, 1987, pp. 4-8.

18. Zinn, B.T., Powell, E.A., Chen, F., and Miller, N.,'The Use of Air Staging to Reduce the NO_x Emissions from Coal Burning Rikje Pulse Combustors', International Symposium on Pulsating Combustion, Monterey, California, U.S.A., 1991.

19. Rajan, S., and Gupta, A., 'Equivalence Ratio and Frequency Effects on the Combustion Characteristics of Micronized Clean Coal in Pulse Combustors', International Symposium on Pulsating Combustion, Monterey, California, U.S.A., 1991.

20. Kentfield, J.A.C., 'Nonsteady, One-dimensional, Internal, Compressible Flows, Theory and Application', Oxford Science Publications, 1993.

21. Belles, F.E., 'R & D and Other Needs for Exploitation of Pulse Combustion in Space Heating Applications', Symposium on Pulse Combustion Technology for Heating Applications, Argonne National Laboratory, 1979.

22. Arpaci, V.S., Dec, J.E. and Keller, J.O., ' Heat transfer in pulse combustor tailpipes', International Symposium on Pulsating Combustion, Monterey, California, U.S.A., 1991.

23. Kunsagi, L., 'Silent Valveless Pulsating Combustors for Industrial Purposes', First International Symposium on Pulsating Combustion, University of Sheffield, 1971.

24. Bertin, J., 'The SNECMA Escopette Pulse-jet', Interavia 8, 1953, pp. 343-347.

25. Persechino, M.A., 'Valveless Pulsejet De-icer application', U.S. NRL. Report 5024, 1957.

26. Keller, J.O. and Saito, K., 'Measurements of the Combusting Flow in a Pulse Combustor', Combustion Science and Technology, Vol. 53, 1987, pp. 137-163.

27. Yerneni, V.N., 'Pulsating Combustion Applied to a Small Gas Turbine' M.Sc. Thesis, The University of Calgary, 1984.

28. O'Blenes, M.J., 'A Pulse Combustor Gas Turbine', M.Sc. Thesis, The University of Calgary, 1987.

29. Corliss, J.M., Putnam, A.A., Murphy, M.J. and Lockin D.W., ' NO_x Emissions from Several Pulse Combustors', ASME 84-JPGC-APC-2, 1984.

30. Keller, J.O. and Hongo, I., 'Pulse Combustion: The Mechanism for NO_x Production', Combustion and Flame, Vol. 80, 1990, pp. 219-237.

31. Michel, Y., 'Effects of Flue-Gas Recirculation on NO_x Production and Performance of Pulse Combustion Hot-water Boilers', International Symposium on Pulsating Combustion, Monterey, California, U.S.A., 1991.

32. Kelly, J., 'Reducing Gas-Fired Pulse Combustor NO_x Emissions' International Symposium on Pulsating Combustion, Monterey, California, U.S.A., 1991.

33. Hanby, V.I., 'Convective Heat Transfer in a Gas-Fired Pulsating Combustor', Journal of Engineering Power 91a, 1966, pp. 48-52.

34. Dec, J.E. and Keller, J.O., 'Pulse Combustor Tail-pipe Heat-Transfer Dependence on Frequency, Amplitude and Mean Flow Rate', Combustion and Flame, Vol. 77, 1989, pp. 359-374.

35. Perry, E.H. and Culick, F.E.C., 'Measurements of Wall Heat Transfer in the Presence of Large-Amplitude Combustion-Driven Oscillations', Combustion Science and Technology, Vol. 9, 1974, pp. 49-53.

36. Lockwood, R.M., 'Guidelines for Design of Pulse Combustion Devices Particularly Valveless Pulse Combustors', Vol. 1 Symposium on Pulse Combustion Applications, Atlanta, Georgia, 1982.

37. Adams, C., 'Performance Results of the Lennox Pulse Combustor Furnace field Trials', Vol. 1 Symposium on Pulse Combustion Applications, Atlanta, Georgia, 1982.

38. Woodworth, L.M., 'R & D Activities in Pulse Combustors', Symposium on Pulse Combustion Technology for Heating Applications, Argonne National Laboratory, 1979.

39. Severyanin, V.S., 'Prospects for Pulsating Combustion in Power Engineering', First International Symposium on Pulsating Combustion, University of Sheffield, 1971.

40. Hongo, I. and Saito, K., 'Development of Small Twin-Valveless Pulse Combustors for Space Heating', International Symposium on Pulsating Combustion, Monterey, California, U.S.A., 1991.

41. Hanby,V.I. and Brown, T.D., 'A Residual Fuel Oil-Fired Pulsating Combustor', Journal of the Institute of Fuel, 1975, pp. 49-51.

42. Zinn, B.T., Carvalho, J.A., Miller, N. and Daniel, B.R., 'Development of a Pulsating Combustor for Burning of Wood', Vol. 1 Symposium on Pulse Combustion Applications, Atlanta, Georgia, 1982.

43. Kentfield, J.A.C. and Fernandes, L.C.V., 'Improvements to the Performance of a Prototype Pulse, Pressure-Gain, Gas Turbine Combustor', Journal of Engineering for Gas Turbines and Power, Vol. 112, 1990.

44. Sran, B.S. and Kentfield, J.A.C., ' Twin Valveless Pulse Combustors Coupled to Operate in Antiphase', Vol. 1 Symposium on Pulse Combustion Applications, Atlanta, Georgia, 1982.

45. Thring, F.H. (Editor), 'Pulsating Combustion, the Collected Works of F.H. Reynst', Pergamon Press, 1961.

46. Porter, C.D., 'Valveless-Gas-Turbine Combustors with Pressure Gain', ASME Paper No. 58-GTP-11, 1958.

47. Kentfield, J.A.C., 'Pressure Gain Combustion, a Review of Recent Progress',Symposium on Pulse Combustion Technology for Heating Applications, Argonne National Laboratory, 1979.

48. Kentfield, J.A.C., 'A New Light Weight Warm-Air Blower for Rapidly Pre-Heating Cold Soaked Equipment', ASME Paper 77-WA/HT-20, 1977.

49. Paquette, R.L., 'Fuel System, Controls, Instrumentation and Accessories', Chapter 10, Vol. 1, Sawyer's Gas Turbine Engineering Handbook (Second edition), Gas Turbine Publications, Inc., Stanford, Connecticut.

50. Odgers, J., Private Communication, 1992.

51. Model H, Two Stage Fuel Unit, Technical Manual, Inglis Limited. Toronto, Canada.

52. Delavan Oil Burner Nozzles and Accessories for Residential and Industrial Applications, Technical Manual, Bamberg, South Carolina, U.S.A.

53. Morzouk, E.S.M., 'Pulsed Pressure-Gain Combustion', Ph.D. Thesis, The University

of Calgary, 1974.

54. Kentfield, J.A.C., Private Communication, 1992.

55. Rehman, M., 'A Study of a Multiple Inlet Valveless Pulsed Combustor', Ph.D. Thesis, The University of Calgary, 1976.

56. Kentfield, J.A.C., Rehman, M., and Morzouk, E.S., 'A Simple Pressure-Gain Combustor for Gas Turbines', Journal of Engineering for Power, Vol. 99, No. 2, 1977.

57. Kentfield, J.A.C., Private Communication, 1992.

APPENDIX A

CONVENTIONAL FUEL PUMPS IN GAS TURBINES

The primary requirement of a fuel system of a gas turbine is to supply an adequate amount of clean fuel at sufficient pressure to the turbine combustor. In a gas turbine fuel systems required for gaseous fuels are entirely different from the types required for liquid fuels. The notes presented here represent a summary of existing, available information (49).

(1) Gaseous Fuels

Gaseous fuels do not require special preparation such as atomization for efficient burning. The gas supply needs only to be at a sufficient pressure to overcome [1] the pressure losses in the fuel lines and control valves; [2] the combustor pressure; [3] the potential maldistribution of fuel in the nozzles caused by pressure losses in the manifold. A supply pressure range of 172 kPa to 345 kPa above compressor discharge pressure is adequate to meet these requirements. In case the gaseous fuel is not available at such a pressure, it is normally compressed by an auxiliary compressor.

(2) Liquid Fuels

Liquid fuel has to be atomised into a fine spray before it can be burnt efficiently in the gas turbine combustor. For this pressure as low as 140 kPa and as high on 689 kPa above the compressor delivery pressure may be required for fuel atomization, depending on the type of fuel system used. These pressure requirements in the liquid fuel system are normally satisfied by a fuel pump. There are three main types of positive displacement fuel pumps used in gas turbines: gear, vane and piston.

(a) Gear Pumps

The gear pump is the most widely used on gas turbines because of its simplicity, ruggedness and low cost. As shown in Figure 3.5, fuel is carried in the spaces between the gear teeth and is forced out of the discharge port as the gear teeth mesh. Clearance between the gear and side plates can become a critical factor because, as this clearance increases, the leakage along the face of the gear from discharge to inlet will increase. To compensate for this wear and growing clearance, pressure loaded side plates made out of bronze are sometimes used.

(b) Vane Pumps

Vane pumps consist of a cam ring, rotor, vanes and two side pressure plates. Vanes are carried in slots in the rotor and are forced against the inner contour of the ring by centrifugal action and the hydraulic pressure. As the rotor revolves, fuel flows through the inlet port into the cavity formed by two adjacent vanes. Fuel is then carried across the sealing lands between the inlet and outlet ports and discharged at the outlet port. Advantages of the vane pumps are high efficiency, ability to compensate for wear and operate at high speeds (up to 20000 rpm).

(c) Piston Pumps

In a piston pump the action of a cam displaces a piston through its stroke. The length of stroke and therefore pump displacement is determined by the cam plate angle for swashplate, or wobble plate type pumps. The pumping action is controlled by the valve port plate which directs flow in the proper direction during the inflow and outflow parts of the stroke. A particular advantage of a piston pump is its ability to provide variable displacement while at constant speed. This is accomplished by varying the cam plate, or swashplate, angle.

Piston pumps are capable of generating high pressures and are less susceptible to internal leakage through pump clearances. However, they are more complex in design and therefore tend to be more costly than other types of pump.

APPENDIX B

DESIGN FEATURES OF THE GEAR PUMP USED

These notes are based upon information available in more detail elsewhere (51). A section of the two stage gear pump is shown in Figure B.1. This unit is capable of pumping kerosene or diesel fuels up to a maximum speed of 1800 rev./min. The basic elements of the pump consist of two sets of gears, a strainer and a combination of pressure regulating and nozzle cut-off valve. The following are the basic design features of the pump.

(1) Rota-Roll Gear

Quiet, efficient operation of the Inglis-Sundstrand fuel pump is ensured by the two hydraulically balanced rota roll pump members. With the rota-roll design the inner smaller member (roller) is keyed to the shaft and drove the outer, internally toothed ring-gear, member (rotor) at a speed 25% slower than motor speed. This arrangement promotes quiet operation. The spiral tooth form of the pumping members minimizes friction and provides positive pumping action with a high maximum efficiency.

(2) Balanced Fast Cut-off Valve

Steady pressure and fast, positive cut-off are characteristics of the piston-type valve. Three bypass ports equally spaced around the piston sleeve distribute pressure evenly, thus hydraulically balancing the piston, which therefore is free acting.

All parts are of durable, corrosion resistant material. The piston, which is chrome plated, slides in a sleeve made separate for easy removal from the fuel unit body. A pliable, resilient neoprene disc on the end of the piston ensures positive cut-off and protection against leakage. Pressure could be easily regulated from 345 kPa gauge to 1034 kPa gauge with the help of a screw driver.

As the valve assembly could be easily removed from the pump, the original spring in a valve was, for the low pressure injection system, replaced with a weaker spring giving a fuel pressure range from 69 kPa gauge to 345 kPa gauge.

(3) Strainer

Foreign particles such as dirt are excluded by a fine mesh monel screen attached to a rigid steel frame. The strainer is positively seated by spring pressure and is readily accessible for cleaning.

(4) Leak proof Diaphragm-Type Shaft Seal

Basic components consist of a special bronze shaft member running against a glass-hard nitralloy ring. An impregnated cloth diaphragm impervious to oil is attached to the nitralloy ring and securely clamped at the body.

(5) Anti Hum Device

This simple devise consisted of a nylon wafer mounted on the end of the gear set. It is impervious to fuel, oil and by absorbing pulsations originating in the intake line, eliminates tank hum.

(6) Large Shaft Bearing

A large shaft diameter and long bearing eliminates shaft noise and permits either direct or belt drive.

(7) Body

The body of the pump is machined out of cast iron to close tolerances.

Other design features include an easy installing and service, compactness and light weight.

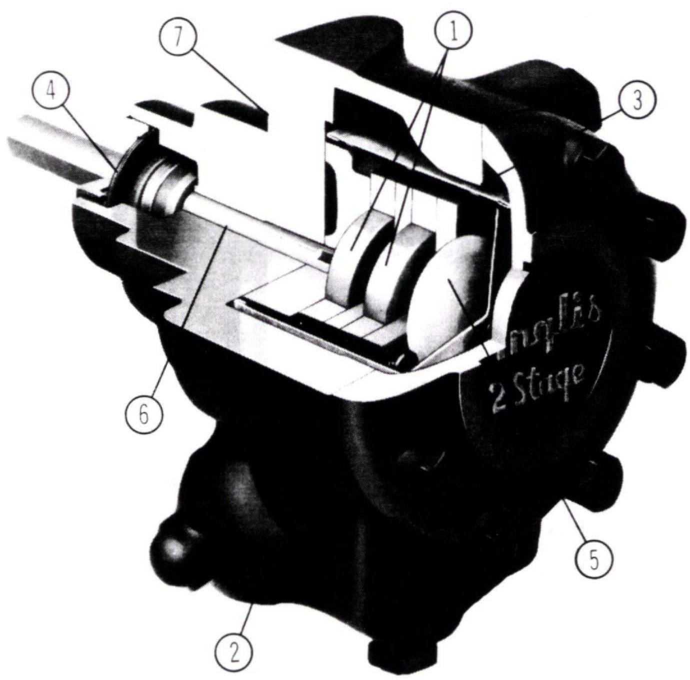

Figure B.1: Cross section of the two stage gear pump